Available online at www.sciencedirect.com

ScienceDirect

Nuclear Physics B 914 (2017) 642–696

NUCLEAR PHYSICS B

www.elsevier.com/locate/nuclphysb

BPS spectra of $\mathcal{N} = 2$ SO_7 and SP_4 models

R. Ahl Laamara [a,b], O. Mellal [a,b], E.H. Saidi [a,b,*]

[a] *LPHE-MS, Science Faculty, Mohammed V University, Rabat, Morocco*
[b] *Centre of Physics and Mathematics, CPM, Morocco*

Received 22 June 2016; received in revised form 5 October 2016; accepted 26 November 2016

Available online 30 November 2016

Editor: Stephan Stieberger

Abstract

Extending the folding method of ADE Dynkin diagrams of Lie algebras to BPS quivers of 4d $\mathcal{N} = 2$ supersymmetric gauge theory with ADE type gauge invariance, we study the BPS spectra for gauge symmetries with non-simply laced Lie algebras. Focussing on the 4d $\mathcal{N} = 2$ SO_7 and SP_4 models, we derive the BPS states of the strong chambers of these theories. We find that for both gauge groups $G_{nsl} = SO_7$ and $SP_4 \simeq SO(5)$, the number of BPS states of the strongly coupled chamber is $2\dim G_{nsl}$ versus $2\dim G_{sl} - 2rank G_{sl}$ for the cousin gauge symmetries $G_{sl} = SO_8$ and $SU_4 \simeq SO(6)$. The relationship between the G_{sl} and G_{nsl} types of BPS quiver mutations is derived. Other features are also studied.

1. Introduction

BPS quiver theory has been proposed few years ago in refs. [1,2] in order to build the complete set of BPS spectra in 4d $\mathcal{N} = 2$ supersymmetric QFT. This approach has been successfully applied to ADE type gauge symmetries [3–10] and to Gaiotto type theories describing the low energy limit of M5-branes wrapped on a punctured Riemann surface [11–14]; see also [15–31] for previous works and [32–37] for other approaches to the $\mathcal{N} = 2$ BPS spectra. A tentative for the generalisation of the BPS quiver construction beyond ADE type groups has been done in [38]; there, BPS quivers with superpotentials have been obtained for a subset of $\mathcal{N} = 2$ QFTs

* Corresponding author.
E-mail address: h-saidi@fsr.ac.ma (E.H. Saidi).

http://dx.doi.org/10.1016/j.nuclphysb.2016.11.021

based on *non-simply* laced Lie algebras of type BCFG. Aspects of this generalisation constitute the main objective of the work developed in this paper; with focus on two selected $\mathcal{N}=2$ supersymmetric gauge theories in order to illustrate explicitly our approach on simple models of non-simply laced type gauge symmetries namely $SO(7,\mathbb{R})$ and $SP(4,\mathbb{R})$.

To introduce our approach, it is interesting to begin by recalling some basic features behind the set up of the BPS quiver theory with underlying gauge symmetry G of simply laced type. First, the idea of a quiver Q^G to encode BPS states is remarkable and a great observation; its power follows from the link with the geometric engineering method of supersymmetric QFT embedded in type II string theory on local fibered manifolds with ADE singularities [39–41]; see also [42–44] for hyperbolic singularities. For the class of $\mathcal{N}=2$ supersymmetric pure gauge theories, the BPS quiver Q^G is formally similar to the usual Dynkin diagram $\mathfrak{D}^G$ of the Lie algebra of the gauge group G [45]; roughly speaking, Q^G is somehow a kind of duplication of nodes corresponding Dynkin graph. The ADE-type diagram $\mathfrak{D}^G$ and the corresponding BPS quiver Q^G share together several basic features; some of them like outer-automorphisms and Coxeter symmetries will be exploited in present study. For example, the Q^G quiver can be defined in terms of a $2r\times 2r$ matrix $\mathcal{A}^G_{IJ}$ in the same manner as for the $\mathfrak{D}^G$ diagram encoding the $r\times r$ Cartan matrix K^G_{ij} [3]. Moreover, like for the ADE type Cartan matrix $\vec{a}_i.\vec{a}_j$ that describes intersections of a given simple roots system $\{\vec{a}_i\}_{1\leq i\leq r}$ of G, the BPS matrix $\mathcal{A}^G_{IJ}$ describes as well intersections of a given system of basis vectors $\{\vec{v}_I\}_{1\leq I\leq 2r}$ defining the electric–magnetic charges of *elementary* monopoles and dyons. Thus, the $2r$ electric–magnetic vectors $\vec{v}_I$ play a similar role as the simple roots $\vec{a}_i$; and so can be thought of as a vector basis giving the positive integral charges $\vec{v}_+=\sum n_I\vec{v}_I$ of BPS particles of the supersymmetric pure gauge theory with symmetry G. The electric–magnetic intersection matrix $\mathcal{A}^G$ encodes therefore the data on the protected massive and charged BPS/anti-BPS states of the Hilbert space of the $\mathcal{N}=2$ QFT_4; the correspondence $\vec{a}_i\leftrightarrow\vec{v}_I$ allows to induce other relationships; in particular the two following ones are useful for present study: (1) the structure of the set $\{\vec{v}_+\}$ of the BPS states may be put into correspondence with the way we construct the set $\{\vec{a}_+\}$ of positive roots of the Lie algebra of G; the same property holds for the anti-BPS states $\{\vec{v}_-=-\vec{v}_+\}$ and the negative roots $\{\vec{a}_-=-\vec{a}_+\}$ of G. This similarity gives a link between the electric–magnetic lattice Γ_{2r} of BPS and anti-BPS states and the root lattice Λ_r of the Lie algebra of G. (2) The set of mutations $\mu: Q^G\to\tilde{Q}^G$ that transform a given quiver Q^G into mutated ones $\tilde{Q}^G$ has also an homologue in the theory of Lie algebra of the gauge symmetry; it is given by the set of all possible ways in choosing a $\{\vec{a}_i\}$ basis of simple roots for describing the full root system of G and so for indexing the diagram $\mathfrak{D}^G$. Therefore, quiver mutations relating distinct quivers Q^G and $\tilde{Q}^G$, describing quantum mechanical dualities [46], may be put into a correspondence with Weyl symmetry group of Lie algebra roots.

In this paper, we contribute to the study of BPS quiver theory of 4d $\mathcal{N}=2$ supersymmetric QFT with BCFG type gauge symmetries and quiver Q^{BCFG} obtained by taking advantage of the $Q^{ADE}\leftrightarrow\mathfrak{D}^{ADE}$ correspondence; and by using a known link between $\mathfrak{D}^{ADE}$ and $\mathfrak{D}^{BCFG}$ Dynkin diagrams (DD). To be explicit, we focus in study on the construction of the set of BPS/anti-BPS states of the strong chamber of two 4d $\mathcal{N}=2$ supersymmetric pure gauge models; the first $\mathcal{N}=2$ model has an $SO(7,\mathbb{R})$ gauge symmetry group; and the second concerns the supersymmetric model with symplectic $SP(4,\mathbb{R})$ gauge symmetry. Our approach is based on *extending* the usual folding method linking $\mathfrak{D}^{ADE}$ and $\mathfrak{D}^{BCFG}$ to the BPS quivers. This extension, which is worked out explicitly in this study, allows us to relate the quivers Q^{ADE} of the BPS theory with ADE type to BPS quivers Q^{BCFG} associated with BCFG type gauge symmetries.

Among our results, we derive the BPS/anti-BPS states of the strong chambers $\mathfrak{Q}_{stg}^{SO_7}$ and $\mathfrak{Q}_{stg}^{SP_4}$ of pure SO$(7,\mathbb{R})$ and SP$(4,\mathbb{R})$ gauge theories by using particular quiver mutation subgroups $H_{stg}^{SO_7}$ and $H_{stg}^{SP_4}$ that have interpretation in terms of alignments of central charges of elementary monopoles and dyons. These $H_{stg}^{SO_7}$ and $H_{stg}^{SP_4}$ are subsets of the usual Coxeter groups $\mathcal{G}_{stg}^{SO_7}$ and $\mathcal{G}_{stg}^{SP_4}$ generated by fundamental mutations $t_i^{SO_7}$ and $t_i^{SP_4}$ satisfying the typical $\left(t_i t_j\right)^{m_{ij}^G} = I_{id}^G$ with m_{ij}^G standing for the Coxeter matrix whose structure is as described in appendix I. We give also the relationship between the obtained strong chamber $\mathfrak{Q}_{stg}^{SO_7}$ (resp. $\mathfrak{Q}_{stg}^{SP_4}$) of the SO$(7,\mathbb{R})$ (resp. SP$(4,\mathbb{R})$) model with the chamber $\mathfrak{Q}_{stg}^{SO_8}$ (resp. $\mathfrak{Q}_{stg}^{SU_4}$) of $\mathcal{N}=2$ supersymmetric models with SO$(8,\mathbb{R})$ (resp. SU(4)) gauge symmetry. We analyse as well the *unexpected* number $N_{bps}^{G^*}$ of BPS states of the strong chambers $\mathfrak{Q}_{stg}^{G^*}$ for gauge invariance $G^* = SO(7,\mathbb{R})$, $SP(4,\mathbb{R})$; and we give the relation between these $N_{bps}^{G^*}$'s with the corresponding N_{bps}^{G} of the chamber $\mathfrak{Q}_{stg}^{G}$ for gauge symmetries $G = SO(8,\mathbb{R})$, $SU(4,\mathbb{R})$.

The presentation of this paper is as follows: In section 2, we recall useful aspects on BPS quivers in $\mathcal{N}=2$ QFT$_4$ with ADE type gauge symmetry; then we describe some aspects of those gauge symmetries with non-simply laced Lie algebras. In section 3, we revisit the BPS quiver model with SO(8) gauge symmetry and fix some convention notations. Like the Dynkin diagram of SO(8), the BPS quivers of the supersymmetric pure SO(8) gauge theory have $\mathbb{Z}_2$ and $\mathbb{Z}_3$ outer-automorphism symmetries. In section 4, we develop *our proposal* based on folding quivers of type $SO(8)$; this approach extends the usual folding method of D$_4$ Dynkin diagram to get the B$_3$ one. Then, we construct explicitly the strong chamber of BPS states for the $SO(7)$ symmetry and derive the quiver mutation group $H_{stg}^{SO_7}$ allowing to generate them starting from a primitive quiver $Q_0^{SO_7}$. In section 5, we first describe the BPS strong chamber of the $\mathcal{N}=2$ $SU(4) \simeq SO(6)$ model; then we use our folding quiver method to construct the strong chamber of BPS states for the $SP(4,\mathbb{R}) \simeq SO(5,\mathbb{R})$ and the quiver mutation group $H_{stg}^{SP_4}$. In section 6, we give the conclusion and make comments. In sections 7 and 8, we give three appendices (I, II, III) where some technical details and extra materials are reported.

2. BPS quivers of $\mathcal{N}=2$ QFT$_4$

In this section, we begin by reviewing some useful tools on ADE type BPS quiver theory of [1,2]; especially those aspects concerning the construction of BPS chambers of 4d $\mathcal{N}=2$ supersymmetric pure gauge theories. Then, we consider the fundamentals of the BPS quivers Q^{BCFG} for the class of supersymmetric theories with gauge symmetries $\boldsymbol{G}$ based on Lie algebras type BCFG having non-simply laced Dynkin diagrams $\mathfrak{D}^{BCFG}$.

2.1. Generalities on BPS chambers of ADE type

Here, we introduce the sets $\mathfrak{Q}_{weak}^G$ and $\mathfrak{Q}_{stg}^G$ of BPS quivers obtained by starting form a primary quiver representative Q_0^G and performing appropriate quiver mutations. Particles living at nodes of the quivers of these sets form respectively the weak and strong chambers of BPS/anti-BPS states of the 4d $\mathcal{N}=2$ supersymmetric gauge theory.

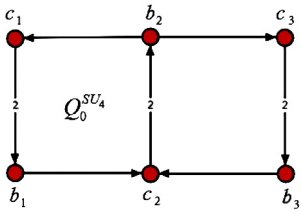

Fig. 1. The primitive BPS quiver $Q_0^{su_4}$ of $\mathcal{N}=2$ supersymmetric model with SU(4) gauge symmetry. Half of nodes are occupied by monopoles and the other half by dyons. The number 2 on vertical links means there are two arrows; for example the link between (b_1, c_1) should be thought of as $\downarrow\downarrow$. This graph has a Z_2 symmetry fixing (b_2, c_2) and exchanging the pairs (b_1, c_1) and (b_3, c_3).

2.1.1. BPS chambers

To start, recall that in BPS quiver theory with gauge symmetry group $\boldsymbol{G}$ having finite dimensional Lie algebra $\boldsymbol{g}$ of ADE type, one encounters a set of basic entities used in the building the BPS/anti-BPS states. Certain of these basic objects are given by the three following ingredients that play an important role in our construction; these are: (i) the primitive quiver Q_0^G, (ii) a sequence of descendent quivers Q_n^G with positive integer n obtained by applying successive quiver mutations; and (iii) the $\mathfrak{Q}_{weak}^G$ and $\mathfrak{Q}_{stg}^G$ sets of quivers underlying the weak and the strong chambers of BPS states.[1] The engineering of these two BPS chambers depends on the ordering of the arguments $\arg Z_i$ of the central charges $Z_i = Z(\gamma_i)$ of the elementary BPS particles γ_i of the quiver Q_0^G. For concreteness and also to fix some terminology used in this study, let us describe rapidly these three ingredients below.

(1) *Primitive quiver* Q_0^{ADE}

This is the quiver Q^G of the $\mathcal{N}=2$ supersymmetric gauge theory described in introduction section with gauge group G in the ADE sector of finite dimensional Lie algebras. Seen that we will encounter below various kinds of BPS quivers, we refer now on to this basic object as the *primitive* quiver and denote it like $Q_0^G \equiv Q^G$. For pure gauge models with a rank r gauge symmetry group $\boldsymbol{G}$, the primitive Q_0^G is made of the following components:

- $2r$ nodes υ_I; half of them occupied by the r *elementary monopoles* $\{b_1, b_2, .., b_r\}$ of the pure gauge theory; and the other half by the r *elementary dyons* $\{c_1, c_2, .., c_r\}$; they play a role quite similar to the role played by simple roots of Lie algebras.
- Oriented links $(\mathcal{A}_0)_{IJ}$ between neighbouring nodes υ_I and υ_J; their number is given by the Dirac pairing $\upsilon_I \circ \upsilon_J$ having integer values. As an illustration and also to fix ideas, see Fig. 1 describing the primitive quiver $Q_0^{su_4}$ of the $\mathcal{N}=2$ pure gauge model with SU(4) gauge symmetry. It will be used later on.
  Moreover, because of orientation of links, the Q_0^G has in general oriented cycles that play as well an important role in the study of the moduli space of the BPS theory. Examples of these cycles are exhibited in Fig. 1 of $Q_0^{su_4}$; explicit representations with bifundamental fields are reported in appendix sections 7 and 8; the simplest example is given by the quiver $Q_0^{su_3}$ of Fig. 17 of subsection 8.1. To each cycle of the quiver Q_0^G, it is associated a gauge invariant monomial in the chiral superpotential W_0^G of the underlying quiver gauge theory. For instance the $Q_0^{su_4}$ quiver of Fig. 1 has four cycles, each one of length 4; and the corresponding

[1] These BPS chambers are CPT invariant; they contain anti-BPS states as well.

superpotential $W_0^{su_4}$ is given by the sum of four quartic monomials constructed by using the prescription of [1]. Illustrating examples of cycles in Q_0^G and corresponding superpotentials W_0^G are given for the quivers of the Figs. 22, 23, 24 and 25 of subsection 8.3 of appendix III.

(2) *Descendent quivers* Q_n^G

Generic BPS states are given by bound states of the r elementary monopoles b_i and the r elementary dyons c_i; they may be also thought of as nodes of some quiver Q_n^G related to Q_0^G by certain transformation known as quiver mutation. These Q_n^G's are therefore new quivers that descend from the primitive Q_0^G; they are classified as Q_1^G, Q_2^G, ... depending on the length of the mutation of Q_0^G. These new quivers have the same number of nodes as Q_0^G; but occupied by new kinds of EM charged particles. So the Q_n^G quivers have in general different links, different cycles and different superpotentials W_n^G. Notice that for a given n-th descendent quiver Q_n^G, the corresponding $2r$ particles $b_i^{(n)}$, $c_i^{(n)}$ living at the $2r$ nodes can be constructed by applying the quiver mutation method of [1,2]. These particles are BPS bound states of the elementary b_i, c_i; and their properties are encoded in the ordering and the alignment of the complex central charges

$$X_i = Z(b_i) \qquad , \qquad Y_i = Z(c_i)\,. \tag{2.1}$$

Examples of descendent quivers will be explicitly constructed in the following sections; see for instance the Figs. 4, 5, 8, 9 and 10. Others are given in appendix sections; for example the graphs of Fig. 13 and Fig. 14 of appendix I.

(3) *Strong and weak chambers*

Given an ordering of the arguments of the $2r$ basic complex central charges X_i, Y_i, the primitive Q_0^G together with the Q_n^G descendants, obtained by performing successive mutations, constitute a set of quivers that we denote like

$$\mathfrak{Q}^G = \left\{ Q_n^G \right\}_{n\geq 0} \tag{2.2}$$

Depending on the ordering of $\arg X_i$ and $\arg Y_i$ in the upper half place of the complex central charge Z, the cardinality of $\mathfrak{Q}^G$ may be finite or infinite. For the case of $\mathcal{N}=2$ supersymmetric pure gauge theory we are interested in here, we distinguish two kinds of $\mathfrak{Q}^G$ sets according to the regime of the gauge coupling constant of the theory; these sets are: (i) the finite $\mathfrak{Q}^G_{stg}$ describing the so-called strong chamber of BPS/anti-BPS states (BPS chamber for short); and (ii) the infinite set $\mathfrak{Q}^G_{weak}$ giving the weak BPS chamber.

The building of these chambers is one of the main purposes of the BPS quiver theory. The general philosophy of the construction of BPS chambers is described in appendix I; examples of explicit construction of chambers and their relations with the central charges ordering are given in appendix III; in particular the Argyres–Douglas A_3 model with quiver given by Fig. 20 and chambers as in table (8.29).

2.1.2. Building BPS chambers

From the presentation given in above subsubsection (§ 2.1.1), in particular the point (3) regarding the sets $\mathfrak{Q}^G_{weak}$ and $\mathfrak{Q}^G_{stg}$, it follows that the Q_n^G quivers of a given chamber $\mathfrak{Q}^G$ of eq. (2.2) have all of them the same number of nodes ($2r$ nodes for pure gauge models); but occupied by different particles having the typical EM charges

$$\upsilon_{m,m'} = \sum m_i b_i + m'_i c_i \tag{2.3}$$

with some positive m_i, m_i' integers for BPS particles and negative ones for anti-BPS particles. The allowed values of the m_i, m_i' integers are, generally speaking, obtained by solving constraint relations coming from the supersymmetric quantum mechanics underlying the quiver Q_0^G [1,2]; for a brief description of two methods to construct the allowed bound states (2.3) see subsubsections 8.2.2 and 8.2.3 of appendix III; see also the two illustrating examples concerning the construction of BPS states in the Argyres–Douglas A_2 and A_3 theories by using quiver representation method of subsubsection 8.2.2. In present study, we will use the quiver mutation method of subsubsection 8.2.3 to derive directly the m_i, m_i' integers; this is achieved by an explicit construction of the mutation operators $\boldsymbol{M}_n$ allowing to build the descendent Q_n^G's from the primitive Q_0^G as follows

$$Q_n^G = \boldsymbol{M}_n \cdot Q_0^G \qquad , \qquad \boldsymbol{M}_0 = I_{id} \tag{2.4}$$

Therefore, the primitive quiver Q_0^G together with the mutation set $\{\boldsymbol{M}_n; n = 0, 1...\}$, encoding the ordering of arg X_i and arg Y_i, play an important role in BPS quiver theory; the knowledge of these objects is capital for building $\mathfrak{Q}^G$.

For a 4d $\mathcal{N} = 2$ pure gauge theory with a given rank r ADE symmetry with simple roots $\vec{a}_1, ..., \vec{a}_r$; the monopoles and dyons are represented by their electric–magnetic (EM) charges respectively given by the $2r$-component vectors

$$b_i = \begin{pmatrix} \vec{0} \\ \vec{a}_i \end{pmatrix} \qquad , \qquad c_i = \begin{pmatrix} \vec{a}_i \\ -\vec{a}_i \end{pmatrix} \tag{2.5}$$

The link between the nodes of the graph of Q_0^G is given by the EM product of these charges which is defined in terms of the Dirac pairing $b_i \circ c_j = -\vec{0}_i.\vec{a}_j - \vec{a}_i.\vec{a}_j$. By using the Cartan matrix $K_{ij} = \vec{a}_i.\vec{a}_j$ of the Lie algebra of the ADE gauge symmetries, the various pairings of the EM charge vectors of monopoles and dyons making Q_0^G read as follows

$$\begin{array}{lll} b_i \circ b_j = 0 & , & c_i \circ b_j = +K_{ij} \\ c_i \circ c_j = 0 & , & b_i \circ c_j = -K_{ij} \end{array} \tag{2.6}$$

With these b_i and c_i EM charges; one can define two interesting related objects that characterise the primitive BPS quiver [3]; these are the $4r^2$-component vector $\upsilon_0^T = (b, c)$, combining monopoles and dyons in a huge vector υ_0; and the corresponding intersection matrix $\mathcal{A}_0^G = \upsilon_0 \circ \upsilon_0^T$ defined by the Dirac pairing of the components of υ_0. In other words the primitive BPS quiver Q_0^G of the $\mathcal{N} = 2$ supersymmetric pure ADE gauge theories can be represented by the pair consisting of υ_0 and $\mathcal{A}_0^G$ that reads in terms of the Cartan matrix of the Lie algebra like

$$\mathcal{A}_0^G = \begin{pmatrix} 0 & -K \\ K & 0 \end{pmatrix} \otimes I_{2r} \tag{2.7}$$

where I_{2r} is the $2r \times 2r$ identity matrix. With this representation, one can generate the υ_n vectors and the corresponding $\mathcal{A}_n^G = \upsilon_n \circ \upsilon_n^T$ matrices describing the Q_n^G quivers by applying mutations on υ_0 and $\mathcal{A}_0^G$. These mutations are as well represented by some matrices $\boldsymbol{M}_n$ that allow to express $\mathcal{A}_n^G$ matrix in terms of the primitive one like $\boldsymbol{M}_n \mathcal{A}_0^G \boldsymbol{M}_n^T$; for explicit details see [3]; see also the generalisation of these mutations to non-simply laced symmetries given by our analysis of sections 4 and 5.

2.2. BPS quivers of BCFG type

The above construction done for 4d $\mathcal{N}=2$ models with ADE-type gauge symmetries can be extended to implement matter [1,2,5]; and, more interestingly for the present study, to supersymmetric models with pure BCFG-type gauge symmetries. Following [38], the BPS quiver description for ADE Lie algebras is also valid for BPS quivers for non-simply laced Lie algebras. For a given rank r non-simply laced type gauge symmetry, the primitive BPS quiver Q_0^G is also made of r elementary monopoles $\{\beta_1, \beta_2, .., \beta_r\}$ and r elementary dyons $\{\delta_1, \delta_2, .., \delta_r\}$; but with EM charges given by

$$\beta_i = \begin{pmatrix} 0 \\ \vec{\alpha}_i^{\,v} \end{pmatrix} \in \mathbb{Z}^{2r} \qquad , \qquad \delta_i = \begin{pmatrix} \vec{\alpha}_i \\ -\vec{\alpha}_i^{\,v} \end{pmatrix} \in \mathbb{Z}^{2r} \tag{2.8}$$

where now the r vectors $\vec{\alpha}_1, ..., \vec{\alpha}_r$ are the simple roots of the non-simply laced Lie algebra; and the $\vec{\alpha}_1^{\,v}, ..., \vec{\alpha}_r^{\,v}$ stand for the corresponding co-roots $\vec{\alpha}_i^{\,v} = \frac{2}{\vec{\alpha}_i.\vec{\alpha}_i}\vec{\alpha}_i$ which, generally speaking, are different from $\vec{\alpha}_i$. Because of the existence of two different lengths of simple roots in non-simply laced algebras, a property which is manifested in practice by the fact that Cartan matrix is no longer symmetric $K_{ji} \neq K_{ij}$, the intersection matrix $\mathcal{A}_0^G$ representing the primitive quiver is no longer equal to the one given by (2.7); this matrix reads as follows

$$\begin{array}{lll} \beta_i \circ \beta_j = 0 & , & \delta_i \circ \beta_j = K_{ij} \\ \delta_i \circ \delta_j = K_{ji} - K_{ij} & , & \beta_i \circ \delta_j = -K_{ji} \end{array} \tag{2.9}$$

it differs from (2.6) by the fact that now the pairing $\delta_i \circ \delta_j$ is different from zero. Therefore, the $\mathcal{A}_0^G$ intersection matrix describing the quiver Q_0^G in 4d $\mathcal{N}=2$ theories with non-simply laced type gauge symmetries has the following form [38]; see also [47,48]

$$\mathcal{A}_0^G = \begin{pmatrix} 0_{r\times r} & -K^T \\ K & K^T - K \end{pmatrix} \otimes I_{2r} \tag{2.10}$$

For the example of the symplectic $\mathrm{SP}(4,\mathbb{R})$ gauge symmetry, the Cartan matrix K and the anti-symmetric $K^T - K$ are given by

$$K = \begin{pmatrix} 2 & -1 \\ -2 & 2 \end{pmatrix} \qquad , \qquad K^T - K = \begin{pmatrix} 0 & -1 \\ 1 & 0 \end{pmatrix} \tag{2.11}$$

and then

$$\mathcal{A}_0^{SP_4} = \begin{pmatrix} 0 & 0 & -2 & 2 \\ 0 & 0 & 1 & -2 \\ 2 & -1 & 0 & -1 \\ -2 & 2 & 1 & 0 \end{pmatrix} \tag{2.12}$$

Because of the non-trivial value of the $\delta_i \circ \delta_j$ pairing, the topology of the graph of the primitive quiver Q_0^G of non-simply laced gauge symmetries is different from their ADE analogues since, in addition to vertical and horizontal links, we have moreover a diagonal link between the δ_r and δ_{r-1} nodes of the graph as shown in Fig. 2 for the illustrating example of 4d $\mathcal{N}=2$ pure $\mathrm{SP}(4,\mathbb{R})$ gauge theory. It turns out that this extra diagonal link makes the usual algorithm of quiver mutations on Q_0^G, with BCFG type gauge symmetry, difficult to apply compared to BPS quiver theory with ADE type algebras; this difficulty will be overcome by using the quiver folding method developed in present study; thanks to outer-automorphisms of BPS quivers of ADE type. But before going into details, let us end this general description on building BPS states by

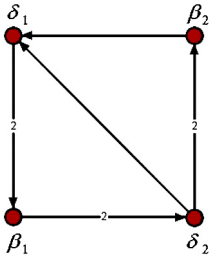

Fig. 2. Primitive BPS quiver $Q_0^{SP_4}$ of the 4d $\mathcal{N}=2$ pure gauge model with SP$(4, R)$ gauge invariance. The diagonal link is because of the pairing $c_i \circ c_j$ which is different from zero. In section 5, we show that this graph is precisely the one obtained by folding $Q_0^{SU_4}$ of Fig. 1 by its Z_2 outer-automorphism.

indicating that Q_n^G quivers of the $\mathcal{N}=2$ supersymmetric QFT with gauge symmetry G are in practice generated as follows:

a) *Strong and weak BPS chambers*
First choose the BPS chamber we are interested in; that is either the weak chamber $\mathfrak{Q}_{weak}^G$ or the strong $\mathfrak{Q}_{stg}^G$; this choice depends on the coupling regime of the gauge theory and is given by an ordering of the arguments of the central charges of the elementary BPS particles. In this study, we will focus on the strong chamber of $\mathcal{N}=2$ theories with pure gauge symmetries SO(8), SO(7), SU(4) and SP(4). This choice has been motivated by two things: (i) by the fact that $\mathfrak{Q}_{stg}^G$ is a priori a finite chamber; and so is a good example to testing the validity of our folding quiver proposal based on extending the folding trick of Dynkin diagrams to BPS quivers. (ii) Because of constraints coming from the lack of complete results on $\mathfrak{Q}_{weak}^G$ of ADE type; the exact content of the weak chambers $\mathfrak{Q}_{weak}^G$ of gauge symmetries with rank $r \geq 2$ is not known; only partial results have been obtained in this matter [3,1,2,4,38].

b) *Gauge invariance and mutation subset* H_{stg}^G
Second distinguish what type of gauge symmetry group G one is considering; that is whether G having a simply laced DD, or a non-simply laced Dynkin diagrams. For the ADE type gauge symmetries, the application of the $\boldsymbol{M}_n$ mutations on the primitive quiver Q_0^{ADE} is straightforward and leads to the usual BPS quivers Q_n^{ADE} [3]. There, it was shown that the number of BPS states of the strong chambers $\mathfrak{Q}_{stg}^{ADE}$ is equal to $2(\dim G - rank G)$; this number can be derived by performing quiver mutations $\boldsymbol{M}_n$ on Q_0^{ADE}; it happens that a particular finite subset H_{stg}^{ADE} of quiver mutation set $(H_{stg}^{ADE} \subset \{\boldsymbol{M}_n\})$ allows to build the BPS states of $\mathfrak{Q}_{stg}^{ADE}$; this subset has a group structure and is generated by the two composite operators L_1 and L_2 given by

$$L_1 = \prod_{i=1}^{r} t_{r+1-i} \qquad , \qquad L_2 = \prod_{i=1}^{r} t_{2r+1-i} \tag{2.13}$$

where the $2r$ reflections $t_1, ..., t_{2r}$ are the fundamental mutations of the Coxeter group $\mathcal{G}_{stg}^{(ADE)_r}$ introduced in appendix I; these two L_1 and L_2 generators satisfy the property $(L_1)^2 = (L_2)^2 = I_{id}$ exactly like for $(t_i)^2 = I_{id}$; and their compositions $(L_2 L_1)^m$ and $L_1 (L_2 L_1)^m$ play an important role in building the BPS states out of the elementary ones. It turns out that the subgroup $H_{stg}^{ADE} \subset \mathcal{G}_{stg}^{ADE}$ is isomorphic to the dihedral group Dih_{n_0}; for rank r ADE Lie algebras, we have the relationship

$$H_{stg}^{(ADE)_r} \simeq Dih_{4(r-1)} \tag{2.14}$$

Notice that the H_{stg}^{G} can interpreted as describing a particular configuration of the X_i of the monopoles and the Y_i of dyons. This configuration is given by the alignment of the r central charges X_i and the same thing for the r central charges Y_i; see (3.6) to fix ideas. In the case of $\mathcal{N}=2$ theories with non-simply laced BCFG gauge symmetries, the construction of Q_n^{BCFG} quivers of BPS chamber $\mathfrak{Q}_{stg}^{BCFG}$ needs an extra algorithm; since a naive application of quiver mutations leads to infinite $\mathfrak{Q}_{stg}^{BCFG}$ with exotic BPS states. To overcome this difficulty, we take advantage of outer-automorphisms of BPS quivers Q_n^{ADE} to build the corresponding Q_n^{BCFG} ones by extending the folding method of Dynkin diagrams of ADE Lie algebras. This BPS quiver folding approach is developed in sections 4 and 5 of this paper.

The mutations of BPS quivers of BCFG type and the quiver folding method need a careful analysis; we have judged interesting to illustrate the construction on particular models. This is done in section 4 for the particular $\mathcal{N}=2$ model with SO$(7,\mathbb{R})$ gauge symmetry; and in section 5 for the $\mathcal{N}=2$ theory with SP$(4,\mathbb{R})$ gauge symmetry. But before that, it is interesting to describe extra helpful tools on BPS quiver theory with SO$(8,\mathbb{R})$ and SU(4) gauge symmetry groups; this is because the DD of the Lie algebra SO$(7,\mathbb{R})$ follows from the DD of SO$(8,\mathbb{R})$ by folding two nodes as shown in Fig. 6. The same link exists between SP$(4,\mathbb{R})$ and SU(4) as shown in Fig. 11.

3. BPS strong chamber of $\mathcal{N}=2$ $SO(8,\mathbb{R})$ theory

In this section we review the main lines of the derivation of the $(24+24)$ BPS/anti-BPS states of the strong chamber $\mathfrak{Q}_{stg}^{D_4}$ of 4d $\mathcal{N}=2$ supersymmetric pure SO$(8,\mathbb{R})$ gauge theory [2,3]. We also describe a remarkable subgroup $H_{stg}^{SO_8} \simeq Dih_{12}$ of the quiver mutation set $\mathcal{G}_{stg}^{SO_8}$ operating in $\mathfrak{Q}_{stg}^{D_4}$. The $\mathcal{G}_{stg}^{SO_8}$ is given by the Coxeter group of quiver mutations generated by eight fundamental reflections; it is succinctly described in appendix I; but for further explicit details see also the appendix of [3].

To begin, it is interesting to notice that the numbers N_{bps}^{ADE} of BPS and $N_{anti\text{-}bps}^{ADE}$ of anti-BPS states in 4d $\mathcal{N}=2$ pure gauge theories with ADE type gauge symmetry G are known; they are given by the formula

$$N_{bps}^{G} + N_{anti\text{-}bps}^{G} = 2\,(\dim G - rank G) \tag{3.1}$$

For $G=SO(8,\mathbb{R})$, we then have $N_{bps}^{SO_8} + N_{anti\text{-}bps}^{SO_8} = 48$ which is equal to $4\times|Dih_{12}|$; but this number can be also factorised like 6×8 which turns out to be the type of factorisation that appears in the cousin $\mathcal{N}=2$ pure SO$(7,\mathbb{R})$ gauge model. There, we find that the number of BPS and anti-BPS states obtained, after applying the folding method to the SO$(8,\mathbb{R})$ quivers, is equal to $N_{bps}^{SO_7} + N_{anti\text{-}bps}^{SO_7} = 6\times 7$; see section 4 for the derivation of this number.

The tools given below are therefore to fix ideas and notations; and also for later use when we study the BPS states of the $\mathcal{N}=2$ supersymmetric SO$(7,\mathbb{R})$ gauge theory which hasn't been considered previously. This study is also important for motivating the quiver folding method and also for comparison of the BPS states content of the $\mathfrak{Q}_{stg}^{D_4}$ and $\mathfrak{Q}_{stg}^{B_3}$ chambers of the SO$(8,\mathbb{R})$ and SO$(7,\mathbb{R})$ twin models.

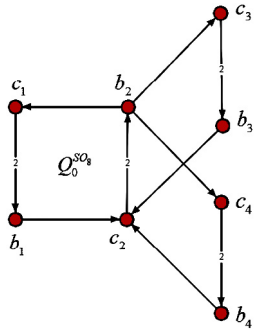

Fig. 3. The primitive quiver $Q_0^{SO_8}$ having 8 nodes describing the 4 monopoles and the 4 dyons. The links are given by the intersection matrix $\mathcal{A}_0$. The quiver $Q_0^{SO_8}$ has two outer-automorphism symmetries: (i) Z_2 exchanging (b_3, c_3) and (b_4, c_4); but fixing the others; and (ii) a Z_3 cycle fixing the central (b_2, c_2) and permuting the three external others.

3.1. Primitive quiver $Q_0^{SO_8}$

The primitive quiver $Q_0^{SO_8}$ is a basic object in the derivation of BPS states of the strongly coupled chamber $\mathfrak{Q}_{stg}^{D_4}$ of the 4d $\mathcal{N} = 2$ pure SO(8) theory; a nice method to get these BPS states is to start with $Q_0^{SO_8}$; and act on it by a particular quiver mutation subgroup $H_{stg}^{SO_8}$ of the group $\mathcal{G}_{stg}^{SO_8}$ generated by 8 fundamental reflections r_1, r_2, r_3, r_4, s_1, s_2, s_3, s_4 whose matrix representations are reported in appendix I.

Let us describe below the key steps of this construction for the case of 4d $\mathcal{N} = 2$ supersymmetric pure $SO(8)$ gauge model. There, the $Q_0^{SO_8}$ quiver is made of the 4 elementary monopoles $\{b_1, b_2, b_3, b_4\}$ and the 4 elementary dyons $\{c_1, c_2, c_3, c_4\}$ as shown by Fig. 3. The electric–magnetic (EM) charges of the b_i monopoles and c_i dyons are expressed in terms of the four $\vec{a}_1$, $\vec{a}_2, \vec{a}_3, \vec{a}_4$ simple roots of the D_4 Lie algebra as well as the corresponding four co-roots $\vec{a}_i^{\,v} = \frac{2}{\vec{a}_i^2}\vec{a}_i$ which coincide with $\vec{a}_i$; these EM vector charges are as follows

$$b_i = \begin{pmatrix} \vec{0} \\ \vec{a}_i \end{pmatrix} \qquad , \qquad c_i = \begin{pmatrix} \vec{a}_i \\ -\vec{a}_i \end{pmatrix} \tag{3.2}$$

Since the $\vec{a}_i$ roots of D_4 are 4-dim vectors, the above EM charges are 8-dim integral vectors; but here they are thought of in terms of eight nodes of the primitive BPS quiver $Q_0^{SO_8}$ which encodes all data on eq. (3.2). So the $Q_0^{SO_8}$ describes the BPS set $\{b_i, c_i\}$ which can be roughly imagined in terms of a 64-component symplectic vector like

$$\upsilon_0^T = (b_1, b_2, b_3, b_4; c_1, c_2, c_3, c_4) \tag{3.3}$$

The links between the eight b_i, c_i nodes are given by Dirac pairing eq. (2.9) between the EM charge vectors of monopoles and dyons. In this view and like the Dynkin diagram, the primitive quiver $Q_0^{SO_8}$ may be represented by an intersection matrix $\mathcal{A}_0^{SO_8} = \upsilon_0 \circ \upsilon_0^T$ like

$$\mathcal{A}_0^{SO_8} = \begin{pmatrix} b_i \circ b_j & b_i \circ c_j \\ c_i \circ b_j & c_i \circ c_j \end{pmatrix} = \begin{pmatrix} 0 & -K \\ K & 0 \end{pmatrix} \otimes I_8 \tag{3.4}$$

with Dirac pairings $b_i \circ b_j = c_i \circ c_j = 0$ and $c_i \circ b_j = -b_i \circ c_j = K_{ij} \otimes I_8$ where I_8 is the 8×8 identity matrix and where K_{ij} is the usual Cartan matrix $\vec{a}_i.\vec{a}_j$ of the so(8) Lie algebra given by

$$K_{D_4} = \begin{pmatrix} 2 & -1 & 0 & 0 \\ -1 & 2 & -1 & -1 \\ 0 & -1 & 2 & 0 \\ 0 & -1 & 0 & 2 \end{pmatrix} \tag{3.5}$$

3.2. Quiver mutations and BPS states

To obtain the BPS/anti-BPS states of the strong coupled chamber of the 4d $\mathcal{N} = 2$ SO$(8, \mathbb{R})$ gauge theory, we follow the approach of [3] by first taking the argument of the complex central charges X_i and Y_i of the 4 monopoles and the 4 dyons as

$$\begin{aligned} &\arg X_1 = \arg X_2 = \arg X_3 = \arg X_4 \\ &\arg Y_1 = \arg Y_2 = \arg Y_3 = \arg Y_4 \\ &\arg Y_i > \arg X_i \end{aligned} \tag{3.6}$$

then applying the quiver mutation method of [1–3,5]. This central charge configuration allows to get the full content of the strong chamber $\mathfrak{Q}_{stg}^{D_4}$ which is known to have 24 BPS states and 24 anti-BPS states. The first set of equalities in (3.6) describes the alignment of the central charge rays associated with the elementary monopoles and the second set of equalities describes the alignment of the central charge rays of dyons; for a physical interpretation of these alignments see the description of § 3.2.1 given below. The inequalities give the ordering of the argument of the elementary BPS states and fix the BPS chamber. Notice that in the strong chamber we are considering, the central charge rays (Y_i) associated with elementary dyons are left-most in the half upper-plane of the complex central charge Z while the rays X_i of elementary monopoles are right-most. In the case of weak chamber, the configuration gets reversed; the Y_i rays are right-most and the X_i's are left-most ones. The terminology left-most and right-most has been used in the basic works [1,2]; it is helpful in the study of ordering the arguments of the central charges of bound states and in the construction of BPS chambers; for instance if $\arg Y > \arg X$, then we have the following property

$$\arg Y > n \arg Y + m \arg X > \arg X \tag{3.7}$$

for any positive definite integers n and m. As the ordering and alignment of the central charge rays in upper half complex plane are important ingredients in using quiver mutation method for the construction of BPS chambers, let us describe briefly known results for this matter by describing the key idea on the SU(N) gauge symmetry. To make the presentation more illustrative, we also give the explicit relations for the leading SU(2) and SU(3) gauge groups; and take the opportunity to give as well some useful comments.

3.2.1. Ordering of central charges

We begin by recalling results on BPS/anti-BPS states of $\mathcal{N} = 2$ QFT with pure SU(2) gauge symmetry as constructed by using the quiver mutation method. In this theory, the BPS states are given by bounds of a monopole $\mathfrak{M}$ and a dyon $\mathfrak{D}$; the monopole has an electric–magnetic charge b, and the dyon has a charge c. The BPS and anti-BPS states in the $\mathfrak{Q}_{weak}^{su_2}$ and $\mathfrak{Q}_{stg}^{su_2}$ chambers of pure SU(2) gauge theory are completely known; and are re-derived in a nice manner by using the language of complex central charge $Z(b) \equiv X$ of monopole and the central charge $Z(c) \equiv Y$ of the dyon. In this method, these two chambers correspond to the two possible ways of ordering the arguments of X and Y in the central charge complex plane Z. For the case $\arg X > \arg Y$, we have the infinite weak chamber $\mathfrak{Q}_{weak}^{su_2}$; the list of BPS states contained in this chamber

is given by eq. (8.1) reported in appendix III; see also the explicit construction of [5]. This BPS spectrum is exactly derived by using quiver mutation method considered in this study. For the other case $\arg Y > \arg X$, we have the strong coupling chamber $\mathfrak{Q}^{su_2}_{stg}$; it consists of the elementary BPS particles $\mathfrak{M}$ and $\mathfrak{D}$ with EM charge b and c and their anti-particles $\bar{\mathfrak{M}}$ and $\bar{\mathfrak{D}}$ with opposite charges.

For $\mathcal{N}=2$ supersymmetric QFTs with rank r ADE gauge group, the construction of the BPS chambers extends the one done for the SU (2) gauge theory; but it is somehow subtle due extra arbitrariness. While the lattice Γ_{ADE} of the EM charges γ of the BPS states has rank $2r$, the moduli space of the supersymmetry pure gauge theory has only $r+1$ physical parameters that can be varied. These physical moduli are given by r moduli $u_1, ..., u_r$, parameterising the Coulomb branch, and the gauge coupling constant. By thinking of the lattice Γ_{ADE} in terms of its $2r$ generators denoted like $\gamma_i^{\pm}$, and using the homomorphism

$$\begin{array}{rcl} Z : \Gamma_{ADE} & \to & \mathbb{C} \\ \gamma_i^{\pm} & \to & Z\left(\gamma_i^{\pm}\right) \end{array} \tag{3.8}$$

one ends with $2r$ complex central charges $Z\left(\gamma_i^{\pm}\right)$ for the elementary BPS states teaching us that an arbitrary configuration of the $2r$ central charges (X_i, Y_i) for the nodes (b_i, c_i) of the quiver Q^{ADE} cannot be chosen arbitrarily. To apply the mutation method we need to find a basis which has central charges lying in a upper half plane with a certain choice of the ordering of the arguments of X_i and Y_i of the elementary monopoles and dyons. This question has been explicitly addressed in [1] by using results on generalised $\mathcal{N}=2$ supersymmetric Seiberg–Witten (SW) gauge theory. There, the nodes (b_i, c_i) of the BPS quiver have been identified with basic cycles $\gamma_i^{\pm}$ in SW geometry. To fix ideas let us focus on $\mathcal{N}=2$ supersymmetry SW theory with pure $SU(N)$ gauge symmetry; the Coulomb branch of this theory has $N-1$ parameters $u = (u_2, ..., u_N)$ given by the Casimirs of $SU(N)$ determining the VEVs of the Cartan elements. These parameters appear as coefficients in the defining equation of the SW complex curve

$$y^2 = P^2_{su_N} - \Lambda^{2N} \qquad , \qquad P_{su_N} = x^N - \sum_{k=2}^{N} u_k x^{N-k} \tag{3.9}$$

where Λ stands for the strong coupling scale. This equation has $2N$ complex roots $x_k^{\pm}$ which are functions of the Coulomb branch parameters $x_k^{\pm}(u, \Lambda)$ and which we denote like $e_i^{\pm}$ for convenience; these roots are used in the building symplectic homology cycles γ in the SW geometry that are interpreted in terms of EM charges of the BPS states. On the other hand, by using the $SP(2N-2, \mathbb{Z})$ duality of SW gauge theory one may select a symplectic homology basis of cycles like $\gamma_i^{\pm} = e_i^{\pm} - e_{i+1}^{\mp}$ and which can be precisely identified with the b_i, c_i electric–magnetic charges of the $2(N-1)$ nodes the BPS quiver $Q_0^{su_N}$. In this SW formulation, BPS particles are represented by vanishing cycles γ on the SW curve and their central charges $Z_u(\gamma)$ are given by the periods

$$Z_u(\gamma) = \int_{\gamma} \lambda(u) \tag{3.10}$$

with 1-form $\lambda(u)$ given by the expression $\frac{x}{2\pi i y} P'_{su_N} dx$. By specifying the analysis to the $SU(3)$ particular gauge symmetry, one can explicitly study the properties of the chambers of BPS states including the passage from of the weak chamber towards the strong one. In this simple example, the SW curve reduces to $y^2 = \left(x^3 - ux - v\right)^2 - \Lambda^6$ with u and v standing for the two Coulomb

branch moduli. The weak coupling chamber $\mathfrak{Q}^{su_3}_{weak}$ corresponds to taking the limit $u \to -\infty$ with $v = \mathrm{Im}\, u = 0$, and the strong chamber $\mathfrak{Q}^{su_3}_{stg}$ to the limit $u \to 0$. The complex curve $y^2 = P^2_{su_3} - \Lambda^6$ has six complex roots $e^{\pm}_1$, $e^{\pm}_2$, $e^{\pm}_3$, and the $SP\,(4, \mathbb{Z})$ homology cycle is generated by the symplectic basis

$$\gamma^-_i \sim e^-_i - e^+_{i+1} \qquad , \qquad \gamma^+_i \sim e^+_i - e^-_{i+1} \tag{3.11}$$

with index $i = 1, 2$. These dual $2 + 2$ symplectic cycles are in one to one with the EM charges (b_1, b_2) of the elementary monopoles and the EM charges (c_1, c_2) of the elementary dyons. They correspond also to the nodes of the BPS quiver $\mathcal{Q}^{su_3}_0$ of the supersymmetric pure SU (3) gauge theory. We have

$$b_i \quad \leftrightarrow \quad \gamma^-_i \qquad , \qquad c_i \quad \leftrightarrow \quad \gamma^+_i \tag{3.12}$$

In the limit of zero coupling constant, the central charges X_i of the monopoles b_i approach the π-separation between BPS and anti-BPS states in the Z complex plane, $\arg X_i \to \pi$. However, the central charges Y_i of the dyons c_i have arguments that tend towards zero, $\arg Y_i \to 0$. In this weak gauge coupling limit, we have the alignments

$$\arg X_i \equiv \arg X \to \pi \qquad , \qquad \arg Y_i \equiv \arg Y \to 0 \tag{3.13}$$

and then the ordering property $\arg X > \arg Y$. As we tune the Coulomb branch parameters from the weak chamber $u = -\infty$ towards the strong chamber $u = 0$, the arguments of the central charges of the monopoles $\{b_1, b_2\}$ and the dyons $\{c_1, c_2\}$ approach increasingly and cross each other at strong coupling limit leading to the reverse ordering

$$\arg Y_i > \arg X_i \qquad , \qquad \arg Y > \arg X \tag{3.14}$$

Notice that at the limit $u = 0$, both the $SU\,(2)$ proper sub-symmetries of $SU\,(3)$ gauge group are strongly coupled in same manner as in the supersymmetric $SU\,(2)$ pure gauge theory introduced in the beginning of this paragraph. Notice also that at the origin $u = v = 0$ of the Coulomb branch of the SU (3) theory, the term $P^2_{su_3} = \left(x^3 - ux - v\right)^2$ in the SW curve reduced to the monomial x^6 and so the roots x_k solving the SW equation in the x-plane are given by the six complex numbers $e^{\frac{2ik\pi}{6}}\Lambda$ showing that the six BPS states in the chamber $\mathfrak{Q}^{su_3}_{stg}$ have as $\mathbb{Z}_6$ symmetry property. The construction of the BPS chambers for the supersymmetric pure SU (N) gauge theory extends straightforwardly for $\mathcal{N} = 2$ supersymmetric pure D_r and E_r gauge theories.

After this digression, we now turn back to our main purpose namely the building of BPS/anti-BPS states of the strong chamber $\mathfrak{Q}^{D_4}_{stg}$.

3.2.2. Cyclic chain of BPS quivers

We start from the primitive $\mathcal{Q}^{SO_8}_0$, represented by the intersection matrix $\mathcal{A}^{SO_8}_0$ given by (3.4); then successive quiver mutations of $\mathcal{Q}^{SO_8}_0$ allow to generate new quivers; say the quiver $\mathcal{Q}^{SO_8}_1$ after first mutation $\boldsymbol{M}_1$, then the quiver $\mathcal{Q}^{SO_8}_2$ after two mutations $\boldsymbol{M}'_1\boldsymbol{M}_1 = \boldsymbol{M}_2$ and so on. Because of the fact that the BPS strong chamber $\mathfrak{Q}^{D_4}_{stg}$ is finite, there should exist an integer n_0 such that $\boldsymbol{M}_{n_0} = I_{id}$; which means that $\mathcal{Q}^{SO_8}_{n_0}$ is precisely the starting $\mathcal{Q}^{SO_8}_0$; the integer n_0 corresponds to a cycle in the mutation set $H^{SO_8}_{stg}$ and turns out to be equal to 12 in present case. The closed chain of quivers

$$\mathcal{Q}^{SO_8}_0 \to \mathcal{Q}^{SO_8}_1 \to \mathcal{Q}^{SO_8}_2 \to ... \to \mathcal{Q}^{SO_8}_{11} \to \mathcal{Q}^{SO_8}_0 \tag{3.15}$$

can be made more explicit by working with $\mathcal{A}_n^{SO_8}$ intersection matrices representing the $Q_n^{SO_8}$ quivers. Indeed, the intersection matrix $\mathcal{A}_1^{SO_8}$, associated with the $Q_1^{SO_8}$ quiver, is obtained by performing a transformation[2] type $\mathcal{A}_1^{SO_8} = \boldsymbol{M}_1 \mathcal{A}_0^{SO_8} \boldsymbol{M}_1^T$ with mutation matrix as follows

$$\boldsymbol{M}_1 = \begin{pmatrix} 1 & 0 & 0 & 0 & 0 & 1 & 0 & 0 \\ 0 & 1 & 0 & 0 & 1 & 0 & 1 & 1 \\ 0 & 0 & 1 & 0 & 0 & 1 & 0 & 0 \\ 0 & 0 & 0 & 1 & 0 & 1 & 0 & 0 \\ 0 & 0 & 0 & 0 & -1 & 0 & 0 & 0 \\ 0 & 0 & 0 & 0 & 0 & -1 & 0 & 0 \\ 0 & 0 & 0 & 0 & 0 & 0 & -1 & 0 \\ 0 & 0 & 0 & 0 & 0 & 0 & 0 & -1 \end{pmatrix} \tag{3.16}$$

This mutation $\boldsymbol{M}_1$ plays an important role in this construction; for convenience we refer to it as L_1; it will be interpreted as one of the two mutation generators of $H_{stg}^{SO_8}$. To make a precise idea on this particular mutation subset $H_{stg}^{SO_8}$ which has a group structure, let us first derive the expression of the second generator L_2 and turn to give a comment.

The $\mathcal{A}_2^{SO_8}$ matrix, associated with the $Q_2^{SO_8}$ quiver, is obtained in an analogous manner to $\mathcal{A}_1^{SO_8}$; but now by operating L_2 on $\mathcal{A}_1^{SO_8}$; that is by performing a transformation type $\mathcal{A}_2^{SO_8} = L_2 \mathcal{A}_1^{SO_8} L_2^T$ where L_2 is the second generator of $H_{stg}^{SO_8}$; it is given by eq. (3.17).

$$L_2 = \begin{pmatrix} -1 & 0 & 0 & 0 & 0 & 0 & 0 & 0 \\ 0 & -1 & 0 & 0 & 0 & 0 & 0 & 0 \\ 0 & 0 & -1 & 0 & 0 & 0 & 0 & 0 \\ 0 & 0 & 0 & -1 & 0 & 0 & 0 & 0 \\ 0 & 1 & 0 & 0 & 1 & 0 & 0 & 0 \\ 1 & 0 & 1 & 1 & 0 & 1 & 0 & 0 \\ 0 & 1 & 0 & 0 & 0 & 0 & 1 & 0 \\ 0 & 1 & 0 & 0 & 0 & 0 & 0 & 1 \end{pmatrix} \tag{3.17}$$

By substituting $\mathcal{A}_1^{SO_8} = L_1 \mathcal{A}_0^{SO_8} L_1^T$, we obtain the direct relation of $\mathcal{A}_2^{SO_8}$ with the primitive quiver namely $\mathcal{A}_2 = \boldsymbol{M}_2 \mathcal{A}_0 \boldsymbol{M}_2^T$ with $\boldsymbol{M}_2 = L_2 L_1$. By repeating the mutation n times, we obtain the 48 BPS states of the strong chamber of the $\mathcal{N} = 2$ pure SO(8) gauge theory. The $\mathcal{A}_n^{SO_8}$ intersection matrix of the n-th $Q_n^{SO_8}$ quivers is given by

$$\mathcal{A}_n^{SO_8} = \boldsymbol{M}_n \mathcal{A}_0^{SO_8} \boldsymbol{M}_n^T \tag{3.18}$$

with

$$\boldsymbol{M}_{2k} = (L_2 L_1)^k \qquad , \qquad \boldsymbol{M}_{2k+1} = L_1 \boldsymbol{M}_{2k} \tag{3.19}$$

3.2.3. Mutation group $H_{stg}^{SO_8}$ and $\mathfrak{Q}_{stg}^{D_4}$

First notice that the two above L_1 and L_2 matrices generating $H_{stg}^{SO_8}$ are in fact composite operators of four successive fundamental reflections of $\mathcal{G}_{stg}^{SO_8}$ generated by 8 fundamental reflec-

[2] This transformation follows from the transformation of (3.3), the EM charge vector of BPS states of the quiver $Q_0^{SO(8)}$; and the expression of the intersection matrix $\mathcal{A}_0^{SO(8)} = \upsilon_0 \circ \upsilon_0^T$.

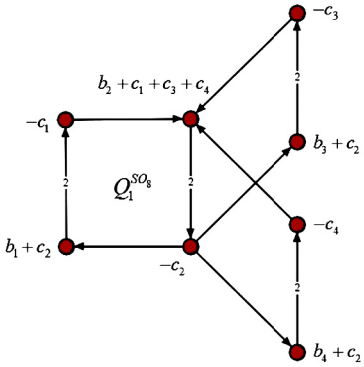

Fig. 4. The quiver $Q_1^{SO_8}$ having 8 nodes describing 8 new BPS states. Like $Q_0^{SO(8)}$, the quiver $Q_1^{SO(8)}$ has also the same two outer-automorphism symmetries: (*i*) a Z_2 symmetry exchanging 3rd and 4-th nodes; but fixing the others; and (*ii*) a Z_3 automorphism fixing the central node; but permuting the three external others.

tions denoted as r_1, r_2, r_3, r_4 and s_1, s_2, s_3, s_4; see also eq. (2.13). The use of composites L_1 and L_2 corresponds to performing four simultaneous reflections as follows

$$L_1 = r_4 r_3 r_2 r_1 \quad , \quad L_2 = s_4 s_3 s_2 s_1 \tag{3.20}$$

The explicit expressions of the fundamental reflections and examples of induced quivers are reported in appendix I. The second feature is that the $\boldsymbol{M}_n$ mutation matrices involved in (3.19) obey the following cyclic relations,

$$\begin{array}{llll} \boldsymbol{M}_{12} & = I_{id} & , & \boldsymbol{M}_6 = -I_{id} \\ \boldsymbol{M}_{n+12} & = \boldsymbol{M}_n & , & \boldsymbol{M}_{n+6} = -\boldsymbol{M}_n \end{array} \tag{3.21}$$

To get the BPS states of the strong chamber, it is enough to compute the expressions of the mutation matrices (3.19); the rows of these matrices give the EM charges of the BPS states of the $\mathfrak{Q}_{stg}^{D_4}$ strong chamber. Let us show how this works in practice by computing the leading $\boldsymbol{M}_n$'s; for $n = 1$ we have $\boldsymbol{M}_1 = L_1$; acting by this matrix on the vector υ_0 with BPS states as in (3.3), we obtain a new vector $\upsilon_1 = \boldsymbol{M}_1 \upsilon_0$ with BPS states as follows

$$\begin{pmatrix} 1 & 0 & 0 & 0 & 0 & 1 & 0 & 0 \\ 0 & 1 & 0 & 0 & 1 & 0 & 1 & 1 \\ 0 & 0 & 1 & 0 & 0 & 1 & 0 & 0 \\ 0 & 0 & 0 & 1 & 0 & 1 & 0 & 0 \\ 0 & 0 & 0 & 0 & -1 & 0 & 0 & 0 \\ 0 & 0 & 0 & 0 & 0 & -1 & 0 & 0 \\ 0 & 0 & 0 & 0 & 0 & 0 & -1 & 0 \\ 0 & 0 & 0 & 0 & 0 & 0 & 0 & -1 \end{pmatrix} \begin{pmatrix} b_1 \\ b_2 \\ b_3 \\ b_4 \\ c_1 \\ c_2 \\ c_3 \\ c_4 \end{pmatrix} = \begin{pmatrix} b_1 + c_2 \\ b_2 + c_1 + c_3 + c_4 \\ b_3 + c_2 \\ b_4 + c_2 \\ -c_1 \\ -c_2 \\ -c_3 \\ -c_4 \end{pmatrix} \tag{3.22}$$

The BPS states obtained by mutation can be then read directly on the rows of the $\boldsymbol{M}_1$ mutation matrix; we have

$$\begin{array}{llll} -c_1, & -c_2, & b_1 + c_2, & b_4 + c_2 \\ -c_3, & -c_4, & b_3 + c_2, & b_2 + c_1 + c_3 + c_4 \end{array} \tag{3.23}$$

The corresponding BPS quiver is given by Fig. 4. Observe that the $\boldsymbol{M}_1$ mutation has generated new eight BPS states; two for each reflection of (3.20). By computing the $\boldsymbol{M}_2 = L_2 L_1$ mutation matrix, we have

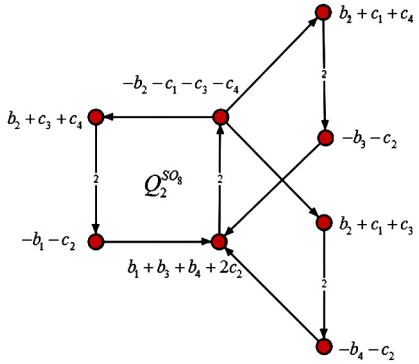

Fig. 5. The quiver $Q_2^{SO_8}$ having 8 nodes describing 8 new BPS states. Like $Q_0^{SO(8)}$ and $Q_1^{SO_8}$, the quiver $Q_2^{SO(8)}$ has also the same two outer-automorphism symmetries.

$$\boldsymbol{M}_2 = \begin{pmatrix} -1 & 0 & 0 & 0 & 0 & -1 & 0 & 0 \\ 0 & -1 & 0 & 0 & -1 & 0 & -1 & -1 \\ 0 & 0 & -1 & 0 & 0 & -1 & 0 & 0 \\ 0 & 0 & 0 & -1 & 0 & -1 & 0 & 0 \\ 0 & 1 & 0 & 0 & 0 & 0 & 1 & 1 \\ 1 & 0 & 1 & 1 & 0 & 2 & 0 & 0 \\ 0 & 1 & 0 & 0 & 1 & 0 & 0 & 1 \\ 0 & 1 & 0 & 0 & 1 & 0 & 1 & 0 \end{pmatrix} \tag{3.24}$$

leading to the following set BPS and anti-BPS states

$$\begin{array}{lll} -b_1-c_2 & , \quad b_2+c_3+c_4 & , \quad -b_2-c_1-c_3-c_4 \\ -b_3-c_2 & , \quad b_2+c_1+c_4 & , \quad b_1+b_3+b_4+2c_2 \\ -b_4-c_2 & , \quad b_2+c_1+c_3 & \end{array} \tag{3.25}$$

They are located at the eight nodes of the BPS quiver $Q_2^{SO_8}$ of Fig. 5. Doing the same thing for the mutation matrices $\boldsymbol{M}_3 = L_1\boldsymbol{M}_2$ and $\boldsymbol{M}_4 = (\boldsymbol{M}_2)^2$ as well as for $\boldsymbol{M}_5 = L_1\boldsymbol{M}_4$; we obtain the remaining BPS states of the strong chamber; the other quivers do not bring anything new because of the properties (3.21). Therefore the BPS states of the strong coupling chamber of $SO(8)$ are given by the following set having $8\times 6 = 48$ BPS states with EM charges

$$\begin{array}{lll} \pm b_1 & \pm(b_1+c_2) & \pm(b_1+b_4+c_2) \\ \pm b_2 & \pm(b_3+c_2) & \pm(b_1+b_3+c_2) \\ \pm b_3 & \pm(b_4+c_2) & \pm(b_2+c_3+c_4) \\ \pm b_4 & \pm(b_2+c_1) & \pm(b_3+b_4+c_2) \\ \pm c_1 & \pm(b_2+c_3) & \pm(b_1+b_3+b_4+c_2) \\ \pm c_2 & \pm(b_2+c_4) & \pm(b_1+b_3+b_4+2c_2) \\ \pm c_3 & \pm(b_2+c_1+c_4) & \pm(2b_2+c_1+c_3+c_4) \\ \pm c_4 & \pm(b_2+c_1+c_3) & \pm(b_2+c_1+c_3+c_4) \end{array} \tag{3.26}$$

In the basis vectors (3.2), these BPS states are read directly from the row of the following set of matrices

$$H_{stg}^{SO_8} = \left\{ \pm I_{id},\ \pm\boldsymbol{M}_1,\ \pm\boldsymbol{M}_2,\ \pm\boldsymbol{M}_3,\ \pm\boldsymbol{M}_4,\ \pm\boldsymbol{M}_5 \right\} \tag{3.27}$$

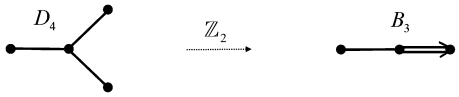

Fig. 6. Z_2 folding simply laced Dynkin diagram of SO (8) down to non-simply laced Dynkin diagram of SO (7).

This $H^{SO_8}_{stg}$ set forms a finite discrete subgroup of the Coxeter group $\mathcal{G}^{SO_8}_{stg}$; the cardinality of this subgroup is equal to 12; a careful inspection of this finite discrete symmetry shows that is isomorphic to the dihedral Dih_{12} group realised by 8×8 matrices type (3.24) with two generators L_1 and L_2 given by the particular mutations $L_1 = \boldsymbol{M}_1$ and $L_2 = -\boldsymbol{M}_5$ in the closed chain (3.15).

4. BPS spectra of strong chamber of SO (7)

In this section, we study the BPS states of the strong chamber of the $\mathcal{N} = 2$ QFT$_4$ with SO (7) gauge symmetry. Our method is based on extending the usual Dynkin diagram folding $D_4 \to B_3$ of Fig. 6 to the corresponding BPS quivers of $\mathcal{N} = 2$ gauge theories. For the case of pure gauge models we are considering here, the quiver folding $\boldsymbol{F}^{bps}_{D_4\to B_3}$ map the $\mathfrak{Q}^{D_4}_{stg}$ chamber of SO (8) model to the $\mathfrak{Q}^{B_3}_{stg}$ chamber of SO (7) model

$$\boldsymbol{F}^{bps}_{D_4\to B_3} : \mathfrak{Q}^{D_4}_{stg} \quad \to \quad \mathfrak{Q}^{B_3}_{stg} \tag{4.1}$$

This particular construction of BPS states of the supersymmetric pure SO (7) gauge model may be also viewed as an illustration of general method for constructing BPS states for the family of $\mathcal{N} = 2$ QFT$_4$ with SO $(2n + 1)$ gauge symmetry. After building the BPS states of the chamber $\mathfrak{Q}^{B_3}_{stg}$, we derive the relationship between the mutation subgroup $H^{SO_8}_{stg}$ and its homologue $H^{SO_7}_{stg}$; and comment on the link between 48 BPS states of $\mathfrak{Q}^{D_4}_{stg}$ and the obtained 42 ones of $\mathfrak{Q}^{B_3}_{stg}$ interpreted as $\frac{7}{8} \times 48$.

4.1. BPS strong chamber of $\mathcal{N} = 2$ $SO(7)$ theory

Here, we use the BPS strong chamber $\mathfrak{Q}^{D_4}_{stg}$ of the supersymmetric pure SO(8) theory to study the BPS states of the strongly coupled chamber of the 4d $\mathcal{N} = 2$ pure SO(7) gauge theory by using a folding quiver method; thanks to the Z_2 automorphism of the BPS quiver $\mathcal{Q}^{SO_8}_0$ inherited from the Z_2 automorphism of the DD of the Lie algebra of the SO(8) gauge symmetry as exhibited by Fig. 6.

To start, recall that the Dynkin diagram of the B_3 Lie algebra can be obtained by folding two nodes of the D_4 Dynkin as shown in Fig. 6. To derive the $\boldsymbol{F}^{bps}_{D_4\to B_3}$ of (4.1), it is interesting to first derive the explicit expression of the folding operator $\mathbf{f}_{D_4\to B_3}$ mapping D_4 diagram to the B_3 one; then turn after to extend this construction to the case of BPS quivers of the corresponding 4d $\mathcal{N} = 2$ gauge theories.

4.1.1. Building the folding operator $f_{D_4\to B_3}$

We begin by noticing that Dynkin diagrams $\mathcal{D}_g$ of finite dimensional Lie algebras g are characterised by intersection of simple roots $\vec{a}_i$ precisely given by their Cartan matrices $K_g = \vec{a}_i.\vec{\alpha}^\vee_j$. Therefore, to describe the folding of the D_4 Dynkin diagram down to the B_3 Dynkin one, we start from the four $\vec{a}_1, \vec{a}_2, \vec{a}_3, \vec{a}_4$ simple roots of the D_4 Lie algebra with intersection matrix as in (3.5); and look for the appropriate manner to reach the simple roots of B_3. To have more insight

into the $\mathbf{f}_{D_4\to B_3}$ folding operator, we also use the canonical basis $\{\vec{e}_1,\vec{e}_2,\vec{e}_3,\vec{e}_4\}$ of the real 4-dim space $\mathbb{R}^4$ in terms of which the four simple roots of D_4 decompose as follows [45]

$$\vec{a}_1=\vec{e}_1-\vec{e}_2\quad,\quad \vec{a}_2=\vec{e}_2-\vec{e}_3\quad,\quad \vec{a}_3=\vec{e}_3-\vec{e}_4\quad,\quad \vec{a}_4=\vec{e}_3+\vec{e}_4 \tag{4.2}$$

having norms $\vec{a}_i.\vec{a}_i=2$ and intersections as in (3.5). To get the structure of the folding mapping between the Dynkin diagrams $\mathcal{D}_{D_4}$ and $\mathcal{D}_{B_3}$; we have to find the way to map the 4×4 Cartan matrix K_{D_4} to the 3×3 Cartan matrix K_{B_3}; that is working out the appropriate rectangular 3×4 matrix $\mathbf{f}$ such that

$$K_{B_3}.\mathbf{f}=\mathbf{f}.K_{D_4} \tag{4.3}$$

Multiplying this constraint relation from the right side first by $\mathbf{f}^T$, we can bring it to the form $K_{B_3}X=\mathbf{f}.K_{D_4}\mathbf{f}^T$ with 3×3 matrix $X=\left(\mathbf{f}\mathbf{f}^T\right)$ and $\det X\neq0$; then by X^{-1}, we end with following relation between the two Cartan matrices

$$K_{B_3}=\mathbf{f}.K_{D_4}.\tilde{\mathbf{f}} \tag{4.4}$$

where we have set $\tilde{\mathbf{f}}=\mathbf{f}^T\left(\mathbf{f}\mathbf{f}^T\right)^{-1}$. Notice that $\mathbf{f}$ and $\tilde{\mathbf{f}}$ are related by the property $\mathbf{f}.\tilde{\mathbf{f}}=I_{3\times3}$; notice also that $\tilde{\mathbf{f}}$ is not uniquely defined since for any non-zero rectangular 4×3 matrix $\mathbf{h}$ with $\det(\mathbf{f}\mathbf{h})\neq0$, the expression $\mathbf{h}\,(\mathbf{f}\mathbf{h})^{-1}$ is also a candidate for $\tilde{\mathbf{f}}$; this feature was expected since folding is a projection; this arbitrariness doesn't affect the result. The mapping $\mathbf{f}$ is explicitly obtained by working out the link between the four $\vec{a}_1,\vec{a}_2,\vec{a}_3,\vec{a}_4$ simple roots of D_4 and the three simple roots of B_3 that we denote as $\vec{\alpha}_1,\vec{\alpha}_2,\vec{\alpha}_3$. Recall that for the B_3 Lie algebra, we have two kinds of simple roots; the $\vec{\alpha}_1,\vec{\alpha}_2$ having a norm equal to 2, and the $\vec{\alpha}_3$ having norm equal to one. In terms of these $\vec{\alpha}_i$'s, the Cartan matrix $K\,(B_3)_{ij}$ is then non-symmetric as shown on the general expression $\frac{2}{\vec{\alpha}_j.\vec{\alpha}_j}\vec{\alpha}_i.\vec{\alpha}_j$; its entries are as follows

$$K\,(B_3)=\begin{pmatrix}2&-1&0\\-1&2&-2\\0&-1&2\end{pmatrix} \tag{4.5}$$

Using the first three canonical basis vectors $\vec{e}_1,\vec{e}_2,\vec{e}_3$, generating a hyperplane $\mathcal{P}_3$ in $\mathbb{R}^4$, the simple $\vec{\alpha}_i$'s can be expressed like $\vec{\alpha}_1=\vec{e}_1-\vec{e}_2$, $\vec{\alpha}_2=\vec{e}_2-\vec{e}_3$ and $\vec{\alpha}_3=\vec{e}_3$; the three $\vec{\alpha}_i$'s are related to the four previous $\vec{a}_i$'s by restrictions to $\mathcal{P}_3$; the folding mapping $\mathbf{f}_{D_4\to B_3}$ between the two sets of simple roots is a projection that read explicitly as follows

$$\vec{\alpha}_1=\vec{a}_1\quad,\quad \vec{\alpha}_2=\vec{a}_2\quad,\quad \vec{\alpha}_3=\frac{1}{2}\,(\vec{a}_3+\vec{a}_4) \tag{4.6}$$

From these relations we learn the matrix $\mathbf{f}$ describing the folding $\mathbf{f}_{D_4\to B_3}$; by help of the expression $\tilde{\mathbf{f}}=\mathbf{f}^T.\left(\mathbf{f}\mathbf{f}^T\right)^{-1}$ satisfying the remarkable $\mathbf{f}.\tilde{\mathbf{f}}=I_{3\times3}$, we have

$$\mathbf{f}=\begin{pmatrix}1&0&0&0\\0&1&0&0\\0&0&\frac{1}{2}&\frac{1}{2}\end{pmatrix}\quad,\quad \tilde{\mathbf{f}}=\begin{pmatrix}1&0&0\\0&1&0\\0&0&1\\0&0&1\end{pmatrix} \tag{4.7}$$

As a check of validity of these expressions, substitute (4.7) into (4.4) with Cartan matrix K_{D_4} as in (3.5), we have

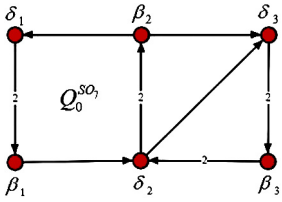

Fig. 7. The primitive BPS quivers $Q_0^{SO_7}$; in addition to usual vertical and horizontal links of ADE type gauge symmetries, we also have a diagonal link; this property is related to the fact that Cartan matrix of so(7) is non-symmetric; it is also related to the existence of two kinds of simple root lengths.

$$K_{B_3} = \begin{pmatrix} 1 & 0 & 0 & 0 \\ 0 & 1 & 0 & 0 \\ 0 & 0 & \frac{1}{2} & \frac{1}{2} \end{pmatrix} \begin{pmatrix} 2 & -1 & 0 & 0 \\ -1 & 2 & -1 & -1 \\ 0 & -1 & 2 & 0 \\ 0 & -1 & 0 & 2 \end{pmatrix} \begin{pmatrix} 1 & 0 & 0 \\ 0 & 1 & 0 \\ 0 & 0 & 1 \\ 0 & 0 & 1 \end{pmatrix} \tag{4.8}$$

leading exactly to the K_{B_3} expression given by (4.5).

4.1.2. Primitive $Q_0^{SO_7}$ as folded $Q_0^{SO_8}$

To build the full set of BPS states of the 4d $\mathcal{N} = 2$ pure SO(7) gauge theory, we proceed as in the case of the SO(8) model; this method requires the knowledge of the primitive quiver $Q_0^{SO_7}$ and the two generators of the mutation group $H_{stg}^{SO_7}$. While $Q_0^{SO_7}$ is obtained in same manner as in SO (8) gauge theory, the set $H_{stg}^{SO_7}$ generating the other $Q_n^{SO_7}$'s is unknown and has to be determined; this will be done by extending the folding method the Dynkin diagram of D_4 into the B_3 one. As we will show in a moment, the $H_{stg}^{SO_7}$ is intimately related to $H_{stg}^{SO_8}$; it has two generators $\mathcal{L}_1$, $\mathcal{L}_2$ related to the L_1, L_2 generators of $H_{stg}^{SO_8}$ like

$$\mathcal{L}_1 = \boldsymbol{F} L_1 \tilde{\boldsymbol{F}} \quad , \quad \mathcal{L}_2 = \boldsymbol{F} L_2 \tilde{\boldsymbol{F}} \tag{4.9}$$

where $\boldsymbol{F}$ and $\tilde{\boldsymbol{F}}$ are extensions of the folding operators $\mathbf{f}$, $\tilde{\mathbf{f}}$ of eqs. (4.4)–(4.7); the exact relations will be given later on; see eqs. (4.15) to fix ideas.

• *Folding operator $\boldsymbol{F}$*

We start from the primitive quiver $Q_0^{SO_7}$ made of the EM charges of the three monopoles $\beta_1, \beta_2, \beta_3$ and three dyons $\delta_1, \delta_2, \delta_3$; these charge-vectors read in terms of the three simple roots $\vec{\alpha}_i$ and co-roots $\vec{\alpha}_i^{\,v} = \frac{2}{\vec{\alpha}_i^2}\vec{\alpha}_i$ as follows

$$\beta_i = \begin{pmatrix} \vec{0} \\ \vec{\alpha}_i^{\,v} \end{pmatrix} \quad , \quad \delta_i = \begin{pmatrix} \vec{\alpha}_i \\ -\vec{\alpha}_i^{\,v} \end{pmatrix} \tag{4.10}$$

with intersection matrix $\mathcal{A}_0^{SO_7} = \upsilon_0^{SO_7} \circ (\upsilon_0^{SO_7})^T$, representing the primitive $Q_0^{SO_7}$ quiver given by Fig. 7, like

$$\mathcal{A}_0^{SO_7} = \begin{pmatrix} \beta_i \circ \beta_j & \beta_i \circ \delta_j \\ \delta_i \circ \beta_j & \delta_i \circ \delta_j \end{pmatrix} = \begin{pmatrix} 0 & -K_{B_3}^T \\ K_{B_3} & K_{B_3}^T - K_{B_3} \end{pmatrix} \otimes I_6 \tag{4.11}$$

where K_{B_3} is as in (4.5). In our approach, we think of this intersection $\mathcal{A}_0^{SO_7}$ matrix as equal to the intersection matrix obtained by folding the $\mathcal{A}_0^{SO_8}$ matrix of the $Q_0^{SO_8}$ quiver (3.4). In other words, we have

$$\upsilon_0^{SO_7} = F.\upsilon_0^{SO_8} \qquad , \qquad \mathcal{A}_0^{SO_7} = F\mathcal{A}_0^{SO_8}F^T \tag{4.12}$$

where the folding rectangular 6×8 matrix F and its transpose are as follows

$$\boldsymbol{F} = \begin{pmatrix} 1 & 0 & 0 & 0 & 0 & 0 & 0 & 0 \\ 0 & 1 & 0 & 0 & 0 & 0 & 0 & 0 \\ 0 & 0 & 1 & 1 & 0 & 0 & 0 & 0 \\ 0 & 0 & 0 & 0 & 1 & 0 & 0 & 0 \\ 0 & 0 & 0 & 0 & 0 & 1 & 0 & 0 \\ 0 & 0 & -\frac{1}{2} & -\frac{1}{2} & 0 & 0 & \frac{1}{2} & \frac{1}{2} \end{pmatrix} \qquad , \qquad \boldsymbol{F}^T = \begin{pmatrix} 1 & 0 & 0 & 0 & 0 & 0 \\ 0 & 1 & 0 & 0 & 0 & 0 \\ 0 & 0 & 1 & 0 & 0 & -\frac{1}{2} \\ 0 & 0 & 1 & 0 & 0 & -\frac{1}{2} \\ 0 & 0 & 0 & 1 & 0 & 0 \\ 0 & 0 & 0 & 0 & 1 & 0 \\ 0 & 0 & 0 & 0 & 0 & \frac{1}{2} \\ 0 & 0 & 0 & 0 & 0 & \frac{1}{2} \end{pmatrix} \tag{4.13}$$

For later use we also need $\tilde{\boldsymbol{F}} = \boldsymbol{F}^T\left(\boldsymbol{F}\boldsymbol{F}^T\right)^{-1}$ obeying the property[3] $\boldsymbol{F}\tilde{\boldsymbol{F}} = I$ and which is given by

$$\tilde{\boldsymbol{F}} = \begin{pmatrix} 1 & 0 & 0 & 0 & 0 & 0 \\ 0 & 1 & 0 & 0 & 0 & 0 \\ 0 & 0 & \frac{1}{2} & 0 & 0 & 0 \\ 0 & 0 & \frac{1}{2} & 0 & 0 & 0 \\ 0 & 0 & 0 & 1 & 0 & 0 \\ 0 & 0 & 0 & 0 & 1 & 0 \\ 0 & 0 & \frac{1}{2} & 0 & 0 & 1 \\ 0 & 0 & \frac{1}{2} & 0 & 0 & 1 \end{pmatrix} \tag{4.14}$$

In terms of the matrices $\mathbf{f}$ and $\tilde{\mathbf{f}}$ of eqs. (4.7), used in the folding of Dynkin diagram D_4 to the Dynkin diagram of B_3, the above $\boldsymbol{F}$ and $\tilde{\boldsymbol{F}}$ read as follows

$$\boldsymbol{F} = \begin{pmatrix} \tilde{\mathbf{f}}^T & 0 \\ \mathbf{f} - \tilde{\mathbf{f}}^T & \mathbf{f} \end{pmatrix} \qquad , \qquad \tilde{\boldsymbol{F}} = \begin{pmatrix} \mathbf{f}^T & 0 \\ \tilde{\mathbf{f}} - \mathbf{f}^T & \tilde{\mathbf{f}} \end{pmatrix} \tag{4.15}$$

With these tools at hand, we can now build mutated BPS quivers $Q_n^{SO_7}$ by applying mutations to the primitive quiver $Q_0^{SO_7}$ by following the same method done for the BPS strong chamber of the SO(8) gauge theory. Let us study how this works by constructing the two leading quivers $Q_1^{SO_7}$ and $Q_2^{SO_7}$ characterised by the intersection matrices $\mathcal{A}_1^{SO_7}$ and $\mathcal{A}_2^{SO_7}$ respectively.

• *Building* $Q_1^{SO_7}$

By using the intersection matrix $\mathcal{A}_1^{SO_7}$ that represents the $Q_1^{SO_7}$ quiver, the mutation mapping $Q_0^{SO_7}$ into $Q_1^{SO_7}$ reads as

$$\mathcal{A}_1^{SO_7} = \boldsymbol{N}_1\mathcal{A}_0^{SO_7}\boldsymbol{N}_1^T \tag{4.16}$$

where $\boldsymbol{N}_1$ is a particular mutation matrix belonging to $H_{stg}^{SO_7}$ and whose explicit expression is not yet known; its form is obtained by applying the folding method to both sides of above relation. By

[3] Notice that $\tilde{\boldsymbol{F}}$ is not uniquely defined since, like for folding Dynkin diagrams, for any non-zero $\mathbf{H}$ with non-singular $(\boldsymbol{F}\boldsymbol{H})^{-1}$, the expressions $\boldsymbol{H}\,(\boldsymbol{F}\boldsymbol{H})^{-1}$ are candidates for $\tilde{\boldsymbol{F}}$.

substituting $\mathcal{A}_0^{SO_7}$ by eq. (4.12) and the $\mathcal{A}_1^{SO_7}$ by its folded expression descending from SO(8) theory namely $\mathcal{A}_1^{SO_7} = \boldsymbol{F}\mathcal{A}_1^{SO_8}\boldsymbol{F}^T$, we can rewrite (4.16) into the form

$$\boldsymbol{F}\mathcal{A}_1^{SO_8}\boldsymbol{F}^T = (\boldsymbol{N}_1\boldsymbol{F})\,\mathcal{A}_0^{SO_8}\,(\boldsymbol{N}_1\boldsymbol{F})^T \tag{4.17}$$

Then by using the mutation eq. (3.18), in particular $\mathcal{A}_1^{SO_8} = \boldsymbol{M}_1\mathcal{A}_0^{SO_8}\boldsymbol{M}_1^T$, we obtain the relation $\boldsymbol{N}_1\boldsymbol{F} = \boldsymbol{F}\boldsymbol{M}_1$ from which we determine $\boldsymbol{N}_1 = \boldsymbol{F}\boldsymbol{M}_1\tilde{\boldsymbol{F}}$. Substituting $\boldsymbol{M}_1 = L_1$, we learn that $\boldsymbol{N}_1$ is also equal to $\mathcal{L}_1 = \boldsymbol{F}L_1\tilde{\boldsymbol{F}}$ as anticipated by eq. (4.9); it is one of the two generators of $H_{stg}^{SO_7}$ with matrix representation

$$\mathcal{L}_1 = \begin{pmatrix} 1 & 0 & 0 & 0 & 1 & 0 \\ 0 & 1 & 1 & 1 & 0 & 2 \\ 0 & 0 & 1 & 0 & 2 & 0 \\ 0 & 0 & 0 & -1 & 0 & 0 \\ 0 & 0 & 0 & 0 & -1 & 0 \\ 0 & 0 & -1 & 0 & -1 & -1 \end{pmatrix} \tag{4.18}$$

from which we can learn directly the 6 BPS states making the $Q_1^{SO_7}$ quiver; these states will be written down later on.

• *Building* $Q_2^{SO_7}$

Doing the same thing for the intersection matrix $\mathcal{A}_2^{SO_7}$ that represent the $Q_2^{SO_7}$ quiver, the mutation mapping $Q_0^{SO_7}$ into $Q_2^{SO_7}$ reads as

$$\mathcal{A}_2^{SO_7} = \boldsymbol{N}_2\mathcal{A}_0^{SO_7}\boldsymbol{N}_2^T \tag{4.19}$$

where $\boldsymbol{N}_2$ is a mutation matrix belonging to $H_{stg}^{SO_7}$; straightforward calculations show that $\boldsymbol{N}_2$ is given by the product of two matrices like $\mathcal{L}_2\mathcal{L}_1$ with $\mathcal{L}_1$ as in (4.18) and $\mathcal{L}_2$ precisely the second generator of $H_{stg}^{SO_7}$ which is related to the L_2 generator of $H_{stg}^{SO_8}$ like $\mathcal{L}_2 = \boldsymbol{F}L_2\tilde{\boldsymbol{F}}$ and whose expression reads as follows

$$\mathcal{L}_2 = \begin{pmatrix} -1 & 0 & 0 & 0 & 0 & 0 \\ 0 & -1 & 0 & 0 & 0 & 0 \\ 0 & 0 & -1 & 0 & 0 & 0 \\ 0 & 1 & 0 & 1 & 0 & 0 \\ 1 & 0 & 1 & 0 & 1 & 0 \\ 0 & 1 & 1 & 0 & 0 & 1 \end{pmatrix} \tag{4.20}$$

From this matrix we can also learn directly the 6 BPS states making the $Q_2^{SO_7}$ quiver; they will be given in the next subsection.

4.2. Building the BPS strong chamber $\mathfrak{Q}_{stg}^{B_3}$

In subsection 4.1, we showed that the strong chamber $\mathfrak{Q}_{stg}^{D_4}$ of the 4d $\mathcal{N}=2$ supersymmetric pure SO(8) gauge theory has 48 BPS states as listed on eq. (3.26). Here, we derive the BPS states content of the strong chamber $\mathfrak{Q}_{stg}^{B_3}$ of the 4d $\mathcal{N}=2$ pure SO(8) theory by using folding method. We show that the number of BPS states $N_{bps}^{B_3}$ of the strong chamber of the SO(7) gauge theory is given by

$$\frac{7}{8}N_{bps}^{D_4} = 42 \neq 36 \tag{4.21}$$

it is different from the expected 36 BPS states following from the heuristic extension of the ADE-type relation (3.1).

To that purpose, we first describe the finite mutation group $H_{stg}^{SO_7}$ of the strong chamber; then we turn to construct the BPS state content of $\mathfrak{Q}_{stg}^{B_3}$.

4.2.1. Mutation group $H_{stg}^{SO_7}$

This is a finite discrete group having two generators $\mathcal{L}_1$ and $\mathcal{L}_2$ with 6×6 matrix representation given by eqs. (4.18)–(4.20). These generators have been induced from their homologue L_1 and L_2 generating particular mutations of primitive $Q_0^{SO_8}$ quiver of the strong chamber of 4d $\mathcal{N}=2$ pure SO(8) gauge theory. Recall that L_1 and L_2 generate $H_{stg}^{SO_8}$ and are realised in terms of 8×8 matrices as in eqs. (3.16)–(3.17). The relations (4.9) and the 6×6 matrix representation of $\mathcal{L}_1$ and $\mathcal{L}_2$ as well as the 8×8 matrix representation of L_1 and L_2 let understand that $H_{stg}^{SO_7}$ and $H_{stg}^{SO_8}$ are intimately related; they are two different representations of same group which turns out to be nothing but the dihedral group Dih_{12}. The link between the $\mathcal{L}_1$, $\mathcal{L}_2$ of the SO(7) theory and the L_1, L_2 involved in SO(8) model is given by the transformation

$$\mathcal{L}_i = \boldsymbol{F} L_i \tilde{\boldsymbol{F}} \tag{4.22}$$

with $\boldsymbol{F}$ standing for the extended folding matrix (4.15) and $\tilde{\boldsymbol{F}}$ is such that $\boldsymbol{F}\tilde{\boldsymbol{F}} = I_{6\times6}$. This link teaches us two useful information: (i) it tells us that $\mathcal{L}_1$, $\mathcal{L}_2$ are the generators of $H_{stg}^{SO_7}$; any element of this mutation symmetry is given by products of $\mathcal{L}_1$ and $\mathcal{L}_2$. (ii) It tells us also that the relationships (4.9) between the L_i's and the $\mathcal{L}_i$'s are in fact particular relations valid for all $\boldsymbol{M}_n$ mutations of the $H_{stg}^{SO_8}$ given by (3.27). In other words, the $\boldsymbol{N}_n$ mutations of $H_{stg}^{SO_7}$ are related to the twelve $\boldsymbol{M}_n$'s of $H_{stg}^{SO_8}$ in the same manner as the $\mathcal{L}_i$'s are related to the L_i's; so we have $\boldsymbol{N}_n = \boldsymbol{F}\boldsymbol{M}_n\tilde{\boldsymbol{F}}$ with

$$\boldsymbol{N}_{2k+1} = \mathcal{L}_1\boldsymbol{N}_{2k} \quad , \quad \boldsymbol{N}_{2k} = (\mathcal{L}_2\mathcal{L}_1)^k \tag{4.23}$$

satisfying the properties

$$\begin{array}{llll} \boldsymbol{N}_{12} & = I_{id} & , & \boldsymbol{N}_6 = -I_{id} \\ \boldsymbol{N}_{n+12} & = \boldsymbol{N}_n & , & \boldsymbol{N}_{n+6} = -\boldsymbol{N}_n \end{array} \tag{4.24}$$

Therefore the finite discrete group $H_{stg}^{SO_7}$ is given by the set

$$H_{stg}^{SO_7} = \left\{ \pm I_{id},\ \pm\boldsymbol{N}_1,\ \pm\boldsymbol{N}_2,\ \pm\boldsymbol{N}_3,\ \pm\boldsymbol{N}_4,\ \pm\boldsymbol{N}_5 \right\} \simeq Dih_{12} \tag{4.25}$$

From this description, we learn that $H_{stg}^{SO_7}$ and $H_{stg}^{SO_8}$ are just two different matrix representations of the dihedral Dih_{12}.

4.2.2. BPS states of $\mathfrak{Q}_{stg}^{B_3}$

The full set of BPS states of the strong chamber of the 4d supersymmetric pure SO(7) gauge theory is determined by quiver mutation method permitting to generate all possible quivers by starting from the primitive quiver $Q_0^{SO_7}$ and acting on it by mutations of $H_{stg}^{SO_7}$. In this way one obtains several BPS quivers $Q_n^{SO_7}$ from which we read the BPS states. Because of the properties

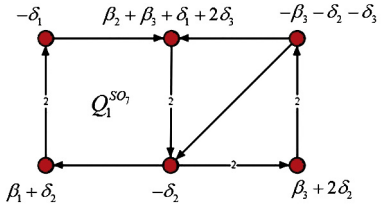

Fig. 8. The BPS quiver $Q_1^{SO_7}$ obtained by mutation of primitive $Q_0^{SO_7}$ by acting by $\mathcal{L}_1$.

(3.21), the following six leading quivers are enough to get the full list of the BPS states of the strong chamber of the 4d supersymmetric pure SO(7) gauge theory

$$Q_0^{SO_7},\ Q_1^{SO_7},\ Q_2^{SO_7},\ Q_3^{SO_7},\ Q_4^{SO_7},\ Q_5^{SO_7} \tag{4.26}$$

Let us describe the BPS states of these quivers with some details. From the primitive quiver $Q_0^{SO_7}$, we have six BPS states; these are the three monopoles $\beta_1, \beta_2, \beta_3$, and three dyons $\delta_1, \delta_2, \delta_3$ with electric–magnetic charges as in (4.10). The quiver $Q_1^{SO_7}$ gives six new BPS states and are as follows

$$\begin{array}{ccccc} -\delta_1 & , & \beta_1+\delta_2 & , & -\beta_3-\delta_3-\delta_2 \\ -\delta_2 & , & \beta_3+2\delta_2 & , & \beta_2+\beta_3+\delta_1+2\delta_3 \end{array} \tag{4.27}$$

They are located at the nodes of the graph of $Q_1^{SO_7}$ of Fig. 8. They are obtained by acting on $\upsilon_0^T=(\beta_1,\beta_2,\beta_3;\delta_1,\delta_2,\delta_3)$ by the mutation transformation $\mathcal{L}_1$ like

$$\begin{pmatrix} 1 & 0 & 0 & 0 & 1 & 0 \\ 0 & 1 & 1 & 1 & 0 & 2 \\ 0 & 0 & 1 & 0 & 2 & 0 \\ 0 & 0 & 0 & -1 & 0 & 0 \\ 0 & 0 & 0 & 0 & -1 & 0 \\ 0 & 0 & -1 & 0 & -1 & -1 \end{pmatrix} \begin{pmatrix} \beta_1 \\ \beta_2 \\ \beta_3 \\ \delta_1 \\ \delta_2 \\ \delta_3 \end{pmatrix} = \begin{pmatrix} \beta_1+\delta_2 \\ \beta_2+\beta_3+\delta_1+2\delta_3 \\ \beta_3+2\delta_2 \\ -\delta_1 \\ -\delta_2 \\ -\beta_3-\delta_2-\delta_3 \end{pmatrix} \tag{4.28}$$

they can be also read directly on the rows of the $\mathcal{L}_1$ matrix generator. Notice that from the view of the full $\mathcal{G}_{stg}^{SO_7}$ mutation group, the $\mathcal{L}_1$ is a composite transformation with three fundamental reflections like $\mathcal{L}_1=r_3r_2r_1$ with

$$r_1=\begin{pmatrix} 1 & 0 & 0 & 0 & 0 & 0 \\ 0 & 1 & 0 & 1 & 0 & 0 \\ 0 & 0 & 1 & 0 & 0 & 0 \\ 0 & 0 & 0 & -1 & 0 & 0 \\ 0 & 0 & 0 & 0 & 1 & 0 \\ 0 & 0 & 0 & 0 & 0 & 1 \end{pmatrix} \quad , \quad r_2=\begin{pmatrix} 1 & 0 & 0 & 0 & 1 & 0 \\ 0 & 1 & 0 & 0 & 0 & 0 \\ 0 & 0 & 1 & 0 & 2 & 0 \\ 0 & 0 & 0 & 1 & 0 & 0 \\ 0 & 0 & 0 & 0 & -1 & 0 \\ 0 & 0 & 0 & 0 & -1 & 1 \end{pmatrix} \tag{4.29}$$

and

$$r_3=\begin{pmatrix} 1 & 0 & 0 & 0 & 0 & 0 \\ 0 & 1 & 1 & 0 & 0 & 2 \\ 0 & 0 & 1 & 0 & 0 & 0 \\ 0 & 0 & 0 & 1 & 0 & 0 \\ 0 & 0 & 0 & 0 & 1 & 0 \\ 0 & 0 & -1 & 0 & 0 & -1 \end{pmatrix} \tag{4.30}$$

Each r_i reflection generates a BPS quiver with two new BPS states; the simultaneous reflections generated by $\mathcal{L}_1 = r_3 r_2 r_1$ on $Q_0^{SO_7}$ give the quiver $Q_1^{SO_7}$ having $3 \times 2 = 6$ BPS states. Using this way of doing, we find that the BPS states coming from $Q_n^{SO_7}$ quivers can be read from the rows of the mutation group elements $\boldsymbol{N}_n$ given by eqs. (4.24). For example, the BPS states resulting from $Q_2^{SO_7}$ are read on the mutation matrix $\boldsymbol{N}_2 = \mathcal{L}_2\mathcal{L}_1$; we have

$$\boldsymbol{N}_2 = \begin{pmatrix} -1 & 0 & 0 & 0 & -1 & 0 \\ 0 & -1 & -1 & -1 & 0 & -2 \\ 0 & 0 & -1 & 0 & -2 & 0 \\ 0 & 1 & 1 & 0 & 0 & 2 \\ 1 & 0 & 1 & 0 & 2 & 0 \\ 0 & 1 & 1 & 1 & 1 & 1 \end{pmatrix} \tag{4.31}$$

it generates the following six new BPS states from the primitive ones

$$\begin{array}{ll} -\beta_1 - \delta_2 & \beta_2 + \beta_3 + 2\delta_3 \\ -\beta_2 - \beta_3 - \delta_1 - 2\delta_3 & \beta_1 + \beta_3 + 2\delta_2 \\ -\beta_3 - 2\delta_2 & \beta_2 + \beta_3 + \delta_1 + \delta_2 + \delta_3 \end{array} \tag{4.32}$$

Similarly, the remaining BPS states come from the $Q_3^{SO_7}$, $Q_4^{SO_7}$ and $Q_5^{SO_7}$ quivers; they are read on the rows of the matrix mutations $\boldsymbol{N}_3 = \mathcal{L}_1\mathcal{L}_2\mathcal{L}_1$, $\boldsymbol{N}_4 = (\mathcal{L}_2\mathcal{L}_1)^2$ and $\boldsymbol{N}_5 = \mathcal{L}\,(\mathcal{L}_2\mathcal{L}_1)^2$. The resulting full set of BPS states of the strong coupling chamber of the $SO(7)$ gauge theory reads therefore as follows

$$\begin{array}{lll} \pm\beta_1 & \pm(\beta_2 + \delta_1) & \pm(2\beta_2 + \beta_3 + \delta_1 + 2\delta_3) \\ \pm\beta_2 & \pm(\beta_3 + \delta_2) & \pm(\beta_2 + \beta_3 + \delta_1 + \delta_2 + \delta_3) \\ \pm\beta_3 & \pm(\beta_3 + 2\delta_2) & \pm(2\beta_1 + \beta_3 + 2\delta_2) \\ \pm\delta_1 & \pm(\beta_1 + \beta_3 + \delta_2) & \pm(\beta_2 + \beta_3 + 2\delta_3) \\ \pm\delta_2 & \pm(\beta_2 + \beta_3 + \delta_3) & \pm(\beta_2 + \beta_3 + \delta_1 + 2\delta_3) \\ \pm\delta_3 & \pm(\beta_3 + \delta_2 + \delta_3) & \pm(\beta_1 + \beta_2 + \beta_3 + \delta_2 + \delta_3) \\ \pm(\beta_1 + \delta_2) & \pm(\beta_1 + \beta_3 + 2\delta_2) & \pm(\beta_1 + \beta_2 + \beta_3 + \delta_1 + \delta_2 + \delta_3) \end{array} \tag{4.33}$$

There are $6 \times 7 = 42$ BPS states in $\mathfrak{Q}_{stg}^{B_3}$ versus the $6 \times 8 = 48$ BPS states in $\mathfrak{Q}_{stg}^{D_4}$; the folding has projected out $\frac{1}{6}$ BPS states.

5. BPS strong chamber of $\mathcal{N} = 2$ SP$(4, \mathbb{R})$ theory

In this section, we build the BPS spectrum of the chamber of the 4d $\mathcal{N} = 2$ supersymmetric SP$(4, \mathbb{R})$ gauge theory. To that purpose, we use the folding quiver method relating BPS quivers $Q_n^{SU_4}$ of the $\mathcal{N} = 2$ SU(4) gauge model to BPS quiver homologue $Q_n^{SP_4}$ of the supersymmetric SP$(4, \mathbb{R})$ theory. This construction extends the usual folding method linking the Dynkin diagrams $\mathcal{D}_{A_3}$ and $\mathcal{D}_{C_2}$ of the simply laced A_3 and the non-simply laced C_2 Lie algebras respectively [45,49,50].

5.1. BPS chamber $\mathfrak{Q}_{stg}^{A_3}$

Here we review the main lines of the derivation of the BPS states of the strong chamber $\mathfrak{Q}_{stg}^{A_3}$ of the 4d $\mathcal{N} = 2$ supersymmetric pure SU(4) gauge theory; and describe the mutation set $\mathcal{G}_{stg}^{SU_4}$

generated by 3+3 reflections r_1, r_2, r_3, s_1, s_2, s_3; especially its subgroup $H_{stg}^{SU_4}$ generated by $L_1 = r_3 r_2 r_1$ and $L_2 = s_3 s_2 s_1$ [3]. These tools are needed for determining the BPS states of the strong chamber $\mathfrak{Q}_{stg}^{C_2}$ of the 4d $\mathcal{N} = 2$ supersymmetric pure SP$(4, \mathbb{R})$ gauge theory.

5.1.1. BPS quivers $Q_0^{SU_4}$ and $Q_1^{SU_4}$

In the 4d $\mathcal{N} = 2$ SU(4) gauge theory, the primitive quiver $Q_0^{SU_4}$ of the strongly coupled chamber $\mathfrak{Q}_{stg}^{A_3}$ is made of the 3 elementary monopoles $\{b_1, b_2, b_3\}$ and the 3 elementary dyons $\{c_1, c_2, c_3\}$ as depicted in Fig. 1. The electric–magnetic charges of the b_i monopoles and the c_i dyons are expressed in terms of the three $\vec{a}_1, \vec{a}_2, \vec{a}_3$ simple roots of the A_3 Lie algebra as follows

$$b_i = \begin{pmatrix} \vec{0} \\ \vec{a}_i \end{pmatrix} \qquad , \qquad c_i = \begin{pmatrix} \vec{a}_i \\ -\vec{a}_i \end{pmatrix} \tag{5.1}$$

These EM charge vectors are thought of in terms of 6 nodes of the primitive BPS quiver $Q_0^{SU_4}$ whose properties may be represented by the EM charge vector $\upsilon_0^T = (b_1, b_2, b_3; c_1, c_2, c_3)$ and, using Dirac pairing, by the intersection matrix[4]

$$\mathcal{A}_0^{SU_4} = \begin{pmatrix} 0 & -K \\ K & 0 \end{pmatrix} \otimes I_6 \tag{5.2}$$

with K_{ij} is the usual 3×3 Cartan matrix $\vec{a}_i.\vec{a}_j$ of the A_3 Lie algebra given by

$$K_{A_3} = \begin{pmatrix} 2 & -1 & 0 \\ -1 & 2 & -1 \\ 0 & -1 & 2 \end{pmatrix} \tag{5.3}$$

Substituting, we have

$$\mathcal{A}_0^{SU_4} = \begin{pmatrix} 0 & 0 & 0 & -2 & 1 & 0 \\ 0 & 0 & 0 & 1 & -2 & 1 \\ 0 & 0 & 0 & 0 & 1 & -2 \\ 2 & -1 & 0 & 0 & 0 & 0 \\ -1 & 2 & -1 & 0 & 0 & 0 \\ 0 & -1 & 2 & 0 & 0 & 0 \end{pmatrix} \tag{5.4}$$

Under simultaneous reflection $L_1 = r_3 r_2 r_1$ of the EM charges of the three dyons, the primitive BPS quiver $Q_0^{SU_4}$ gets mapped to the mutated quiver $Q_1^{SU_4}$ whose new BPS states have the EM charge vector $\upsilon_1^T = (c_2 + b_1, c_1 + c_3 + b_2, c_2 + b_3; -c_1, -c_2, -c_3)$. The intersection matrix $\mathcal{A}_1^{SU_4}$ associated with $Q_1^{SU_4}$ is equal to $\boldsymbol{M}_1 \mathcal{A}_0^{SU_4} \boldsymbol{M}_1^T$ where the transformation $\boldsymbol{M}_1$ is a 6×6 mutation matrix given by

$$L_1 = \begin{pmatrix} 1 & 0 & 0 & 0 & 1 & 0 \\ 0 & 1 & 0 & 1 & 0 & 1 \\ 0 & 0 & 1 & 0 & 1 & 0 \\ 0 & 0 & 0 & -1 & 0 & 0 \\ 0 & 0 & 0 & 0 & -1 & 0 \\ 0 & 0 & 0 & 0 & 0 & -1 \end{pmatrix} \tag{5.5}$$

[4] In what follows we shall hide the factor $\otimes I_6$.

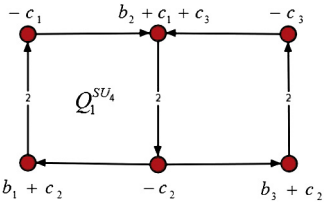

Fig. 9. The mutated quiver $Q_1^{SU_4}$ having 6 nodes describing BPS states and a Z_2 outer-automorphism symmetry fixing the two central nodes and exchanging the external ones.

where, for convenience, we have set $\boldsymbol{M}_1 = L_1$. This matrix L_1 is one of two matrix generators of $H_{stg}^{SU_4}$. Notice that the primitive quiver $Q_0^{SU_4}$ has 6 BPS states; by performing the mutation by L_1, we obtain 6 new BPS states making $Q_1^{SU_4}$ given by Fig. 9 having a Z_2 outer-automorphism symmetry inherited from the Dynkin diagram of SU (4); these BPS states are as follows

$$Q_0^{SU_4}: \begin{matrix} b_1\ ,\ c_1 \\ b_2\ ,\ c_2 \\ b_3\ ,\ c_3 \end{matrix} \quad ; \quad Q_1^{SU_4}: \begin{matrix} c_2+b_1 & ,\ -c_1 \\ c_1+c_3+b_2 & ,\ -c_2 \\ c_2+b_3 & ,\ -c_3 \end{matrix} \tag{5.6}$$

The remaining BPS states of $\mathfrak{Q}_{stg}^{A_3}$ are derived in a similar manner as in the case of SO (8) model described in section 3; they are obtained by acting on $Q_1^{SU_4}$ by the generator L_2 and repeating the mutations of $H_{stg}^{SU_4}$ until reaching $Q_0^{SU_4}$; some steps of this construction are described in what follows.

5.1.2. *BPS states of chamber* $\mathfrak{Q}_{stg}^{A_3}$

The set of BPS states of the strong chamber $\mathfrak{Q}_{stg}^{A_3}$ of the 4d $\mathcal{N}=2$ supersymmetric SU (4) gauge theory has $24 = 2 \times 12$ BPS states; they include the ones given by (5.6), and are as follows

$$\begin{array}{llll} \pm b_1 & \pm c_1 & \pm(b_1+c_2) & \pm(b_2+c_1) \\ \pm b_2 & \pm c_2 & \pm(b_2+c_1+c_3) & \pm(b_2+c_3) \\ \pm b_3 & \pm c_3 & \pm(b_3+c_2) & \pm(b_1+b_3+c_2) \end{array} \tag{5.7}$$

A way to obtain this set is to start from the primitive quiver $Q_0^{SU_4}$ of Fig. 1, and apply mutations. As done in section 3, it turns out that the subset $H_{stg}^{SU_4}$ of the quiver mutations set $\mathcal{G}_{stg}^{SU_4}$ is enough to generate the spectrum (5.7). It happens also that $H_{stg}^{SU_4}$ is nothing but the 6×6 matrix representation of the dihedral group Dih_8 with two non-commuting matrix generators L_1 and L_2; the first L_1 is as in (5.5) and the second is as follows

$$L_2 = \begin{pmatrix} -1 & 0 & 0 & 0 & 0 & 0 \\ 0 & -1 & 0 & 0 & 0 & 0 \\ 0 & 0 & -1 & 0 & 0 & 0 \\ 0 & 1 & 0 & 1 & 0 & 0 \\ 1 & 0 & 1 & 0 & 1 & 0 \\ 0 & 1 & 0 & 0 & 0 & 1 \end{pmatrix} \tag{5.8}$$

These matrix generators obey the property $(L_2L_1)^4 = I_{6\times6}$; using the same notations as in section 3 by setting $\boldsymbol{M}_{2k} = (L_2L_1)^k$ and $\boldsymbol{M}_{2k+1} = L_1\boldsymbol{M}_{2k}$, the mutations of $H_{stg}^{SU_4}$ are given by

$$H_{stg}^{SU_4} = \{\ I_{id},\quad \boldsymbol{M}_1,\quad \boldsymbol{M}_2,\quad \boldsymbol{M}_3,\quad \boldsymbol{M}_4,\quad \boldsymbol{M}_5,\quad \boldsymbol{M}_6,\quad \boldsymbol{M}_7\ \} \tag{5.9}$$

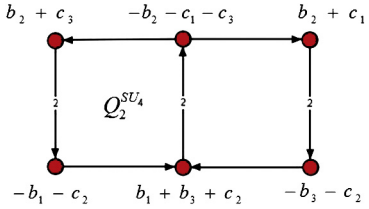

Fig. 10. The quiver $Q_2^{SU_4}$ having 6 nodes describing BPS states and a Z_2 outer-automorphism symmetry fixing the two central nodes and exchanging the external ones.

with the "cyclic" property

$$\boldsymbol{M}_{4+n} = \boldsymbol{M}_4 \boldsymbol{M}_n \tag{5.10}$$

These seven $\boldsymbol{M}_n$ mutations allow to build the corresponding mutated quivers $Q_n^{SU_4}$ from which we read the 24 BPS states of the strong chamber of this theory. Let us briefly describe the derivation of these states; the primitive quiver $Q_0^{SU_4}$ has 6 BPS states; by performing the mutation by L_1, we obtain 6 new BPS states making $Q_1^{SU_4}$; they are as in eqs. (5.6). The quiver $Q_2^{SU_4}$ is obtained by applying the $\boldsymbol{M}_2$ mutation on the primitive quiver $Q_0^{SU_4}$; and the quiver $Q_3^{SU_4}$ is obtained by applying the $\boldsymbol{M}_3$ mutation on the primitive $Q_0^{SU_4}$ and so on. Similar calculations as done for $Q_1^{SU_4}$ give the other remaining BPS quivers; they lead to the following 24 BPS states

$$\begin{array}{l} Q_2^{SU_4}: \begin{array}{ll} -c_2 - b_1 & , \ c_3 + b_2 \\ -c_1 - c_3 - b_2 & , \ c_2 + b_1 + b_3 \\ -c_2 - b_3 & , \ c_1 + b_2 \end{array} \end{array} \quad ; \quad \begin{array}{l} Q_3^{SU_4}: \begin{array}{ll} b_3 & , \ -c_3 - b_2 \\ b_2 & , \ -c_2 - b_1 - b_3 \\ b_1 & , \ -c_1 - b_2 \end{array} \end{array}$$

$$\begin{array}{l} Q_4^{SU_4}: \begin{array}{ll} -b_3 & , \ -c_3 \\ -b_2 & , \ -c_2 \\ -b_1 & , \ -c_1 \end{array} \end{array} \quad ; \quad \begin{array}{l} Q_5^{SU_4}: \begin{array}{ll} -c_2 - b_3 & , \ c_3 \\ -c_1 - c_3 - b_2 & , \ c_2 \\ -c_2 - b_1 & , \ c_1 \end{array} \end{array}$$

$$\begin{array}{l} Q_6^{SU_4}: \begin{array}{ll} c_2 + b_3 & , \ -c_1 - b_2 \\ c_1 + c_3 + b_2 & , \ -c_2 - b_1 - b_3 \\ c_2 + b_1 & , \ -c_3 - b_2 \end{array} \end{array} \quad ; \quad \begin{array}{l} Q_7^{SU_4}: \begin{array}{ll} -b_1 & , \ c_1 + b_2 \\ -b_2 & , \ c_2 + b_1 + b_3 \\ -b_3 & , \ c_3 + b_2 \end{array} \end{array} \tag{5.11}$$

The graph representing the quiver $Q_2^{SU_4}$ is given by Fig. 10; it has a Z_2 outer-automorphism symmetry.

5.2. *BPS chamber* $\mathfrak{Q}_{stg}^{C_2}$

In this subsection, we construct the BPS states of the strong chamber $\mathfrak{Q}_{stg}^{C_2}$ of the supersymmetric pure $SP(4,\mathbb{R})$ gauge theory by extending the idea of folding method for building the Dynkin diagram of the non-simply laced Lie algebras C_2 out of the DD of A_3. This extension is because BPS quivers of $\mathcal{N}=2$ supersymmetric pure SU (4) gauge theory has a Z_2 outer-automorphism symmetry. Recall that the non-simply laced Dynkin diagram of C_2 symplectic Lie algebra can be obtained by folding two nodes of the simply laced A_3 Dynkin diagram as shown in Fig. 11. To that purpose, we begin by constructing the folding operator $\mathbf{f}_{A_3 \to C_2}$ which

Fig. 11. Folding simply laced Dynkin diagram of SU (4) down to non-simply laced Dynkin diagram of SP (4).

maps A_3 Dynkin diagram to the C_2 Dynkin one; then we extend this construction the case of BPS quivers of the corresponding 4d $\mathcal{N}=2$ pure SP$(4,\mathbb{R})$ gauge theory.

5.2.1. Folding operator $\mathbf{f}_{A_3\to C_2}$

To describe the folding of the A_3 Dynkin diagram down to the C_2 one, we start from the three $\vec{a}_1, \vec{a}_2, \vec{a}_3$ simple roots of the A_3 Lie algebra; and look for reaching the two $\vec{\alpha}_1, \vec{\alpha}_2$ simple roots of the C_2 Lie algebra. In terms of the canonical basis $\{\vec{e}_1, \vec{e}_2, \vec{e}_3\}$ of the real 3-dim space $\mathbb{R}^4$, the three simple roots of A_3 decompose as

$$\vec{a}_1 = \vec{e}_1 - \vec{e}_2 \quad , \quad \vec{a}_2 = \vec{e}_2 - \vec{e}_3 \quad , \quad \vec{a}_3 = \vec{e}_3 - \vec{e}_4 \tag{5.12}$$

with $\vec{a}_i.\vec{a}_i = 2$ and intersections given by the Cartan matrix K_{A_3} (5.3). The simple roots of C_2 of the Lie algebra are realised in quite similar manner like $\vec{\alpha}_1 = \vec{e}'_1 - \vec{e}'_2$, $\vec{\alpha}_2 = 2\vec{e}'_2$ with Cartan matrix $K_{C_3} = \frac{2}{\vec{\alpha}_j^2}\vec{\alpha}_i.\vec{\alpha}_j$ given by

$$K_{C_2} = \begin{pmatrix} 2 & -1 \\ -2 & 2 \end{pmatrix} \tag{5.13}$$

But here we will use the realisation following from the folding of the A_3 Dynkin diagram namely [49,50],

$$\vec{\alpha}_1 = \frac{1}{2}(\vec{a}_1 + \vec{a}_3) \qquad , \qquad \vec{\alpha}_2 = \vec{a}_2 \tag{5.14}$$

Applying the same method as done in subsection 4.2.1, the folding operator $\mathbf{f}_{A_3\to C_2}$ (for short $\mathbf{f}$), mapping the Dynkin diagram $\mathcal{D}_{A_3}$ to the $\mathcal{D}_{C_2}$ one, may be defined as a link between the two Cartan matrices as follows

$$K_{C_2} = \mathbf{f}.K_{A_3}.\tilde{\mathbf{f}} \tag{5.15}$$

where $\tilde{\mathbf{f}}$ is such that $\mathbf{f}.\tilde{\mathbf{f}} = I_{3\times 3}$; it is related to the transpose of the folding matrix like $\tilde{\mathbf{f}} = \mathbf{f}^T.\left(\mathbf{f}\mathbf{f}^T\right)^{-1}$; see eqs. (4.4) for the derivation of this relation. Straightforward calculations lead to the following rectangular matrices

$$\mathbf{f} = \begin{pmatrix} \frac{1}{2} & 0 & \frac{1}{2} \\ 0 & 1 & 0 \end{pmatrix} \qquad , \qquad \tilde{\mathbf{f}} = \begin{pmatrix} 1 & 0 \\ 0 & 1 \\ 1 & 0 \end{pmatrix} \tag{5.16}$$

By substituting K_{A_3} by its expression (5.3) and using above relations, we have

$$K_{C_2} = \begin{pmatrix} \frac{1}{2} & 0 & \frac{1}{2} \\ 0 & 1 & 0 \end{pmatrix} \begin{pmatrix} 2 & -1 & 0 \\ -1 & 2 & -1 \\ 0 & -1 & 2 \end{pmatrix} \begin{pmatrix} 1 & 0 \\ 0 & 1 \\ 1 & 0 \end{pmatrix} \tag{5.17}$$

which is precisely the Cartan matrix K_{C_2} given by eq. (5.13).

5.2.2. Folding quiver map and $H_{stg}^{SP_4}$ symmetry

To build the set of BPS states of the 4d $\mathcal{N}=2$ supersymmetric pure SP$(4,\mathbb{R})$ gauge theory, we extend the folding method between the Dynkin diagrams $\mathcal{D}_{A_3}$ and $\mathcal{D}_{C_2}$ to the corresponding BPS quivers; thanks to the Z_2 outer-automorphism of the primitive $Q_0^{SU_4}$ which is inherited from the Dynkin diagram of A_3 Lie algebra. First, we construct the folding quiver mapping $\boldsymbol{F}$; then we use it to build the BPS quivers of the $\mathfrak{Q}_{stg}^{C_2}$ strong chamber as well the $H_{stg}^{SP_4}$ mutation subset.

• *Folding quiver operator*

To construct the folding quiver operator $\boldsymbol{F}$ mapping the primitive quiver $Q_0^{SU_4}$ of Fig. 1 into the primitive $Q_0^{SP_4}$ of Fig. 2, we consider their respective matrix representatives $\mathcal{A}_0^{SU_4}$ of eq. (5.2) and $\mathcal{A}_0^{SP_4}$ given by

$$\mathcal{A}_0^{SP_4}=\begin{pmatrix}0 & -K_{C_2}^T\\ K_{C_2} & K_{C_2}^T-K_{C_2}\end{pmatrix}\otimes I_4 \tag{5.18}$$

In the folding BPS quiver approach, the intersection matrix $\mathcal{A}_0^{SP_4}$ is identified with intersection matrix $\boldsymbol{F}\mathcal{A}_0^{SU_4}\boldsymbol{F}^T$ following from the folding of primitive quiver $Q_0^{SU_4}$ of the $\mathcal{N}=2$ $SU(4)$ theory. Put differently, we require the identification

$$\mathcal{A}_0^{SP_4}=\boldsymbol{F}\mathcal{A}_0^{SU_4}\boldsymbol{F}^T \tag{5.19}$$

The rectangular 4×6 matrix $\boldsymbol{F}$ encodes the folding operator of $Q_0^{SU_4}$ down to $Q_0^{SP_4}$; it is obtained by solving the constraint relation (5.19). These $\boldsymbol{F}$ and $\boldsymbol{F}^T$ folding quiver operators as well as their partner $\tilde{\boldsymbol{F}}=\boldsymbol{F}^T.\left(\boldsymbol{F}\boldsymbol{F}^T\right)^{-1}$ obeying the property $\boldsymbol{F}\tilde{\boldsymbol{F}}=I_{4\times 4}$ are related to those $\mathbf{f}$ and $\tilde{\mathbf{f}}$ used in linking Dynkin $\mathcal{D}_{A_3}$ and $\mathcal{D}_{C_2}$ diagrams as follows

$$\boldsymbol{F}=\begin{pmatrix}\tilde{\mathbf{f}}^T & 0\\ \mathbf{f}-\tilde{\mathbf{f}}^T & \mathbf{f}\end{pmatrix}\qquad,\qquad \tilde{\boldsymbol{F}}=\begin{pmatrix}\mathbf{f}^T & 0\\ \tilde{\mathbf{f}}-\mathbf{f}^T & \tilde{\mathbf{f}}\end{pmatrix} \tag{5.20}$$

Their explicit forms are given by

$$\boldsymbol{F}=\begin{pmatrix}1 & 0 & 1 & 0 & 0 & 0\\ 0 & 1 & 0 & 0 & 0 & 0\\ -\frac{1}{2} & 0 & -\frac{1}{2} & \frac{1}{2} & 0 & \frac{1}{2}\\ 0 & 0 & 0 & 0 & 1 & 0\end{pmatrix}\qquad,\qquad \boldsymbol{F}^T=\begin{pmatrix}1 & 0 & -\frac{1}{2} & 0\\ 0 & 1 & 0 & 0\\ 1 & 0 & -\frac{1}{2} & 0\\ 0 & 0 & \frac{1}{2} & 0\\ 0 & 0 & 0 & 1\\ 0 & 0 & \frac{1}{2} & 0\end{pmatrix} \tag{5.21}$$

and

$$\tilde{\boldsymbol{F}}=\begin{pmatrix}\frac{1}{2} & 0 & 0 & 0\\ 0 & 1 & 0 & 0\\ \frac{1}{2} & 0 & 0 & 0\\ \frac{1}{2} & 0 & 1 & 0\\ 0 & 0 & 0 & 1\\ \frac{1}{2} & 0 & 1 & 0\end{pmatrix} \tag{5.22}$$

To test the validity of these relations, we substitute the above quantities back into $\mathcal{A}_0^{SP_4}=\boldsymbol{F}\mathcal{A}_0^{SU_4}\boldsymbol{F}^T$ of eq. (5.19), we obtain the following intersection matrix of the primitive $Q_0^{SP_4}$ quiver

$$\mathcal{A}_0^{SP_4} = \begin{pmatrix} 1 & 0 & 1 & 0 & 0 & 0 \\ 0 & 1 & 0 & 0 & 0 & 0 \\ -\frac{1}{2} & 0 & -\frac{1}{2} & \frac{1}{2} & 0 & \frac{1}{2} \\ 0 & 0 & 0 & 0 & 1 & 0 \end{pmatrix} \times \begin{pmatrix} 0 & 0 & 0 & -2 & 1 & 0 \\ 0 & 0 & 0 & 1 & -2 & 1 \\ 0 & 0 & 0 & 0 & 1 & -2 \\ 2 & -1 & 0 & 0 & 0 & 0 \\ -1 & 2 & -1 & 0 & 0 & 0 \\ 0 & -1 & 2 & 0 & 0 & 0 \end{pmatrix} \begin{pmatrix} 1 & 0 & -\frac{1}{2} & 0 \\ 0 & 1 & 0 & 0 \\ 1 & 0 & -\frac{1}{2} & 0 \\ 0 & 0 & \frac{1}{2} & 0 \\ 0 & 0 & 0 & 1 \\ 0 & 0 & \frac{1}{2} & 0 \end{pmatrix}$$

which coincides exactly with the $\mathcal{A}_0^{SP_4}$ given by eq. (2.12).

• *The mutation subgroup* $H_{stg}^{SP_4}$

The set $H_{stg}^{SP_4}$ is a particular subgroup of the set of mutations of the BPS quivers of the strong chamber $\mathcal{G}_{stg}^{SP_4}$ described in appendix I. It has two non-commuting generators $\mathcal{L}_1$, $\mathcal{L}_2$ related to the L_1, L_2 generators of $H_{stg}^{SU_4}$ like

$$\mathcal{L}_1 = \boldsymbol{F} L_1 \tilde{\boldsymbol{F}} \quad , \quad \mathcal{L}_2 = \boldsymbol{F} L_2 \tilde{\boldsymbol{F}} \tag{5.23}$$

where $\boldsymbol{F}$ and $\tilde{\boldsymbol{F}}$ are as in eqs. (5.20)–(5.21). Substituting L_1 and L_2 by their expressions (5.5)–(5.8), the above relations give

$$\mathcal{L}_1 = \begin{pmatrix} 1 & 0 & 0 & 2 \\ 1 & 1 & 2 & 0 \\ -1 & 0 & -1 & -1 \\ 0 & 0 & 0 & -1 \end{pmatrix} \quad , \quad \mathcal{L}_2 = \begin{pmatrix} -1 & 0 & 0 & 0 \\ 0 & -1 & 0 & 0 \\ 1 & 1 & 1 & 0 \\ 1 & 0 & 0 & 1 \end{pmatrix} \tag{5.24}$$

obeying the property $\mathcal{L}_1^2 = \mathcal{L}_2^2 = I_{4\times 4}$. Using the same notations as in section 4 by setting $\boldsymbol{N}_{2k} = (\mathcal{L}_2\mathcal{L}_1)^k$ and $\boldsymbol{N}_{2k+1} = \mathcal{L}_1\boldsymbol{N}_{2k}$, the mutations $\boldsymbol{N}_n$ of the set $H_{stg}^{SP_4}$ are related to those transformations of the $\mathfrak{Q}_{stg}^{A_3}$ strong chamber like $\boldsymbol{N}_n = \boldsymbol{F}\boldsymbol{M}_n\tilde{\boldsymbol{F}}$; so we have

$$H_{strong}^{SP(4)} = \{\, I_{id}, \quad \boldsymbol{N}_1, \quad \boldsymbol{N}_2, \quad \boldsymbol{N}_3, \quad \boldsymbol{N}_4, \quad \boldsymbol{N}_5, \quad \boldsymbol{N}_6, \quad \boldsymbol{N}_7 \,\} \tag{5.25}$$

with the remarkable properties $\boldsymbol{N}_4 = -I_{id}$ and $\boldsymbol{N}_{n+4} = -\boldsymbol{N}_n$. These $\boldsymbol{N}_n$ mutations allow to build the corresponding mutated quivers $Q_n^{SU_4}$ from which we read the 24 BPS states of the strong chamber of this theory.

5.2.3. *BPS spectrum of* $\mathfrak{Q}_{stg}^{C_2}$

The obtained 20 BPS states of the strong chamber $\mathfrak{Q}_{stg}^{C_2}$ of the 4d $\mathcal{N}=2$ pure SP(4, $\mathbb{R}$) gauge theory are collected in the following table

$\pm\beta_1$	$\pm(\beta_1 + 2\delta_2)$	$\pm(\beta_1+\beta_2+2\delta_1)$
$\pm\delta_1$	$\pm(\beta_1 + \delta_2)$	$\pm(\beta_1+\beta_2+\delta_1+\delta_2)$
$\pm\beta_2$	$\pm(\beta_1 + \delta_1 + \delta_2)$	
$\pm\delta_2$	$\pm(\beta_1 + \beta_2 + \delta_1)$	

(5.26)

They are derived by applying the mutation operators on the primitive quiver $Q_0^{SP_4}$; by following the same method as in unfolded SU(4) theory; we find

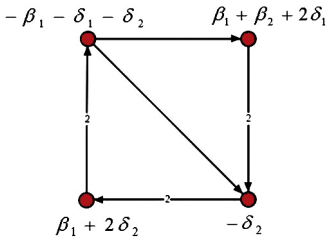

Fig. 12. The quiver $Q_1^{SP_4}$ having 4 nodes describing BPS states.

$$
\begin{aligned}
Q_1^{SP_4} &: \begin{cases} \beta_1+2\delta_2 \ , & -\beta_1-\delta_1-\delta_2 \\ \beta_1+\beta_2+2\delta_1 \ , & -\delta_2 \end{cases} \\
Q_2^{SP_4} &: \begin{cases} -\beta_1-2\delta_2 \ , & \beta_1+\beta_2+\delta_1+\delta_2 \\ -\beta_1-\beta_2-2\delta_1 \ , & \beta_1+\delta_2 \end{cases} \\
Q_3^{SP_4} &: \begin{cases} \beta_1 \ , & -\beta_1-\beta_2-\delta_1 \\ \beta_2 \ , & -\beta_1-\delta_2 \end{cases} \\
Q_4^{SP_4} &: \begin{cases} -\beta_1 \ , & -\delta_1 \\ -\beta_2 \ , & -\delta_2 \end{cases}
\end{aligned}
\tag{5.27}
$$

The graph of $Q_1^{SP_4}$ is given by Fig. 12.

In the end, we notice that the mutation groups $H_{stg}^{SU_4}$ and $H_{stg}^{SP_4}$ are two different representations of the dihedral Dih_8 group. Notice also that the 20 BPS states are precisely given by the number

$$2\times \dim SP\,(4) \tag{5.28}$$

which is equal to $\frac{5}{6}N_{bps}^{SU_4}$. By using the group homomorphisms $SP\,(4)\simeq SO\,(5)$ and $SU\,(4)\simeq SO\,(6)$; it follows that the number of BPS and anti-BPS states of the $\mathfrak{Q}_{stg}^{B_2}$ chamber is $\frac{5}{6}$ of the $\mathfrak{Q}_{stg}^{D_3}$ chamber where D_3 refers to $so\,(6)$. This property can be compared with the number $2\times\dim SO\,(7)$ obtained in section 4 where the number of the BPS states of $\mathfrak{Q}_{stg}^{B_3}$ chamber is $\frac{7}{8}$ time the number of BPS states of the $\mathfrak{Q}_{stg}^{D_4}$ chamber. With these two results it seems natural to conjecture that the number $N_{bps}^{SO_{2r-1}}$ BPS states of the strong $\mathfrak{Q}_{stg}^{B_{r-1}}$ chamber is $\frac{2r-1}{2r}$ times the number $N_{bps}^{SO_{2r}}$ of BPS states of the $\mathfrak{Q}_{stg}^{D_r}$ chamber; in other words we have the following relation between the two numbers of BPS states

$$N_{bps}^{SO_{2r-1}}=\frac{2r-1}{2r}N_{bps}^{SO_{2r}} \tag{5.29}$$

for finite dimensional Lie algebra B_r series with rank $r\geq 3$.

6. Conclusion

In this paper, we have developed the basis of a method to study the BPS states of 4d $\mathcal{N}=2$ supersymmetric gauge theories with non-simply laced type gauge invariance. To obtain the set of these BPS states for non-simply laced type gauge symmetries, we have taken advantage of

three helpful things: (i) known results on BPS spectra of 4d $\mathcal{N}=2$ QFT with ADE type gauge symmetries; (ii) the folding link between ADE and BCFG Dynkin diagrams; and (iii) outer-automorphisms of the BPS quivers Q_n^G of ADE type; these outer-automorphisms are inherited from the corresponding ADE Dynkin diagrams. To illustrate the approach, we have considered in present study the explicit construction of the BPS states of the strong chamber of two particular $\mathcal{N}=2$ models namely the supersymmetric pure SO$(7,\mathbb{R})$ and SP$(4,\mathbb{R})$ gauge theories. To derive the BPS spectra of these typical models, we have developed a *quiver folding method* extending the usual folding of simply laced Dynkin diagrams to obtain non-simply laced Dynkin graphs. This quiver folding approach has taught us an interesting feature which, to our knowledge, was unknown before; the particular quiver mutation sets $H_{stg}^{SO_7}$ given by eq. (4.25) and $H_{strg}^{SO_8}$ of eq. (3.27) respectively generating BPS states in the strong chambers $\mathfrak{Q}_{stg}^{SO_7}$ and $\mathfrak{Q}_{stg}^{SO_8}$ are in fact intimately related quiver mutation symmetry groups; they are just two different representations of the dihedral group Dih_{12}. The same result has been found to be valid for the mutation sets $H_{stg}^{SP_4}$ given by eq. (5.25) and $H_{stg}^{SU_4}$ of eq. (5.9) generating BPS states in the corresponding chambers $\mathfrak{Q}_{stg}^{SP_4}$ and $\mathfrak{Q}_{stg}^{SU_4}$; here also the two mutation groups $H_{stg}^{SP_4}$ and $H_{stg}^{SU_4}$ are two different representations of the dihedral group Dih_8; we suspect that this feature is a general property that holds for mutation sets $H_{stg}^{SO_{2n-1}}$ and $H_{stg}^{SO_{2n}}$ as well as for those $\mathcal{N}=2$ supersymmetric theories with exceptional F_4 and G_2 gauge symmetries. Recall that the Dynkin diagram of SO$(7,\mathbb{R})$ can be obtained by folding the Dynkin diagram of SO$(8,\mathbb{R})$ as in Fig. 6; and the Dynkin diagram of SP$(4,\mathbb{R})$ is obtained by folding the Dynkin diagram of SU(4) like in Fig. 11. Using these graph relationships, and knowing the BPS spectra of the strong chamber of $\mathcal{N}=2$ pure SO$(8,\mathbb{R})$ and SU(4) gauge models, we have derived those BPS spectra of the corresponding SO$(7,\mathbb{R})$ and SP$(4,\mathbb{R})$ models by help of the quiver folding method; we have found that for the non-simply laced SO$(7,\mathbb{R})$ and SP$(4,\mathbb{R})$ gauge symmetries, the number of BPS states of the strong chamber is not given by the ADE-type formula $2(\dim G - rank G)$; but just by $2\dim G$; we suspect that this feature holds for all supersymmetric models with BCFG gauge invariance as shown on eq. (5.29) for the SO$(2n+1,\mathbb{R})$ series; but a refined analysis is still needed before a final answer. The next step in this study aims to extend the construction done for $\mathcal{N}=2$ pure SO$(7,\mathbb{R})$ and SP$(4,\mathbb{R})$ gauge models to the general supersymmetric gauge theories; in particular to the study of 4d $\mathcal{N}=2$ theories with non-simply laced exceptional F_4 and G_2 gauge symmetries; and also to the building of the weak coupling chambers. Progress in these directions will be reported in a future occasion.

7. Appendices

In this section, we give three appendices where we report some technical details, first on the set of quiver mutations and second on the derivation of the folding operator both for Dynkin diagrams and BPS quivers.

7.1. Appendix I: mutation set of strong chamber

In this section, we first describe aspects of the quiver mutations for the strong chamber of the BPS quiver theory with underlying gauge symmetries given by SU(4) and SP$(4,\mathbb{R})$; then we make comments on the extension to those with SO(8) and SO(7) gauge symmetries. Recall that the Dynkin diagrams of the Lie algebra of SP$(4,\mathbb{R})$ and SO(7) are respectively obtained by folding the Dynkin diagrams of SU(4) and SO(8).

7.1.1. Quiver mutation set $\mathcal{G}_{stg}^{SU_4}$

The set of quiver mutations of the strong chamber of 4d $\mathcal{N}=2$ supersymmetric pure SU(4) gauge model is a group generated by 6 fundamental reflections; say three $t_1=r_1, t_2=r_2, t_3=r_3$ generators for the dyons in the primitive quiver; and three $t_4=s_1, t_5=s_2, t_6=s_3$ for monopoles partner. These reflections can be realised by 6×6 matrices as follows

$$r_1^{su_4}=\begin{pmatrix}1&0&0&0&0&0\\0&1&0&1&0&0\\0&0&1&0&0&0\\0&0&0&-1&0&0\\0&0&0&0&1&0\\0&0&0&0&0&1\end{pmatrix}\quad,\quad r_2^{su_4}=\begin{pmatrix}1&0&0&0&1&0\\0&1&0&0&0&0\\0&0&1&0&1&0\\0&0&0&1&0&0\\0&0&0&0&-1&0\\0&0&0&0&0&1\end{pmatrix}\tag{7.1}$$

and

$$r_3^{su_4}=\begin{pmatrix}1&0&0&0&0&0\\0&1&0&0&0&1\\0&0&1&0&0&0\\0&0&0&1&0&0\\0&0&0&0&1&0\\0&0&0&0&0&-1\end{pmatrix}\quad,\quad s_1^{su_4}=\begin{pmatrix}-1&0&0&0&0&0\\0&1&0&0&0&0\\0&0&1&0&0&0\\0&0&0&1&0&0\\1&0&0&0&1&0\\0&0&0&0&0&1\end{pmatrix}\tag{7.2}$$

as well as

$$s_2^{su_4}=\begin{pmatrix}1&0&0&0&0&0\\0&-1&0&0&0&0\\0&0&1&0&0&0\\0&1&0&1&0&0\\0&0&0&0&1&0\\0&1&0&0&0&1\end{pmatrix}\quad,\quad s_3^{su_4}=\begin{pmatrix}1&0&0&0&0&0\\0&1&0&0&0&0\\0&0&-1&0&0&0\\0&0&0&1&0&0\\0&0&1&0&1&0\\0&0&0&0&0&1\end{pmatrix}\tag{7.3}$$

The set of mutations $\mathcal{G}_{stg}^{SU_4}$ has a Coxeter group structure generated by the generators t_i satisfying the following relations $\left(t_it_j\right)^{m_{ij}^{SU_4}}=I_{id}^{SU_4}$ where $m_{ij}^{SU_4}$ stand for the elements of an integral 6×6 symmetric matrix M^{SU_4} known as the Coxeter matrix which is given by

$$M^{SU_4}=\begin{pmatrix}1&2&2&2&3&2\\2&1&2&3&2&3\\2&2&1&2&3&2\\2&3&2&1&2&2\\3&2&3&2&1&2\\2&3&2&2&2&1\end{pmatrix}\tag{7.4}$$

For the particular case $m_{ij}=2$, the condition $\left(t_it_j\right)^2=I_{id}$ leads as well to $t_it_j=t_jt_i$. To generate the BPS states of the strong chamber of 4d $\mathcal{N}=2$ supersymmetric pure SU(4) gauge theory, we have used the particular subgroup $H_{stg}^{SU_4}$ (2.14) of the Coxeter $\mathcal{G}_{stg}^{SU_4}$; this subgroup is generated by the two composite mutations $L_1=r_3r_2r_1$ and $L_2=s_3s_2s_1$ acting as depicted by Figs. 13–14. This construction extends straightforwardly to the Coxeter group $\mathcal{G}_{stg}^{SO_8}$ of the strong chamber 4d $\mathcal{N}=2$ supersymmetric pure SO(8) gauge theory. There, we have 8 reflections realised by 8×8 matrices obeying $\left(t_it_j\right)^{m_{ij}^{SO_8}}=I_{id}^{SO_8}$ where now the $m_{ij}^{SO_8}$'s are the entries of 8×8 Coxeter

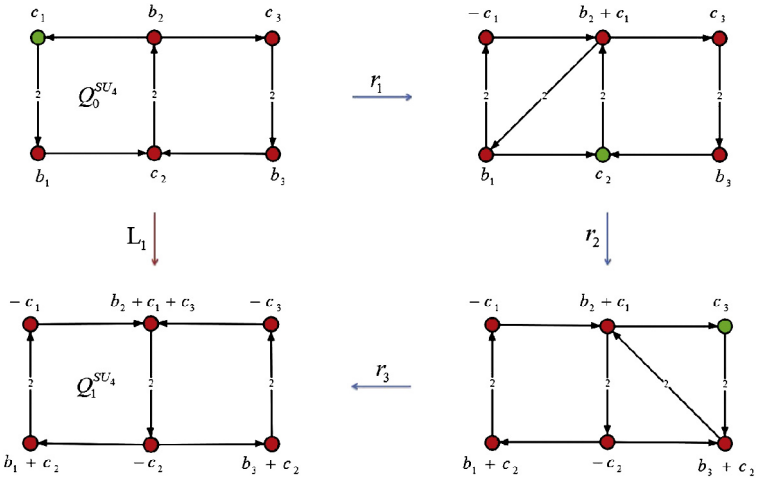

Fig. 13. BPS quiver $Q_1^{SU_4}$ of the 4d $\mathcal{N}=2$ pure gauge model with SU(4) gauge invariance after performing three successive fundamental reflections $L_1 = r_3 r_2 r_1$ on $Q_0^{SU_4}$.

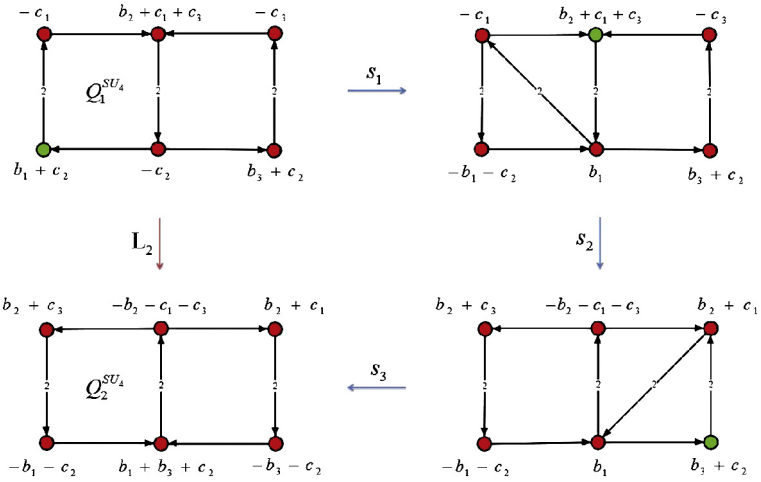

Fig. 14. BPS quiver $Q_2^{SU_4}$ of the 4d $\mathcal{N}=2$ pure gauge model with SU(4) gauge invariance after performing three successive fundamental reflections $L_2 = s_3 s_2 s_1$ on $Q_1^{SU_4}$.

matrix M^{SO_8}. The analogue of the subgroup $H_{stg}^{SU_4}$ is given by $H_{stg}^{SO_8}$; it has two generators given by $L_1^{SO_8} = r_4 r_3 r_2 r_1$ and $L_2^{SO_8} = s_4 s_3 s_2 s_1$. For completeness, the explicit expressions of these 8 fundamental reflections are given in eqs. (7.9)–(7.11). Notice by the way that $SU(4) \simeq SO(6)$; and so the above results can be straightforwardly generalised to the full series of SO$(2n)$ gauge symmetries.

7.1.2. Mutation group $\mathcal{G}_{stg}^{SP_4}$

The set $\mathcal{G}_{stg}^{SP_4}$ of mutations of the strong chamber of 4d $\mathcal{N}=2$ supersymmetric pure SP$(4,\mathbb{R})$ gauge model is a group generated by 4 reflections: $t_1 = r_1$, $t_2 = r_2$ generators for the dyons in the

primitive quiver; and $t_3 = s_1$, $t_4 = s_2$ for corresponding monopoles. These reflections are realised by 4×4 matrices like

$$r_1^{sp_4} = \begin{pmatrix} 1 & 0 & 0 & 0 \\ 1 & 1 & 2 & 0 \\ -1 & 0 & -1 & 0 \\ 0 & 0 & 0 & 1 \end{pmatrix} \quad , \quad r_2^{sp_4} = \begin{pmatrix} 1 & 0 & 0 & 2 \\ 0 & 1 & 0 & 0 \\ 0 & 0 & 1 & -1 \\ 0 & 0 & 0 & -1 \end{pmatrix} \tag{7.5}$$

and

$$s_1^{sp_4} = \begin{pmatrix} -1 & 0 & 0 & 0 \\ 0 & 1 & 0 & 0 \\ 1 & 0 & 1 & 0 \\ 1 & 0 & 0 & 1 \end{pmatrix} \quad , \quad s_2^{sp_4} = \begin{pmatrix} 1 & 0 & 0 & 0 \\ 0 & -1 & 0 & 0 \\ 0 & 1 & 1 & 0 \\ 0 & 0 & 0 & 1 \end{pmatrix} \tag{7.6}$$

The set of mutation $\mathcal{G}_{stg}^{SP_4}$ has a Coxeter group structure with generators t_i satisfying $\left(t_i t_j\right)^{m_{ij}^{SP_4}} = I^{SP_4}$ where the $m_{ij}^{SP_4}$ integers are the entries of the Coxeter matrix

$$M^{SP_4} = \begin{pmatrix} 1 & 2 & 2 & 4 \\ 2 & 1 & 4 & 2 \\ 2 & 4 & 1 & 2 \\ 4 & 2 & 2 & 1 \end{pmatrix} \tag{7.7}$$

These reflections are related to the $\mathcal{G}_{stg}^{SU_4}$ ones by using Folding matrices $\boldsymbol{F}$ and $\tilde{\boldsymbol{F}}$ obeying $\boldsymbol{F}\tilde{\boldsymbol{F}} = I$; these matrices have been explicitly constructed in section 5 of present study; we have:

$$\begin{aligned} r_1^{sp_4} &= \boldsymbol{F}\left(r_1^{su_4} r_3^{su_4}\right)\tilde{\boldsymbol{F}} \\ r_2^{sp_4} &= \boldsymbol{F} r_2^{su_4}\tilde{\boldsymbol{F}} \\ s_1^{sp_4} &= \boldsymbol{F}\left(s_1^{su_4} s_3^{su_4}\right)\tilde{\boldsymbol{F}} \\ s_2^{sp_4} &= \boldsymbol{F} s_2^{su_4}\tilde{\boldsymbol{F}} \end{aligned} \tag{7.8}$$

To generate BPS states in the strong chamber of 4d $\mathcal{N}=2$ supersymmetric pure $\mathrm{SP}(4,\mathbb{R})$ gauge theory, we have used the two composite mutation operators $\mathcal{L}_1 = r_2 r_1$ and $\mathcal{L}_2 = s_2 s_1$.

7.1.3. Quiver mutation set $\mathcal{G}_{stg}^{SO_8}$

The set of mutations of the strong chamber of 4d $\mathcal{N}=2$ supersymmetric pure $\mathrm{SO}(8)$ gauge model is a group generated by 8 fundamental reflections; say four $t_1 = r_1$, $t_2 = r_2$, $t_3 = r_3$, $t_4 = r_4$ generators for the dyons in the primitive quiver; and four $t_5 = s_1$, $t_6 = s_2$, $t_7 = s_3$, $t_8 = s_4$ for monopoles. These reflections can be realised by 8×8 matrices as follows:

$$r_1^{so_8} = \begin{pmatrix} 1 & 0 & 0 & 0 & 0 & 0 & 0 & 0 \\ 0 & 1 & 0 & 0 & 1 & 0 & 0 & 0 \\ 0 & 0 & 1 & 0 & 0 & 0 & 0 & 0 \\ 0 & 0 & 0 & 1 & 0 & 0 & 0 & 0 \\ 0 & 0 & 0 & 0 & -1 & 0 & 0 & 0 \\ 0 & 0 & 0 & 0 & 0 & 1 & 0 & 0 \\ 0 & 0 & 0 & 0 & 0 & 0 & 1 & 0 \\ 0 & 0 & 0 & 0 & 0 & 0 & 0 & 1 \end{pmatrix} \quad , \quad r_2^{so_8} = \begin{pmatrix} 1 & 0 & 0 & 0 & 0 & 1 & 0 & 0 \\ 0 & 1 & 0 & 0 & 0 & 0 & 0 & 0 \\ 0 & 0 & 1 & 0 & 0 & 1 & 0 & 0 \\ 0 & 0 & 0 & 1 & 0 & 1 & 0 & 0 \\ 0 & 0 & 0 & 0 & 1 & 0 & 0 & 0 \\ 0 & 0 & 0 & 0 & 0 & -1 & 0 & 0 \\ 0 & 0 & 0 & 0 & 0 & 0 & 1 & 0 \\ 0 & 0 & 0 & 0 & 0 & 0 & 0 & 1 \end{pmatrix} \tag{7.9}$$

$$r_3^{so_8} = \begin{pmatrix} 1 & 0 & 0 & 0 & 0 & 0 & 0 & 0 \\ 0 & 1 & 0 & 0 & 0 & 0 & 1 & 0 \\ 0 & 0 & 1 & 0 & 0 & 0 & 0 & 0 \\ 0 & 0 & 0 & 1 & 0 & 0 & 0 & 0 \\ 0 & 0 & 0 & 0 & 1 & 0 & 0 & 0 \\ 0 & 0 & 0 & 0 & 0 & 1 & 0 & 0 \\ 0 & 0 & 0 & 0 & 0 & 0 & -1 & 0 \\ 0 & 0 & 0 & 0 & 0 & 0 & 0 & 1 \end{pmatrix} \quad , \quad r_4^{so_8} = \begin{pmatrix} 1 & 0 & 0 & 0 & 0 & 0 & 0 & 0 \\ 0 & 1 & 0 & 0 & 0 & 0 & 0 & 1 \\ 0 & 0 & 1 & 0 & 0 & 0 & 0 & 0 \\ 0 & 0 & 0 & 1 & 0 & 0 & 0 & 0 \\ 0 & 0 & 0 & 0 & 1 & 0 & 0 & 0 \\ 0 & 0 & 0 & 0 & 0 & 1 & 0 & 0 \\ 0 & 0 & 0 & 0 & 0 & 0 & 1 & 0 \\ 0 & 0 & 0 & 0 & 0 & 0 & 0 & -1 \end{pmatrix} \tag{7.10}$$

$$s_1^{so_8} = \begin{pmatrix} -1 & 0 & 0 & 0 & 0 & 0 & 0 & 0 \\ 0 & 1 & 0 & 0 & 0 & 0 & 0 & 0 \\ 0 & 0 & 1 & 0 & 0 & 0 & 0 & 0 \\ 0 & 0 & 0 & 1 & 0 & 0 & 0 & 0 \\ 0 & 0 & 0 & 0 & 1 & 0 & 0 & 0 \\ 1 & 0 & 0 & 0 & 0 & 1 & 0 & 0 \\ 0 & 0 & 0 & 0 & 0 & 0 & 1 & 0 \\ 0 & 0 & 0 & 0 & 0 & 0 & 0 & 1 \end{pmatrix} \quad , \quad s_2^{so_8} = \begin{pmatrix} 1 & 0 & 0 & 0 & 0 & 0 & 0 & 0 \\ 0 & -1 & 0 & 0 & 0 & 0 & 0 & 0 \\ 0 & 0 & 1 & 0 & 0 & 0 & 0 & 0 \\ 0 & 0 & 0 & 1 & 0 & 0 & 0 & 0 \\ 0 & 1 & 0 & 0 & 1 & 0 & 0 & 0 \\ 0 & 0 & 0 & 0 & 0 & 1 & 0 & 0 \\ 0 & 1 & 0 & 0 & 0 & 0 & 1 & 0 \\ 0 & 1 & 0 & 0 & 0 & 0 & 0 & 1 \end{pmatrix} \tag{7.11}$$

$$s_3^{so_8} = \begin{pmatrix} 1 & 0 & 0 & 0 & 0 & 0 & 0 & 0 \\ 0 & 1 & 0 & 0 & 0 & 0 & 0 & 0 \\ 0 & 0 & -1 & 0 & 0 & 0 & 0 & 0 \\ 0 & 0 & 0 & 1 & 0 & 0 & 0 & 0 \\ 0 & 0 & 0 & 0 & 1 & 0 & 0 & 0 \\ 0 & 0 & 1 & 0 & 0 & 1 & 0 & 0 \\ 0 & 0 & 0 & 0 & 0 & 0 & 1 & 0 \\ 0 & 0 & 0 & 0 & 0 & 0 & 0 & 1 \end{pmatrix} \quad , \quad s_4^{so_8} = \begin{pmatrix} 1 & 0 & 0 & 0 & 0 & 0 & 0 & 0 \\ 0 & 1 & 0 & 0 & 0 & 0 & 0 & 0 \\ 0 & 0 & 1 & 0 & 0 & 0 & 0 & 0 \\ 0 & 0 & 0 & -1 & 0 & 0 & 0 & 0 \\ 0 & 0 & 0 & 0 & 1 & 0 & 0 & 0 \\ 0 & 0 & 0 & 1 & 0 & 1 & 0 & 0 \\ 0 & 0 & 0 & 0 & 0 & 0 & 1 & 0 \\ 0 & 0 & 0 & 0 & 0 & 0 & 0 & 1 \end{pmatrix} \tag{7.12}$$

The set of quiver mutation $\mathcal{G}_{stg}^{SO_8}$ has a Coxeter group structure, with generators satisfying the following features $\left(t_i t_j\right)^{m_{ij}^{SO_8}} = I_{id}^{SO_8}$ where $m_{ij}^{SO_8}$ is the elements of the Coxeter 8×8 matrix

$$M^{SO_8} = \begin{pmatrix} 1 & 2 & 2 & 2 & 2 & 3 & 2 & 2 \\ 2 & 1 & 2 & 2 & 3 & 2 & 3 & 3 \\ 2 & 2 & 1 & 2 & 2 & 3 & 2 & 2 \\ 2 & 2 & 2 & 1 & 2 & 3 & 2 & 2 \\ 2 & 3 & 2 & 2 & 1 & 2 & 2 & 2 \\ 3 & 2 & 3 & 3 & 2 & 1 & 2 & 2 \\ 2 & 3 & 2 & 2 & 2 & 2 & 1 & 2 \\ 2 & 3 & 2 & 2 & 2 & 2 & 2 & 1 \end{pmatrix} \tag{7.13}$$

To generate BPS states in the strong chamber of the supersymmetric pure SO(8) gauge theory, we have used the two composite mutation operators $L_1^{SO_8} = r_4 r_3 r_2 r_1$, $L_2^{SO_8} = s_4 s_3 s_2 s_1$ generating a subgroup $H_{stg}^{SO_8} \simeq Dih_{12}$ of the Coxeter $\mathcal{G}_{stg}^{SO_8}$.

7.1.4. Quiver mutation group $\mathcal{G}_{stg}^{SO_7}$

The group $\mathcal{G}_{stg}^{SO_7}$ of quiver mutations on the strong chamber of 4d $\mathcal{N}=2$ supersymmetric pure SO(7) gauge model is a group generated by 6 fundamental reflections namely $t_1 = r_1$, $t_2 = r_2$, $t_3 = r_3$ for dyons in the primitive quiver; and $t_4 = s_1$, $t_5 = s_2$, $t_6 = s_3$ for corresponding monopoles. These reflections are realised by 6×6 matrices like

$$r_1^{so_7} = \begin{pmatrix} 1 & 0 & 0 & 0 & 0 & 0 \\ 0 & 1 & 0 & 1 & 0 & 0 \\ 0 & 0 & 1 & 0 & 0 & 0 \\ 0 & 0 & 0 & -1 & 0 & 0 \\ 0 & 0 & 0 & 0 & 1 & 0 \\ 0 & 0 & 0 & 0 & 0 & 1 \end{pmatrix} \quad , \quad r_2^{so_7} = \begin{pmatrix} 1 & 0 & 0 & 0 & 1 & 0 \\ 0 & 1 & 0 & 0 & 0 & 0 \\ 0 & 0 & 1 & 0 & 2 & 0 \\ 0 & 0 & 0 & 1 & 0 & 0 \\ 0 & 0 & 0 & 0 & -1 & 0 \\ 0 & 0 & 0 & 0 & -1 & 1 \end{pmatrix} \tag{7.14}$$

and

$$r_3^{so_7} = \begin{pmatrix} 1 & 0 & 0 & 0 & 0 & 0 \\ 0 & 1 & 1 & 0 & 0 & 2 \\ 0 & 0 & 1 & 0 & 0 & 0 \\ 0 & 0 & 0 & 1 & 0 & 0 \\ 0 & 0 & 0 & 0 & 1 & 0 \\ 0 & 0 & -1 & 0 & 0 & -1 \end{pmatrix} \quad , \quad s_1^{so_7} = \begin{pmatrix} -1 & 0 & 0 & 0 & 0 & 0 \\ 0 & 1 & 0 & 0 & 0 & 0 \\ 0 & 0 & 1 & 0 & 0 & 0 \\ 0 & 0 & 0 & 1 & 0 & 0 \\ 1 & 0 & 0 & 0 & 1 & 0 \\ 0 & 0 & 0 & 0 & 0 & 1 \end{pmatrix} \tag{7.15}$$

as well as

$$s_2^{so_7} = \begin{pmatrix} 1 & 0 & 0 & 0 & 0 & 0 \\ 0 & -1 & 0 & 0 & 0 & 0 \\ 0 & 0 & 1 & 0 & 0 & 0 \\ 0 & 1 & 0 & 1 & 0 & 0 \\ 0 & 0 & 0 & 0 & 1 & 0 \\ 0 & 1 & 0 & 0 & 0 & 1 \end{pmatrix} \quad , \quad s_3^{so_7} = \begin{pmatrix} 1 & 0 & 0 & 0 & 0 & 0 \\ 0 & 1 & 0 & 0 & 0 & 0 \\ 0 & 0 & -1 & 0 & 0 & 0 \\ 0 & 0 & 0 & 1 & 0 & 0 \\ 0 & 0 & 1 & 0 & 1 & 0 \\ 0 & 0 & 1 & 0 & 0 & 1 \end{pmatrix} \tag{7.16}$$

The set of quiver mutation $\mathcal{G}_{stg}^{SO_7}$ has a Coxeter group structure with group law $\left(t_i t_j\right)^{m_{ij}^{so_7}} = I_{id}^{so_7}$ where $m_{ij}^{so_7}$'s are entries of the Coxeter 6×6 matrix

$$M^{so_7} = \begin{pmatrix} 1 & 2 & 2 & 2 & 3 & 2 \\ 2 & 1 & 2 & 3 & 2 & 4 \\ 2 & 2 & 1 & 2 & 4 & 2 \\ 2 & 3 & 2 & 1 & 2 & 2 \\ 3 & 2 & 4 & 2 & 1 & 2 \\ 2 & 4 & 2 & 2 & 2 & 1 \end{pmatrix} \tag{7.17}$$

The analogue of eqs. (7.8) read in present case as follows

$$\begin{aligned} r_1^{so_7} &= \boldsymbol{F} r_1^{so_8} \tilde{\boldsymbol{F}} \quad , \quad s_1^{so_7} = \boldsymbol{F}.s_1^{so_8}.\tilde{\boldsymbol{F}} \\ r_2^{so_7} &= \boldsymbol{F} r_2^{so_8} \tilde{\boldsymbol{F}} \quad , \quad s_2^{so_7} = \boldsymbol{F}.s_2^{so_8}.\tilde{\boldsymbol{F}} \\ r_3^{so_7} &= \boldsymbol{F}\left(r_4^{so_8} r_3^{so_8}\right)\tilde{\boldsymbol{F}} \quad , \quad s_3^{so_7} = \boldsymbol{F}\left(s_4^{so_8}.s_3^{so_8}\right)\tilde{\boldsymbol{F}} \end{aligned} \tag{7.18}$$

BPS states in the strong chamber of the $\mathcal{N}=2$ supersymmetric pure SO(7) gauge theory have been obtained by using the two composite mutation operators $\mathcal{L}_1 = r_3 r_2 r_1$, $\mathcal{L}_2 = s_3 s_2 s_1$ generating the subgroup $H_{stg}^{so_7}$ as shown in section 4 of this paper.

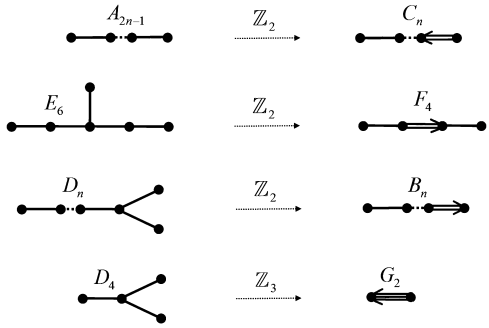

Fig. 15. Folding simply laced Dynkin diagrams.

7.2. Appendix II: folding operators

In this section, we first derive the folding operator mapping ADE type Dynkin diagrams of finite dimensional Lie algebras into BCFG type descendent. Then we extend the construction to describe BPS quivers of BCFG type by folding BPS quivers of ADE type.

7.2.1. Folding ADE Dynkin diagrams

Every non-laced Dynkin diagram of finite dimensional Lie algebra type BCFG can be obtained by folding simply laced diagrams of ADE type as shown in Fig. 15. Indeed certain simply laced ADE Dynkin diagrams admit outer-automorphisms; for example the $\mathbb{Z}_2$ type automorphisms of A_{2r} and D_r lead respectively the C_r and B_r series. Notice that the Dynkin diagram of D_4 has $\mathbb{Z}_2$ and $\mathbb{Z}_3$ outer-automorphisms; folding by $\mathbb{Z}_3$ automorphism leads to the Dynkin diagram of the G_2 Lie algebra.

Using the fact that each Dynkin diagram D_G is the graphic representation of the Cartan matrix K_G describing the intersection of the simple roots of the Lie algebra of G, it is natural to define the folding map between simply laced diagrams and non-simply laced ones in terms of the corresponding intersection matrices. To that purpose, let D_G be the Dynkin diagram of a given simply laced Lie algebra of a gauge symmetry G with Cartan matrix K_G; and let D_{G^*} be the Dynkin diagram of the corresponding non-simply laced Lie algebra of G^* with Cartan matrix K_{G^*}. Thinking by the folding D_G/D_{G^*} as a mapping $\mathbf{f}: D_G \to D_{G^*}$, one can check that the corresponding Cartan matrices are related as

$$K_{G^*}.\mathbf{f} = \mathbf{f}.K_G \tag{7.19}$$

From this relation, we learn that by considering a $\tilde{\mathbf{f}}$ such that $\mathbf{f}.\tilde{\mathbf{f}} = I$, we obtain

$$K_{\hat{G}} = \mathbf{f}.K_G.\tilde{\mathbf{f}} \tag{7.20}$$

As noticed in sections 4 of this paper, the "adjoint" operator $\tilde{\mathbf{f}}$ is not uniquely defined; but can be chosen like $\mathbf{f}^T\left(\mathbf{f}\mathbf{f}^T\right)^{-1}$.

7.2.2. Folding BPS quivers

The derivation of folding in BPS quiver theory, for gauge symmetries with BCFG type, is quite similar to the folding of Dynkin diagrams of finite dimensional Lie algebras; thanks to outer-automorphisms of BPS quivers and to the intersection matrix which are expressed in terms of the Cartan Matrix. These properties allow to extend the folding method of Dynkin diagrams of

Lie algebras to BPS quivers of 4d $\mathcal{N}=2$ supersymmetric gauge theory. In this case, the folding operator F mapping the set $\mathfrak{Q}^G$ to $\mathfrak{Q}^{G^*}$ respectively characterised by the intersection matrices $\mathcal{A}^G$ and $\mathcal{A}^{G^*}$ given by eq. (2.7) and (2.10)

$$\mathcal{A}^G=\begin{pmatrix}0 & -K_G\\ K_G & 0\end{pmatrix} \quad , \quad \mathcal{A}^{G^*}=\begin{pmatrix}0 & -K_{G^*}^T\\ K_{G^*} & K_{G^*}^T-K_{G^*}\end{pmatrix} \tag{7.21}$$

is expressed in terms of $\mathbf{f}$ and $\tilde{\mathbf{f}}$ of Dynkin diagrams as follows

$$\boldsymbol{F}=\begin{pmatrix}\tilde{\mathbf{f}}^T & 0\\ \mathbf{f}-\tilde{\mathbf{f}}^T & \mathbf{f}\end{pmatrix} \tag{7.22}$$

By using eqs. (7.20), (7.21), (7.22), a straightforward calculation leads to the relation

$$\mathcal{A}^{G^*}=\boldsymbol{F}\mathcal{A}^G\boldsymbol{F}^T \tag{7.23}$$

leading in turns to $\boldsymbol{N}_n=\boldsymbol{F}\boldsymbol{M}_n\tilde{\boldsymbol{F}}$ giving the relationship between $\boldsymbol{N}_n$ mutations of type BCFG to $\boldsymbol{M}_n$ mutations of type ADE. This link implies that quiver mutation groups $H_{stg}^{G^*}$ and H_{stg}^{G} of the strong chambers are homomorphic.

8. Appendix III: BPS quivers of $\mathcal{N}=2$ QFT$_4$

In this appendix, we collect helpful tools behind the quiver mutation method for building the BPS spectra of 4d $\mathcal{N}=2$ supersymmetric gauge theories with ADE gauge symmetry groups. This quiver mutation method *augmented* by quiver folding ideas of Dynkin diagrams of ADE Lie algebras has been used in this paper for approaching the construction of BPS spectra of $\mathcal{N}=2$ QFTs with non-simply laced gauge symmetries. More details on the basis underlying the mutation method and explicit illustrations can be found in the defining works of refs. [1,2]; see also [3,4] for discrete group theoretical interpretations. Here, we focus on those aspects relevant for our study.

The organisation of this appendix is as follows: First, we introduce the BPS quivers Q^G encoding the data on BPS states of supersymmetric pure gauge theories with gauge group G. Then, we show through simple examples how to build BPS bound states by using the so-called stable quiver representations encoding the solutions of F- and D-term equations of the supersymmetric quantum mechanics underlying BPS quiver theory. After that, we describe succinctly the quiver mutation method for building chambers of BPS/anti-BPS states; this is a powerful method that has been used in this paper; it knows about non-degenerate superpotential W^G; and allows to overcome the problem of solving the non-trivial representation theory problem. We end this appendix by studying superpotentials W^{SO_8}, W^{SU_4} and W^{SO_7}, W^{SP_4} that are associated with the quivers considered in this study; the general structure of this kind of superpotentials has been obtained by Cecotti and Del Zotto in [38].

8.1. From BPS states to BPS quivers

Given a $\mathcal{N}=2$ supersymmetric QFT$_4$ like the ones studied in this paper with pure ADE type gauge symmetry G, one has in general a great number of BPS/anti-BPS states living in the BPS chambers of this theory. It is a very remarkable observation that all these states can be generated by starting from a simple quiver Q_0^G. A direct way to introduce the idea behind the link between the BPS states of $\mathcal{N}=2$ gauge theory and the primitive quiver Q_0^G is through

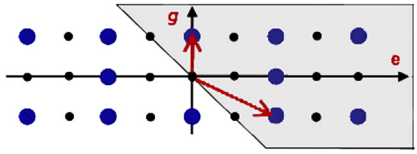

Fig. 16. The BPS and anti-BPS states of infinite weak chamber of the pure $\mathcal{N}=2$ SU(2) gauge theory. Blue dots correspond to the EM charges of the BPS/anti-BPS states. Notice that the strong chamber is finite; it has four states, a monopole; a dyon and their antiparticles. BPS states live in upper half-plane given by the gray region. (For interpretation of the references to colour in this figure legend, the reader is referred to the web version of this article.)

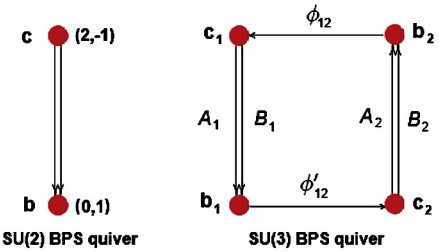

Fig. 17. On left, the BPS quiver Q_{su_2} of pure $\mathcal{N}=2$ SU(2) gauge theory. The electric–magnetic product $b\circ c=-c\circ b=-2$. On right, the BPS quiver Q_{su_3} pure $\mathcal{N}=2$ SU(3) gauge theory; this quiver has two oriented cycles; the chiral superfields A_1, A_2, B_1, B_2, Φ_{12}, Φ'_{12} and their superpotential will be discussed later.

illustrating examples like the SU(2) and SU(3) models without matter; other useful examples are given by the Argyres–Douglas A-models whose general aspects will be described latter. Once we learn how the machinery works on these models, one can then extend the construction to $\mathcal{N}=2$ supersymmetric theories with bigger gauge symmetries.

8.1.1. The $Q_0^{su_2}$ and $Q_0^{su_3}$ examples

The simplest example of BPS quiver theory is certainly the $\mathcal{N}=2$ pure gauge model with SU(2) gauge group which, in language of quivers, is described with a $Q_0^{su_2}$ having two nodes. In this theory, the BPS/anti-BPS states sit in two chambers: weak $\mathfrak{Q}_{weak}^{su_2}$ and strong $\mathfrak{Q}_{stg}^{su_2}$. While $\mathfrak{Q}_{stg}^{su_2}$ is finite with cardinality equals to 4, the number of BPS and anti-BPS particles contained in $\mathfrak{Q}_{weak}^{su_2}$ is infinite. The electric–magnetic (EM) charges of the BPS (resp. anti-BPS) states of weak chamber are well known; they read in the $\{e, g\}$ basis as follows

$$\begin{aligned}\gamma_{n,+}^{bps} &= 2ne+g\\ \gamma_{1,0}^{bps} &= 2e\\ \gamma_{n,-}^{bps} &= 2(n+1)e-g\end{aligned}\tag{8.1}$$

these sequences include the purely electrical charged $W^{\pm}$-boson with charge $\pm 2e$. The EM charges of BPS and anti-BPS states form a 2-dim lattice Γ_{su_2} as in Fig. 16 with generators (b, c) given by the EM charge $b=0e+g$ of the monopole $\mathfrak{M}$ and the charge $c=2e-g$ of the dyon $\mathfrak{D}$. The BPS quiver $Q_0^{su_2}$ encoding data on BPS states in Fig. 16 is given by the left diagram of Fig. 17 with two nodes b and c linked by two arrows. Each node of the pure SU(2) BPS quiver represents therefore a basis vector of the BPS spectrum; and the double arrow encodes the Dirac pairing $b\circ c=-2$.

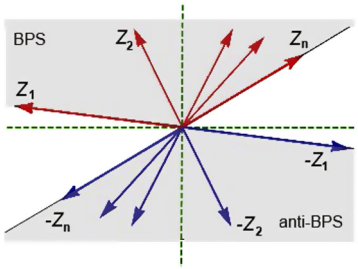

Fig. 18. Cones of BPS and anti-BPS states represented by rays in the in central charge complex plane. The arguments of the complex charges are ordered like in eq. (8.4). Left most Z_1 and right most Z_n are central charges of nodes of a BPS quiver.

From this example, one can easily extend the construction to gauge symmetry groups G of type ADE; the primitive Q_0^G quivers extending $Q_0^{su_2}$ can be straightforwardly drawn just by linking copies of SU (2) as in the building of higher rank Dynkin diagrams. A simple example of this extension is given by $Q_0^{su_3}$, the right diagram of Fig. 17 describing the BPS quiver of the pure SU (3) gauge model; it has four nodes $\{b_1, c_1, b_2, c_2\}$ associated with four elementary BPS states. The construction of BPS quivers for the family of pure SU $(r+1)$ theory is therefore direct; it is just a linear replication of the BPS quiver for pure SU (2). In this case we have $2r$ elementary BPS states with EM charges $\{b_i, c_i\}_{1\leq i\leq r}$. Similar BPS quivers can be drawn for the D_r and E_r series; they are obtained by mimicking the corresponding Dynkin diagrams with each node replaced by two nodes as in the examples given by Fig. 17. Notice moreover, that this BPS quiver description applies as well for more general supersymmetric theories; in particular in the presence of matter and flavor symmetries.

8.1.2. EM lattice Γ_{2r} and central charge plane

A nice way to deal with the EM charges γ of the BPS states of a $\mathcal{N}=2$ QFT$_4$ with symmetry group G is to use the complex central charge Z_u at a given point u in the Coulomb branch $\mathcal{U}$ of the gauge theory. This is obtained by mapping EM charge vectors γ of generic BPS states into complex numbers $Z_u(\gamma)$ thought in terms of rays in the complex plane of the central charge

$$\begin{array}{rccl} Z_u & : & \Gamma_{2r} & \to & \mathbb{C} \\ & & \gamma & \to & Z(\gamma) \end{array} \tag{8.2}$$

the amplitudes $|Z_u(\gamma)|$ describe the masses M_γ of BPS particle. Notice that the BPS quiver Q_0^G whose nodes were associated with the lattice basis $\gamma_i^{\pm} = (b_i, c_i)$ of the elementary BPS particles can be also interpreted in terms of the central charges $Z_u\left(\gamma_i^{\pm}\right)$ of elementary monopoles and dyons. BPS bound states with EM charge γ given by positive integral linear combinations $n_i^+\gamma_i^- + n_i^-\gamma_i^+$ have complex charges given by the sums

$$Z_u(\gamma) = \sum n_i^+ Z_u\left(\gamma_i^-\right) + n_i^- Z_u\left(\gamma_i^+\right) \tag{8.3}$$

They are represented by rays in the upper half plane of the complex charge as in Fig. 18. Given that $Z_u(\gamma)$'s are complex functions, we then have two kinds of real degrees: the masses M_γ of the BPS particles; and the phases $\arg Z(\gamma)$ playing an important role in ordering the BPS particle rays in the upper half plane of the central charge. In Fig. 18, we exhibit an ordering of the BPS particle rays by using the arguments of the complex central charges

$$\pi + \varphi_0 > \arg Z_1 > \arg Z_2 > \ldots > \arg Z_n > \varphi_0 \tag{8.4}$$

where φ_0 stands for some origin of phases. The above cone (8.4) lives in the upper half plane; the central charge Z_1 has the largest phase and is the left-most; the Z_n has the smallest phase, it is right-most. If taking $\varphi_0 = 0$, one has the usual canonical complex plane frame represented in green shaded line. In this graphic representation, the BPS states are located in the upper half plane $]0, \pi[$.

8.2. From BPS quivers to BPS spectra

In this subsection, we consider the reverse of the idea presented in above previous subsection by showing how to construct BPS bound states of $\mathcal{N} = 2$ QFTs with ADE gauge symmetries by starting form quivers Q_0^G.

After introducing the moduli space of supersymmetric ground states of SQM describing BPS states, we describe briefly the so-called quiver representation method for building BPS spectra. This method, which uses linear algebra requirements, relies on the solving of the F- and D-term equations of SQM; and so needs the knowledge of the superpotential as well as data on Fayet–Iliopoulos terms. Notice that though it allows to build the BPS spectra, the use of the quiver representation method is in practice some how cumbersome; especially that we have a more powerful one that knows about superpotentials and that leads to the same result. In what follows, let us describe rapidly the main line of the quiver representation approach; and turn after to introducing the quiver mutation method.

8.2.1. BPS bound states

BPS quivers Q_0^G based on a rank r gauge symmetry group and having a structure like the $Q_0^{su_2}$ and $Q_0^{su_3}$ of Fig. 17 encode a basis of $2r$ elementary BPS states with EM charges $\{\gamma_i\}$. Starting with a given Q_0^G, the question is how to get the full set of BPS states from it; this is a hard question since one needs extra information. To answer this central question, one borrows results from quiver gauge theories, embedded in compactified type II strings and D-branes wrapping cycles, dimensionally reduced to supersymmetric quantum mechanics (SQM). To know whether a bound state $|\Psi_\gamma\rangle$ with EM charge $\gamma = \sum n_i \gamma_i$ and central charge $Z(\gamma) = \sum n_i Z(\gamma_i)$ with positive integers n_i is indeed a BPS state, we proceed as follows:

(1) we think of the state $|\Psi_\gamma\rangle$ as a supersymmetric quantum mechanical bound state made of n_i copies of each basis particle γ_i

$$|\Psi_\gamma\rangle = \prod_i |\Psi_{\gamma_i}\rangle^{n_i} \tag{8.5}$$

(2) we deal with the BPS quiver Q_0^G in the same manner as the quiver gauge diagram used in the geometric engineering of QFTs embedded in type II strings on local Calabi–Yau manifolds [39–41]. With this interpretation, a $U(n_i)$ gauge group factor is inserted on each i-node of the quiver; and $U(n_i) \times U(n_j)$ bifundamental fields B_{ij}^a are attributed to arrows pointing from i node to j one. In other words, the BPS quiver Q_0^G whose nodes and arrows were originally a basis of hypermultiplets, now encodes the gauge group and bifundamental matter of a supersymmetric quiver quantum mechanics. Moreover, to ensure that γ is the charge of a BPS particle, we look for supersymmetric ground states described by the usual D- and F-term equations that we briefly describe in what follows.

• *D-term equations*

The existence of Fayet–Iliopoulos (FI) terms with coupling constants ν_i are due to the presence of a $U(1)^{2r}$ abelian factor coming from the diagonal abelian subgroups of the gauge group

factors $U(n_i) = U(1) \times SU(n_i)$ living at each node the quiver. These $2r$ coupling constants ν_i are related to the complex fields B^a_{ij} through the usual D-term equations $D_i = 0$ which read as follows

$$\nu_i = \sum_{\substack{\text{arrows} \\ \text{starting from i}}} \left|B^a_{ij}\right|^2 - \sum_{\substack{\text{arrows} \\ \text{ending at i}}} \left|B^a_{ki}\right|^2 \tag{8.6}$$

These parameters ν_i are related to the absolute values $|Z_i| = |Z(\gamma_i)|$ and the shifted arguments $\vartheta_i = \arg Z(\gamma_i) - \arg Z(\gamma)$ of the central charges like $\vartheta_i \times |Z_i|$ where the $Z(\gamma_i)$'s are as before and $Z(\gamma) = \sum n_i Z(\gamma_i)$, the central charge of the composite BPS particle.

• *F-term equations*

These equations are given by the vanishing of the gradient of the superpotential $W = W\left(B^a_{ij}\right)$ which is built out of concatenations of bifundamental chiral superfields involved in the cycles in the Q_0^G quiver according to the prescription of ref. [2]. This superpotential yields the F-term equations

$$F^a_{ij} = \frac{\partial W}{\partial B^a_{ij}} = 0 \tag{8.7}$$

and leads therefore to relations amongst the bifundamental fields B^a_{ij}. For the example of $Q_0^{su_3}$ quiver of the supersymmetric pure SU(3) gauge theory given by the right diagram of Fig. 17, we have six chiral superfields A_1, A_2, B_1, B_2, Φ_{12}, Φ'_{12} and two oriented cycles from which we have the following chiral superpotential [1]

$$W^{su_3} = A_1\Phi_{12}A_2\Phi'_{12} - B_1\Phi_{12}B_2\Phi'_{12} \tag{8.8}$$

In this model, there are six F-term equations leading to six constraint relations that can solved explicitly. With this description, the moduli space $\boldsymbol{M}_\gamma$ of supersymmetric ground states with charge γ is simply the solution to the F- and D-terms quotiented by the action of the unitary gauge groups

$$\boldsymbol{M}_\gamma = \left\{ B^a_{ij} \;\mid\; F^a_{ij} = 0 \;;\; D_i = 0 \right\} / \prod\nolimits_{i=1}^{r} U(n_i) \tag{8.9}$$

To deal with the space $\boldsymbol{M}_\gamma$, an approach has been developed in [1,2] taking advantage of the complex nature of the formalism by combining the power of complex analyticity of extended supersymmetry with quiver representation theory. This is achieved by promoting the unitary gauge symmetries $U(n_i)$ into the complexified groups $Gl(n_i, \mathbb{C})$; and replacing the D-term equations $D_i = 0$ by stability conditions of quiver representations as described in what follows.

8.2.2. Quiver representation method

In the language of quiver representation theory, the bifundamental fields B^a_{ij} associated with the links of the Q_0^G are thought of in terms of complex linear maps B^a_{ij}: $\mathbb{C}^{n_i} \to \mathbb{C}^{n_j}$; and the problem of determining the ground state of the supersymmetric quantum mechanics is recast into the study of stable representations R of the complex holomorphic B^a_{ij} maps obeying (8.7). The defining eq. (8.9) is reformulated as follows

$$\boldsymbol{M}_\gamma = \left\{ R = \left\{ B^a_{ij} : \mathbb{C}^{n_i} \to \mathbb{C}^{n_j} \right\} \;\mid\; F^a_{ij} = 0 \;;\; R \text{ stable} \right\} / \prod\nolimits_{i=1}^{r} Gl(n_i, C) \tag{8.10}$$

Fig. 19. Quiver of A_2 Argyres–Douglas theory.

where quiver representation R is defined by attributing a complex vector space $\mathbb{C}^{n_i}$'s for each node of the quiver, and linear maps B^a_{ij}: $\mathbb{C}^{n_i} \to \mathbb{C}^{n_j}$ for the arrows. These B^a_{ij}'s are subject to the F-term equations $F^a_{ij} = 0$ and are given modulo the action of the complexified gauge group $\prod_{i=1}^r GL(n_i, C)$. In this complex holomorphic formulation, the $D_i = 0$ equations are interpreted in terms of stability conditions of the quiver representation R. By stability of R it is meant that for all non trivial sub-representation S,

$$\begin{array}{ccc} \mathbb{C}^{n_i} & \xrightarrow{B_{ij}} & \mathbb{C}^{n_j} \\ \uparrow f & & \uparrow g \\ \mathbb{C}^{m_i} & \xrightarrow{b_{ij}} & \mathbb{C}^{m_j} \end{array} \tag{8.11}$$

with associated central charges $Z_u(\gamma_R) = \sum n_i Z_u(\gamma_i)$ and $Z_u(\gamma_s) = \sum m_i Z_u(\gamma_i)$ and positive integers $m_i \leq n_i$, we have

$$\arg Z_u(\gamma_S) < \arg Z_u(\gamma_R) \tag{8.12}$$

Any sub-representation S that violates the above condition is a destabilising sub-representation; it leads to a constraint relation amongst the n_i integers. As an illustration, notice that nodes γ_i of a quiver Q^G are always stable representations; in this particular example, the central charge vector γ_R is given by $\sum_k n^R_k \gamma_k$ with $n^R_k = \delta_{ik}$; and, by using the so-called dimension vector $d = (n_1, n_2, ..., n_{2r})$, can be written like $(0, ..., 0, 1_i, 0, ..., 0)$. This special representation R is always stable since it has no non-trivial S, and thus no destabilising sub-representations. Each node of the quiver gives a multiplicity one hypermultiplet BPS state. Below, we give two simple examples that help to illustrate the idea of the quiver representation method; they concern the A_2 and A_3 Argyres–Douglas theories [2,51,52].

• *Argyres–Douglas A_2 theory*

Consider the primitive quiver of the Argyres–Douglas A_2 theory having two nodes with central charges Z_1 and Z_2 as shown in Fig. 19; and let us work out the conditions for a bound state $\gamma = n_1\gamma_1 + n_2\gamma_2$ made of n_1 particles of type γ_1 and n_2 particles of type γ_2 to be a BPS state.

To that purpose, we can use quiver representation theory approach or more interestingly the powerful quiver mutation method. In the case of quiver representation manner, that we want to illustrate here, we think of the two nodes of the A_2 quiver in terms of the complex spaces $\mathbb{C}^{n_1}$ and $\mathbb{C}^{n_2}$ with dimension vector $d = (n_1, n_2)$ and of the arrow between the two nodes in term of a linear mapping $B : \mathbb{C}^{n_1} \longrightarrow \mathbb{C}^{n_2}$.

To determine stability of the representation $\gamma_R = n_1\gamma_1 + n_2\gamma_2$, we investigate the conditions following from eq. (8.12) for non-trivial sub-representations S. Let us start with the S_1 associated with the dimension vector $d_1 = (0, 1)$ and study the commutativity of the following diagram

$$\begin{array}{ccc} \mathbb{C}^{n_1} & \xrightarrow{B} & \mathbb{C}^{n_2} \\ \uparrow f & & \uparrow g \\ 0 & \xrightarrow{0} & \mathbb{C} \end{array} \tag{8.13}$$

There is no condition on the mapping B for this diagram to commute; and so the S_1 associated with $d_1 = (0, 1)$ is always a sub-representation. As a consequence, the stability condition (8.12)

reads as $\arg(Z_2) < \arg(n_1 Z_1 + n_2 Z_2)$. Moreover, seen that the n_1 and n_2 are positive, it follows that the bound state $\gamma_R = n_1\gamma_1 + n_2\gamma_2$ should belong to the chamber $\arg(Z_2) < \arg(Z_1)$ since

$$\arg(Z_2) < \arg(n_1 Z_1 + n_2 Z_2) < \arg(Z_1) \tag{8.14}$$

This relation shows that the ray associated with Z_2 is right-most in the upper half plane of the complex central charge Z_1 is left-most. Next we consider another sub-representation S_2; for instance the one associated with the dimension vector $d_2 = (1, 0)$ as shown in the following diagram

$$\begin{array}{ccc} \mathbb{C}^{n_1} & \xrightarrow{B} & \mathbb{C}^{n_2} \\ \uparrow{\scriptstyle f} & & \uparrow{\scriptstyle g} \\ \mathbb{C} & \xrightarrow{0} & 0 \end{array} \tag{8.15}$$

The stability of the $\gamma_R = n_1\gamma_1 + n_2\gamma_2$ demands that we should have $\arg(Z_1) < \arg(Z_2)$; but this prediction contradicts (8.14) and the S_2 with dimension vector $d_2 = (1, 0)$ is a destabilising sub-representation of R. To ensure that $\gamma_R = n_1\gamma_1 + n_2\gamma_2$ is indeed a bound state, we must forbid this sub-representation; this leads to a constraint on integers n_1 and n_2 as follows

$$n_1 \leq n_2 \tag{8.16}$$

The reason for this condition is that in this situation the diagram (8.15) don't commute; hence the linear mapping B should be injective and therefore the above condition of the complex dimensions of the $\mathbb{C}^{n_i}$ spaces associated with the two nodes of the quiver. To determine the expression of the integers n_1 and n_2, we continue the process by considering the sub-representation S_3 associated with the dimension vector $d_3 = (1, 1)$ and diagram

$$\begin{array}{ccc} \mathbb{C}^{n_1} & \xrightarrow{B} & \mathbb{C}^{n_2} \\ \uparrow{\scriptstyle f} & & \uparrow{\scriptstyle g} \\ \mathbb{C} & \xrightarrow{b} & \mathbb{C} \end{array} \tag{8.17}$$

The stability of our bound state $\gamma_R = n_1\gamma_1 + n_2\gamma_2$ requires $\arg(Z_1 + Z_2) < \arg(n_1 Z_1 + n_2 Z_2)$ which we rewrite like

$$\arg(Z_1 + Z_2) < \arg(Z_1 + \frac{n_2}{n_1} Z_2) \tag{8.18}$$

However, given that $n_1 \leq n_2$ as required by (8.16), and seen that $\arg(Z_2) < \arg(Z_1)$, we have $\arg(Z_1 + Z_2) > \arg(n_1 Z_1 + n_2 Z_2)$, and then should be forbidden. Therefore the only possibility for the bound state $\gamma = n_1\gamma_1 + n_2\gamma_2$ to be a BPS state is that the diagram (8.17) is trivial; that is $n_1 = n_2 = 1$.

To conclude, we have the BPS spectra as collected in the following table

chambers	BPS particles
$\arg(Z_2) < \arg(Z_1)$	$\gamma_1, \gamma_2, \gamma_1 + \gamma_2$
$\arg(Z_1) < \arg(Z_2)$	γ_1, γ_2

(8.19)

the BPS particles in the chamber $\arg(Z_2) < \arg(Z_1)$ of the A_2 Argyres–Douglas theory consists of the elementary BPS particles γ_1, γ_2 representing the nodes of the quiver and the bound state with charge $\gamma_1 + \gamma_2$. In the BPS chamber $\arg(Z_1) < \arg(Z_2)$, the bound state $\gamma_1 + \gamma_2$ is unstable and decays into γ_1 and γ_2. The moduli space of representations of the charge $\gamma = \gamma_1 + \gamma_2$ is given

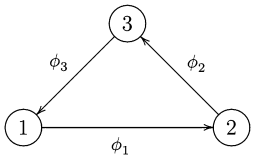

Fig. 20. Quiver of A_3 Argyres–Douglas theory.

by the quotient of a single non-zero complex number B modulo the action of the complexified gauge group which in this case is given by $\mathbb{C}^*$. Then the moduli space $\boldsymbol{M}_{\gamma_1+\gamma_2}$ is just a point; it has complex dimension $\delta = 0$ and so this representation describes a BPS multiplet of spin $\frac{1}{2}$. Recall that for $\gamma = \sum n_i \gamma_i$, the complex dimension δ of the moduli space $\boldsymbol{M}_\gamma$ is given by

$$\delta = 1 - \lambda_F + \sum_{B^a_{ij}} (n_i n_j) - \sum_{nodes\ i} n_i^2 \tag{8.20}$$

where the integer λ_F stands for the number of F-term constraints; the space $\boldsymbol{M}_\gamma$ describes a BPS multiplet of spin $\frac{\delta+1}{2}$.

• *Argyres–Douglas A_3 theory*

This is the second example we give for building BPS chambers by using quiver representation theory. The A_3 Argyres–Douglas theory described by the quiver given by Fig. 20. This quiver has three nodes and a cycle; and therefore a non-trivial superpotential which reads as follows $W = \phi_3\phi_2\phi_1$.

The three resulting F-term equations are

$$\phi_2 \circ \phi_1 = 0, \qquad \phi_3 \circ \phi_2 = 0, \qquad \phi_1 \circ \phi_3 = 0 \tag{8.21}$$

In addition to the stable node representations R_1, R_2, R_3 respectively associated with the vector dimensions $d_1 = (1,0,0)$, $d_2 = (0,1,0)$ and $d_3 = (0,0,1)$, we search for bound states $\gamma_R = n_1\gamma_1 + n_2\gamma_2 + n_3\gamma_3$ involving n_1 particles of type γ_1, n_2 particles of type γ_2 and n_3 particles of type γ_3; that is a dimension vector $d_R = (n_1, n_2, n_3)$. These bound states are described by the linear mapping $\phi_i : \mathbb{C}^{n_i} \longrightarrow \mathbb{C}^{n_{i+1}}$ mod 3

$$\mathbb{C}^{n_1} \xrightarrow{\phi_1} \mathbb{C}^{n_2} \xrightarrow{\phi_1} \mathbb{C}^{n_3} \xrightarrow{\phi_3} \mathbb{C}^{n_1} \tag{8.22}$$

To determine stability of $\gamma_R = n_1\gamma_1 + n_2\gamma_2 + n_3\gamma_3$, we study the constraints coming from eq. (8.12). Depending on the values of the integers n_i; and using the arguments of the central charges Z_i of the elementary BPS states, the bound state γ_R may sit in one of the six following chambers

$$\begin{aligned}
&\arg(Z_1) > \arg(Z_2) > \arg(Z_3)\\
&\arg(Z_1) > \arg(Z_3) > \arg(Z_2)\\
&\arg(Z_2) > \arg(Z_1) > \arg(Z_3)\\
&\arg(Z_2) > \arg(Z_3) > \arg(Z_1)\\
&\arg(Z_3) > \arg(Z_2) > \arg(Z_1)\\
&\arg(Z_3) > \arg(Z_1) > \arg(Z_2)
\end{aligned} \tag{8.23}$$

A way to work out the appropriate bound states γ_R for each of the 6 above chambers is by taking advantage of the result obtained for the example of A_2 theory since the quiver of A_3

Argyres–Douglas theory may be roughly viewed as the gluing of three copies of A_2 quivers. This observation allows to consider the stability of those bound states γ_R of the following form

$$\gamma_R = n_i\gamma_i + n_j\gamma_j \quad \text{with } i \neq j \tag{8.24}$$

These states correspond to representations with vector dimensions as $(n_1, n_2, 0)$, $(n_1, 0, n_3)$ and $(0, n_2, n_3)$; hence the analysis reduces to the A_2 model of previous example. Indeed consider bound states γ_{R_3} with dimension vector $d_{R_3} = (n_1, n_2, 0)$, these states are described by the following linear mappings

$$\mathbb{C}^{n_1} \xrightarrow{\phi_1} \mathbb{C}^{n_2} \xrightarrow{\phi_1} 0 \xrightarrow{0} \mathbb{C}^{n_1} \tag{8.25}$$

Repeating the same analysis as in the previous A_2 example, it is easy to check that stability requires that when $\arg(Z_2) < \arg(Z_1)$ regardless $\arg(Z_3)$, there is a bound states $\gamma_{R_3} = \gamma_1 + \gamma_2$ arising from the stable representation with dimension vector $d_{R_3} = (1, 1, 0)$. Hence, the BPS states of A_3 Argyres–Douglas theory contain at least the states collected in the following table

chambers	BPS particles
$\arg(Z_2) < \arg(Z_1)$	$\gamma_1, \gamma_2, \gamma_3, \gamma_1 + \gamma_2$
$\arg(Z_1) < \arg(Z_2)$	$\gamma_1, \gamma_2, \gamma_3$

(8.26)

The other remaining BPS states will arise from the ordering of the arguments of Z_3 with respect to Z_1 and to Z_2. In this regards, notice that the analysis of those other bound states γ_R with dimension vectors $d_{R_1} = (0, n_2, n_3)$ and $d_{R_2} = (n_1, 0, n_3)$ are related to $d_{R_3} = (n_1, n_1, 0)$ one just by changing the indices of the nodes γ_1, γ_2 and γ_3. Then, the representation with dimension vector $d_{R_2} = (n_1, 0, n_3)$ is just the representation with dimension vector $d_{R_3} = (n_1, n_2, 0)$ by replacing γ_3 with γ_2, γ_1 with γ_3; and γ_2 with γ_1; that by performing the cyclic permutation (132). Then BPS states of A_3 Argyres–Douglas theory living in the $\arg Z_1 < \arg Z_3$ and $\arg Z_3 < \arg Z_1$ chambers are as follows

chambers	BPS particles
$\arg(Z_1) < \arg(Z_3)$	$\gamma_1, \gamma_2, \gamma_3, \gamma_1 + \gamma_3$
$\arg(Z_3) < \arg(Z_1)$	$\gamma_1, \gamma_2, \gamma_3$

(8.27)

Similarly, the analysis of stability of representation with dimension vector $d_{R_1} = (0, n_2, n_3)$ is equivalent to the analysis of stability of representation with dimension vector $d_{R_3} = (n_1, n_2, 0)$ by preforming the cyclic permutation (123), the inverse of the previous (132). Then, BPS states of A_3 Argyres–Douglas theory which living in the $\arg Z_3 < \arg Z_2$ and $\arg Z_3 < \arg Z_2$ chambers are

chambers	BPS particles
$\arg(Z_3) < \arg(Z_2)$	$\gamma_1, \gamma_2, \gamma_3, \gamma_2 + \gamma_3$
$\arg(Z_2) < \arg(Z_3)$	$\gamma_1, \gamma_2, \gamma_3$

(8.28)

Combining (8.26), (8.27) and (8.28), we deduce the BPS spectrum of A_3 Argyres–Douglas theory as follows

Chambers	BPS states
$\arg(Z_2) < \arg(Z_1) < \arg(Z_3)$	$\gamma_1,\ \gamma_2,\ \gamma_3,\ \gamma_1+\gamma_2,\ \gamma_1+\gamma_3$
$\arg(Z_3) < \arg(Z_2) < \arg(Z_1)$	$\gamma_1,\ \gamma_2,\ \gamma_3,\ \gamma_1+\gamma_2,\ \gamma_2+\gamma_3$
$\arg(Z_1) < \arg(Z_3) < \arg(Z_2)$	$\gamma_1,\ \gamma_2,\ \gamma_3,\ \gamma_2+\gamma_3,\ \gamma_1+\gamma_3$
$\arg(Z_2) < \arg(Z_3) < \arg(Z_1)$	$\gamma_1,\ \gamma_2,\ \gamma_3,\ \gamma_1+\gamma_2$
$\arg(Z_1) < \arg(Z_2) < \arg(Z_3)$	$\gamma_1,\ \gamma_2,\ \gamma_3,\ \gamma_1+\gamma_3$
$\arg(Z_3) < \arg(Z_1) < \arg(Z_2)$	$\gamma_1,\ \gamma_2,\ \gamma_3,\ \gamma_2+\gamma_3$

(8.29)

Notice that these BPS states can be derived in a nice way by applying quiver mutation on the A_3 quiver depicted in Fig. 20.

Notice also that naive application of quiver representation theory predicts existence of another bound state namely the one with charge $\gamma_1+\gamma_2+\gamma_3$; but it is ruled out by the F-term equations.

8.2.3. Quiver mutation method

In quiver representation description illustrated above on Argyres–Douglas theory, one is restricted into BPS quivers encoding the spectrum of an $\mathcal{N}=2$ quantum field theory at a specific point u on the Coulomb branch $\mathcal{U}$. For small deformations of the stability condition in moduli space, the set of quiver representations are unchanged and the corresponding BPS states are stable. This property means that quiver representation theory can be viewed as local theory of BPS particles on a patch in $\mathcal{U}$ where (8.12) still holds. However at certain real codimension one loci in moduli space, one may encounter one of the two following situations:

- *A marginal stability wall* corresponding to the situation where the central charge $Z_u(\gamma_R)$ of some representation R and the central charge $Z_u(\gamma_S)$ of a sub-representation S become aligned $\arg Z_u(\gamma_S)=\arg Z_u(\gamma_R)$. On one side of this wall of marginal stability we have the property $\arg Z_u(S)<\arg Z_u(R)$; so the quiver representation R is stable and hence the corresponding BPS particle exists. On the other side of the wall, we have $\arg Z_u(S)>\arg Z_u(R)$ and then the R is no longer stable. On this side of the wall; the associated particle γ_R disappears from the BPS spectrum; it decays into lighter BPS states.
- *A wall of second kind* [53,2]; it is given by the situation where the central charge of a basis BPS particle γ_i of a quiver Q^G becomes real, $Z_u(\gamma_i)\in\mathbb{R}$. Across this wall, the quiver description of the BPS spectrum breaks down entirely; on the left the wall we have the BPS quiver Q^G describing a set BPS states with EM charges γ_i and central charges $Z(\gamma_i)$ as in Fig. 18; and on the right of the wall we have another BPS quiver $\tilde{Q}^G$ describing BPS state with EM charge $\tilde{\gamma}_i$ and central charges $Z(\tilde{\gamma}_i)$ as in Fig. 21. The transformation of a quiver across the wall of the second kind is given by the so-called quiver mutation $\tilde{\mu}$ describing a quantum mechanical duality relating the states of two distinct quivers.

$$\tilde{\mu}: Q^G \to \tilde{Q}^G \tag{8.30}$$

With this mutation, we then dispose of a quiver description at any point in moduli space by following a path connecting them; this path is given by quiver mutations which, in case of strong chambers with finite cardinality, have a discrete group structure.

Following [1,2], the same quiver transformation can be performed on different quiver basis living at a fixed point in moduli space. In this case the mutation $\tilde{\mu}$ will take us between quivers that describe the same physics. This local duality is a powerful equivalence; it allows us to circumvent the computation problem involved in solving stability condition of quiver representations. Using EM charge bases $\{\gamma_i\}$ for the BPS quiver Q and the $\{\tilde{\gamma}_i\}$ the dual quiver $\tilde{Q}$ obtained by mutating the BPS particle with central charge $Z_1=Z(\gamma_1)$ associated with the node γ_1. Under this mutation which rigorously speaking is defined by

$$\begin{aligned}\tilde{\gamma}_1 &= -\gamma_1\\ \tilde{\gamma}_k &= \begin{cases}\gamma_k+(\gamma_k\circ\gamma_1)\,\gamma_1 & \text{if} \quad \gamma_k\circ\gamma_1>0\\ \gamma_k & \text{if} \quad \gamma_k\circ\gamma_1\leq 0\end{cases}\end{aligned} \tag{8.31}$$

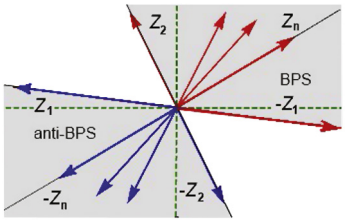

Fig. 21. BPS and anti-BPS states represented by rays $\pm\tilde{Z}_i$ in the in central charge complex plane. The BPS particle Z_1 of Fig. 18 has been mutated into an anti-BPS particle.

the central charge $Z(\gamma_1)$ (see Fig. 18) is rotated out of the complex central charge half-plane of BPS particles as shown by Fig. 21. From the view of the dual $\tilde{Q}^G$, the mutated particle with central charge $\tilde{Z}(\tilde{\gamma}_1) = -Z(\gamma_1)$ is now interpreted as a BPS particle.

Notice that the building of mutated quivers is nicely done by starting from of primitive quiver Q^G and using diagrams to implement the transformations. Given the graph describing a quiver Q^G with $2r$ nodes $\{\gamma_1, ..., \gamma_{2r}\}$, one can construct the dual quiver $\tilde{Q}$ associated with the mutation of node γ_1. The nodes of the new BPS quiver $\tilde{Q}^G$ are in one to one with the nodes in Q^G; the arrows of $\tilde{Q}^G$ are constructed from those of Q^G and the same thing for the superpotential $\tilde{W}$ of $\tilde{Q}^G$ which is constructed from the superpotential W of Q^G. For technical details, we refer to the illustrative examples of [2].

8.3. *Superpotentials*

In this subsection, we collect some information on the structure of the superpotential W^G of the BPS quiver theory; in particular the superfield expressions of the W^G's of those models considered in this paper having $G = SO(8,\mathbb{R})$, $SU(4)$ and $SO(7,\mathbb{R})$, $SP(4,\mathbb{R})$. We also give the corresponding F-term equations constraining the linear mappings $B^a_{ij} : \mathbb{C}^{n_i} \longrightarrow \mathbb{C}^{n_n}$ of the quiver representations R describing bound states $\gamma_R = \sum n_i \gamma_i$ of elementary monopoles and dyons. First, we give the expressions of the superpotentials $\mathrm{W}_0^{SO_8}$ and $\mathrm{W}_0^{SU_4}$ of the supersymmetric SO$(8,\mathbb{R})$ and SU(4) gauge theories; then we turn to their $\mathrm{W}_0^{SO_7}$ and $\mathrm{W}_0^{SP_4}$ cousins.

8.3.1. SO$(8,\mathbb{R})$ *and* SU(4) *gauge models*

We begin by the study of the superpotential $\mathrm{W}_0^{SO_8}$ associated with the primitive quiver $\mathrm{Q}_0^{SO_8}$ of supersymmetric pure gauge model with $SO(8,\mathbb{R})$ gauge symmetry group; we give its explicit expression in terms of chiral superfields and draw the main lines of the method to deal with corresponding F-term equations. Then, we turn to the study of the superpotential $\mathrm{W}_0^{SU_4}$, here also we construct $\mathrm{W}_0^{SU_4}$ in terms of the superfields and describe relevant solutions of their F-term equations.

• *Supersymmetric* $SO(8,\mathbb{R})$ model

The primitive quiver $Q_0^{SO_8}$ of this theory is given by Fig. 3; it has six cycles as shown in Fig. 22; the length of each cycle is equal to four. By using the prescription of ref. [2] for building superpotentials, we learn that the corresponding superpotential $W_0^{SO_8}$ is a quartic chiral function involving 14 chiral superfields; these are the $4+4$ superfields A_i, B_i $i = 1, 2, 3, 4$; and the $3+3$ superfields ϕ_k, ϕ_k^*, $k = 1, 2, 3$.

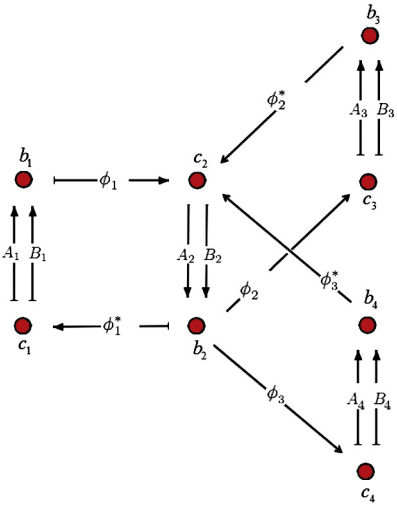

Fig. 22. Cycles of the primitive quiver $Q_0^{SO_8}$; the superfields in the superpotential (8.32) are as represented on the arrows.

The explicit expression of $W_0^{SO_8}$ reads as follows

$$\begin{aligned} W_0^{SO_8} \;=\; & \left(A_1\phi_1^* A_2\phi_1 - B_1\phi_1^* B_2\phi_1\right) + \\ & \left(A_2\phi_2^* A_3\phi_2 - B_2\phi_2^* B_3\phi_2\right) + \\ & \left(A_2\phi_3^* A_4\phi_3 - B_2\phi_3^* B_4\phi_3\right) \end{aligned} \tag{8.32}$$

and the F-term equations are given by

$$\begin{array}{llll} \phi_1^* A_2\phi_1 = 0 & , & B_2\phi_2^*\phi_2 & = 0 \\ A_2\phi_2^*\phi_2 = 0 & , & B_2\phi_3^*\phi_3 & = 0 \\ A_2\phi_3^*\phi_3 = 0 & , & A_1\phi_1^*\phi_1 + A_3\phi_2^*\phi_2 + A_4\phi_3^*\phi_3 & = 0 \\ \phi_1^* B_2\phi_1 = 0 & , & B_1\phi_1^*\phi_1 + B_3\phi_2^*\phi_2 + B_4\phi_3^*\phi_3 & = 0 \end{array} \tag{8.33}$$

and

$$\begin{array}{llll} (A_1A_2 - B_1B_2)\,\phi_1 = 0 & , & (A_1A_2 - B_1B_2)\,\phi_1^* & = 0 \\ (A_2A_3 - B_2B_3)\,\phi_2 = 0 & , & (A_2A_3 - B_2B_3)\,\phi_2^* & = 0 \\ (A_2A_4 - B_2B_4)\,\phi_3 = 0 & , & (A_2A_4 - B_2B_4)\,\phi_3^* & = 0 \end{array} \tag{8.34}$$

These superfield constraint relations are the analogue of eqs. (8.21) describing the conditions on the linear mappings in the Argyres–Douglas A_3 model studied in previous subsection. They have to be imposed when solving the stability condition (8.12) of quiver representation for the pure $SO\,(8,\mathbb{R})$ model. Recall that bound states of elementary monopoles and dyons have the form $\gamma_R = \sum_{i=1}^{8} n_i\gamma_i$ with n_i positive integers; for these bound states γ_R to be BPS, one has to perform a similar analysis as done for the A_2 and A_3 Argyres–Douglas model of subsection 8.2. To deal with the moduli space of the F-term eqs. (8.33)–(8.34) of the $SO\,(8,\mathbb{R})$ theory, one can follow the analysis done for A_3 Argyres–Douglas model; or more interestingly extend the approach of [2] explicitly performed for the supersymmetric pure SU (3) model. The latter has a simple quiver with two cycles and therefore a simple superpotential $W_0^{SU_3}$ like

$$W_0^{SU_3} = A_1\phi_1^* A_2\phi_1 - B_1\phi_1^* B_2\phi_1 \tag{8.35}$$

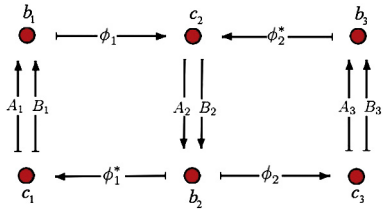

Fig. 23. Cycles of the primitive quiver $Q_0^{SU_4}$.

and F-term equations as follows

$$\begin{array}{llll} (A_1A_2 - B_1B_2)\,\phi_1 & = 0 \quad , & (A_1A_2 - B_1B_2)\,\phi_1^* & = 0 \\ A_1\phi_1^*\phi_1 & = 0 \quad , & B_1\phi_1^*\phi_1 & = 0 \\ A_2\phi_1^*\phi_1 & = 0 \quad , & B_2\phi_1^*\phi_1 & = 0 \end{array} \tag{8.36}$$

Non-trivial solutions of these equations are given by requiring $A_1A_2 = B_1B_2$ and by choosing $\phi_1 = 0$, $\phi_1^* \neq 0$; or by taking $A_1A_2 = B_1B_2$ and $\phi_1 \neq 0$, $\phi_1^* = 0$. The analysis done in [2] for the group SU (3) can be extended straightforwardly to gauge symmetries of ADE type; in particular for $SO\,(8,\mathbb{R})$ and SU (4) we are interested in here. For the example of $SO\,(8,\mathbb{R})$ theory, the corresponding F-term eqs. (8.33)–(8.34) can be non-trivially solved by setting $A_1A_2 = B_1B_2$ and $A_2A_3 = B_2B_3$ as well as $A_2A_4 = B_2B_4$; and by requiring the vanishing of half of the six superfields $\{\phi_1,\ \phi_2,\ \phi_3,\ \phi_1^*,\ \phi_2^*,\ \phi_3^*\}$; for instance by taking the three $\phi_i = 0$ and the three others $\phi_i^* \neq 0$ and vice versa. Clearly the moduli space analysis for higher rank gauge symmetries, though straightforward, is some how cumbersome; fortunately this kind of calculations can be overcome by using the quiver mutation approach that knows about the constraint relations coming from the superpotential of the theory; thanks to quantum mechanical dualities behind the power of mutation method.

• *SU*(4) *gauge model*

The analysis done for the supersymmetric models with gauge group SU (3) and $SO\,(8,\mathbb{R})$ can be repeated for the SU (4) gauge theory. In this case the primitive BPS quiver $Q_0^{SU_4}$ has $2+2$ cycles with length 4 and bifundamental superfields as in Fig. 23.

The corresponding superpotential $W_0^{SU_4}$ involves 10 chiral superfields; the $3+3$ superfields A_i, B_i $i = 1, 2, 3$; and the $2+2$ superfields ϕ_k, ϕ_k^*, $k = 1, 2$. The chiral $W_0^{SU_4}$ is constructed in same manner as before; it is given by

$$\begin{aligned} W_0^{SU_4} \;=\; & \left(A_1\phi_1^*A_2\phi_1 - B_1\phi_1^*B_2\phi_1\right) + \\ & \left(A_2\phi_2^*A_3\phi_2 - B_2\phi_2^*B_3\phi_2\right) \end{aligned} \tag{8.37}$$

The F-term equations following from the superpotential $W_0^{SU_4}$ are given by

$$\begin{array}{llll} A_2\phi_1^*\phi_1 & = 0 \quad , & A_1\phi_1^*\phi_1 + A_3\phi_2^*\phi_2 & = 0 \\ B_2\phi_1^*\phi_1 & = 0 \quad , & B_1\phi_1^*\phi_1 + B_3\phi_2^*\phi_2 & = 0 \\ A_2\phi_2^*\phi_2 & = 0 \quad , & B_2\phi_2^*\phi_2 & = 0 \end{array} \tag{8.38}$$

and

$$\begin{array}{llll} (A_1A_2 - B_1B_2)\,\phi_1 & = 0 \quad , & (A_1A_2 - B_1B_2)\,\phi_1^* & = 0 \\ (A_2A_3 - B_2B_3)\,\phi_2 & = 0 \quad , & (A_2A_3 - B_2B_3)\,\phi_2^* & = 0 \end{array} \tag{8.39}$$

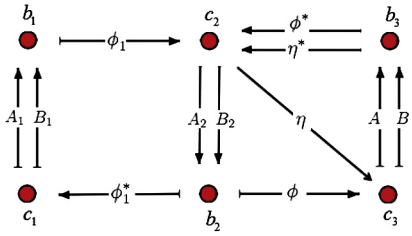

Fig. 24. Cycles of the primitive quiver $Q_0^{SO_7}$; the superfields in the superpotential (8.34) are as represented on the arrows.

Non-trivial solutions of these equations can be also written down; they are directly read from eqs. (8.38)–(8.39); for instance by choosing non vanishing A_i and B_i satisfying $\frac{A_1}{B_1} = \frac{B_2}{A_2}$ and $\frac{A_2}{B_2} = \frac{B_3}{A_3}$ as well as $\phi_i = 0$ but $\phi_i^* \neq 0$. In this pure gauge model, bound states have $\gamma_R = \sum_{i=1}^{6} n_i \gamma_i$ with n_i six positive integers are determined by solving the stability conditions $\arg Z_u(\gamma_S) < \arg Z_u(\gamma_R)$ for sub-representation S of R by following the same method as done for the A_3 Argyres–Douglas model and the supersymmetric pure SU(3) theory.

8.3.2. $\mathrm{SO}(7,\mathbb{R})$ *and* $\mathrm{SP}(4,\mathbb{R})$ *models*

The structure of the superpotentials W^G for non-simply laced gauge symmetry groups type BCFG have been first obtained by Cecotti and Del Zotto in [38]. Here we restrict our analysis to the cases of pure $\mathrm{SO}(7,R)$ and $\mathrm{SP}(4,\mathbb{R})$ gauge theories. First, we give the superpotential $W_0^{SO_7}$ and the corresponding F-term equations; then we turn to $W_0^{SP_4}$ and the induced constraint equations on linear mapping associated with the bifundamentals of the quiver $\mathrm{Q}_0^{SP_4}$.

• *$SO(7,\mathbb{R})$ gauge theory*

The primitive quiver $Q_0^{SO_7}$ of the supersymmetric pure $\mathrm{SO}(7,\mathbb{R})$ gauge theory is given by Fig. 7; it has 6 cycles with chiral superfields as shown in Fig. 24.

Contrary to $Q_0^{SO_8}$, there are different kinds of cycles in $Q_0^{SO_7}$; two cycles of length 3 and the four others of length 4. By using the prescription of ref. [2] for building superpotentials and the convention notation of [38], the superpotential of the $\mathrm{SO}(7,\mathbb{R})$ theory reads as follows

$$\begin{aligned} W_0^{SO_7} \;=\; & A_1\phi_1^* B_2\phi_1 - B_1\phi_1^* A_2\phi_1 + A_2\phi^* B\phi + \\ & A\phi B_2\eta^* + A\eta\phi^* + B\eta\eta^* \end{aligned} \tag{8.40}$$

It involves twelve chiral superfields related to those of $\mathrm{SO}(8,\mathbb{R})$ theory like: (α) the usual 4 superfields A_i and B_i with $i = 1,2$ as well as the new 2 superfields A, B corresponding to the folding of the chiral superfields A_i, B_i with $i = 3,4$ of Fig. 22; (β) the usual 2 superfields ϕ_1, ϕ_1^* and the 4 new superfields ϕ, ϕ^*, η and η^* corresponding to the folding of the chiral superfields ϕ_2, ϕ_3 and ϕ_2^*, ϕ_3^* of Fig. 22. The F-term equations following from the superpotential $W_0^{SO_7}$ are as follows

$$\begin{array}{lll} \phi_1^* B_2\phi_1 = 0 & , & B\phi^*\phi - B_1\phi_1^*\phi_1 = 0 \\ \phi_1^* A_2\phi_1 = 0 & , & A_1\phi_1^*\phi_1 + A\eta^*\phi = 0 \\ B_2\eta^*\phi + \phi^*\eta = 0 & , & A_2\phi^*\phi + \eta^*\eta = 0 \end{array} \tag{8.41}$$

and

$$\begin{array}{l} A_2 B\phi + A\eta = 0 \\ AB_2\phi + B\eta = 0 \\ (A_1B_2 - B_1A_2)\,\phi_1 = 0 \end{array} \tag{8.42}$$

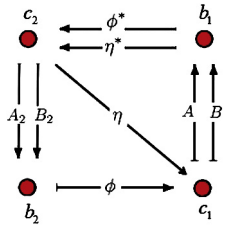

Fig. 25. Cycles of the primitive quiver $Q_0^{SP_4}$.

as well as

$$\begin{array}{ll} A\phi^* + B\eta^* & = 0 \\ A_2 B\phi^* + A B_2 \eta^* & = 0 \\ (A_1 B_2 - B_1 A_2)\,\phi_1^* & = 0 \end{array} \tag{8.43}$$

Solutions of the above relations can be written down by extending the method used for the SO$(8,\mathbb{R})$ gauge model; for example eqs. (8.41)–(8.43) may be solved by taking for instance $\phi_1 = \phi = \eta = 0$ and $\phi_1^* \neq 0$, $\phi^* \neq 0$, $\eta^* \neq 0$. The remaining eqs. (8.43) are ensured by taking $\frac{A_1}{A_2} = \frac{B_1}{B_2}$, $\frac{A}{B} = -\frac{\eta^*}{\phi^*}$ and $\frac{A_2}{B_2} = \left(\frac{A}{B}\right)^2$.

• *SP*$(4,\mathbb{R})$ *model*

The primitive quiver $Q_0^{SP_4}$ of the supersymmetric pure SP$(4, R)$ gauge theory is given by Fig. 12; it has $2+2$ cycles with chiral superfields as shown in Fig. 25.

Following the same method used above, the superpotential of the supersymmetric pure SP$(4,\mathbb{R})$ theory reads as follows

$$W_0^{SP_4} = A_2\phi^* B\phi + B_2\eta^* A\phi + A\eta\phi^* + B\eta\eta^* \tag{8.44}$$

The F-term equations following from this superpotential are as follows

$$\begin{array}{llll} B\phi^*\phi = 0 & , & B_2\eta^*\phi + \phi^*\eta = 0 \\ A\eta^*\phi = 0 & , & A_2\phi^*\phi + \eta^*\eta = 0 \end{array} \tag{8.45}$$

and

$$\begin{array}{llll} A_2 B\phi + A\eta = 0 & , & A_2\phi^* B + B_2\eta^* A = 0 \\ B_2 A\phi + B\eta = 0 & , & A\phi^* + B\eta^* = 0 \end{array} \tag{8.46}$$

Here also we can write down the non-trivial solutions of above relations which are similar to those described in [2] for SU(3) and which have been extended in this subsection to the cases of SO$(8,\mathbb{R})$, SO$(7,\mathbb{R})$ and SU(4). A class of these solutions is given by taking for instance $\phi = \eta = 0$, but $\phi^* \neq 0$, $\eta^* \neq 0$; and the others constrained relations solved by taking $\frac{A}{B} = -\frac{\eta^*}{\phi^*}$ and $\frac{A_2}{B_2} = \left(\frac{\eta^*}{\phi^*}\right)^2$.

Acknowledgements

O. Mellal would like to thank M. Del Zotto for discussions.

References

[1] Murad Alim, Sergio Cecotti, Clay Cordova, Sam Espahbodi, Ashwin Rastogi, Cumrun Vafa, BPS quivers and spectra of complete $N = 2$ quantum field theories, arXiv:1109.4941.
[2] Murad Alim, Sergio Cecotti, Clay Cordova, Sam Espahbodi, Ashwin Rastogi, Cumrun Vafa, $N = 2$ quantum field theories and their BPS quivers, arXiv:1112.3984.
[3] E.H. Saidi, Mutations symmetries in BPS quiver theory: building the BPS spectra, J. High Energy Phys. 8 (2012) 18, arXiv:1204.0395.
[4] S. Cecotti, M. Del Zotto, Half-hypers and quivers, J. High Energy Phys. 09 (2012) 135, arXiv:1207.2275.
[5] E.H. Saidi, Weak coupling chambers in $N = 2$ BPS quiver theory, Nucl. Phys. B 864 (2012), arXiv:1208.2887.
[6] Sergio Cecotti, The quiver approach to the BPS spectrum of a 4d $N = 2$ gauge theory, arXiv:1212.3431.
[7] M. Del Zotto, Four-Dimensional $N = 2$ Superconformal Quantum Field Theories and BPS-Quivers, Scuola Internazionale Superiore di Studi Avanzati, 2013.
[8] Sergio Cecotti, Michele Del Zotto, Infinitely many $N = 2$ SCFT with ADE flavor symmetry, arXiv:1210.2886.
[9] Sergio Cecotti, Proceedings of String Math, 2012, Bonn, arXiv:1212.3431.
[10] Sergio Cecotti, Michele Del Zotto, The BPS spectrum of the 4d $N = 2$ SCFT's H_1, H_2, D_4, E_6, E_7, E_8, arXiv:1304.0614 [hep-th].
[11] D. Gaiotto, $N = 2$ dualities, arXiv:0904.2715 [hep-th].
[12] D. Gaiotto, G.W. Moore, A. Neitzke, Wall-crossing, Hitchin systems, and the WKB approximation, arXiv:0907.3987 [hep-th].
[13] S. Cecotti, C. Vafa, Classification of complete $N = 2$ supersymmetric theories in 4 dimensions, arXiv:1103.5832.
[14] A. Klemm, W. Lerche, P. Mayr, C. Vafa, N.P. Warner, Selfdual strings and $N = 2$ supersymmetric field theory, Nucl. Phys. B 477 (1996) 746–766, arXiv:hep-th/9604034.
[15] N. Seiberg, E. Witten, Monopoles, duality and chiral symmetry breaking in $N = 2$ supersymmetric QCD, Nucl. Phys. B 431 (1994) 484550, arXiv:hep-th/9408099.
[16] N. Seiberg, E. Witten, Electric–magnetic duality, monopole condensation, and confinement in $N = 2$ supersymmetric Yang–Mills theory, Nucl. Phys. B 426 (1994) 1952, arXiv:hep-th/9407087.
[17] A. Klemm, W. Lerche, S. Yankielowicz, S. Theisen, Simple singularities and $N = 2$ supersymmetric Yang–Mills theory, Phys. Lett. B 344 (1995) 169–175, arXiv:hep-th/9411048.
[18] Philip C. Argyres, Alon E. Faraggi, The vacuum structure and spectrum of $N = 2$ supersymmetric $su(n)$ gauge theory, Phys. Rev. Lett. 74 (1995) 3931–3934.
[19] F. Denef, Supergravity flows and D-brane stability, J. High Energy Phys. 0008 (2000) 050, arXiv:hep-th/0005049.
[20] M.R. Douglas, G.W. Moore, D-branes, quivers, and ALE instantons, arXiv:hep-th/9603167.
[21] D. Diaconescu, J. Gomis, Fractional branes and boundary states in orbifold theories, J. High Energy Phys. 0010 (2000) 001, arXiv:hep-th/9906242.
[22] M.R. Douglas, B. Fiol, C. Romelsberger, The spectrum of BPS branes on a noncompact Calabi–Yau, J. High Energy Phys. 0509 (2005) 057, arXiv:hep-th/0003263.
[23] B. Fiol, M. Marino, BPS states and algebras from quivers, J. High Energy Phys. 0007 (2000) 031, arXiv:hep-th/0006189.
[24] B. Fiol, The BPS spectrum of $N = 2$ SU(N) SYM and parton branes, arXiv:hep-th/0012079.
[25] B. Feng, A. Hanany, Y.H. He, A. Iqbal, Quiver theories, soliton spectra and Picard–Lefschetz transformations, J. High Energy Phys. 0302 (2003) 056, arXiv:hep-th/0206152.
[26] B. Feng, A. Hanany, Y.-H. He, D-brane gauge theories from toric singularities and toric duality, Nucl. Phys. B 595 (2001) 165–200, arXiv:hep-th/0003085.
[27] Kazutoshi Ohta, Yuya Sasai, Exact results in quiver quantum mechanics and BPS bound state counting, J. High Energy Phys. 11 (2014) 123, arXiv:1408.0582.
[28] Seung-Joo Lee, Zhao-Long Wang, Piljin Yi, Abelianization of BPS quivers and the refined Higgs index, arXiv:1310.1265.
[29] Michele Cirafici, Line defects and (framed) BPS quivers, arXiv:1307.7134.
[30] M. Kontsevich, Y. Soibelman, Stability structures, motivic Donaldson–Thomas invariants and cluster transformations, arXiv:0811.2435 [math.AG].
[31] Michael Yu. Kuchiev, Supersymmetric $N = 2$ gauge theory with arbitrary gauge group, Nucl. Phys. B 838 (2010) 331–357, arXiv:0907.2010.
[32] A.D. Shapere, C. Vafa, BPS structure of Argyres–Douglas superconformal theories, arXiv:hep-th/9910182.
[33] D. Gaiotto, G.W. Moore, A. Neitzke, Framed BPS states, arXiv:1006.0146 [hep-th].
[34] D. Gaiotto, G.W. Moore, A. Neitzke, Wall-crossing in coupled 2d–4d systems, arXiv:1103.2598 [hep-th].

[35] D. Gaiotto, G.W. Moore, A. Neitzke, Spectral networks, arXiv:1204.4824 [hep-th].
[36] R. Ahl Laamara, M.N. El Kinani, E.H. Saidi, M. Vall, $N = 2$ supersymmetry partial breaking and tadpole anomaly, Nucl. Phys. B 901 (2015) 480–509, arXiv:1512.00704 [hep-th].
[37] S. Cecotti, M. Del Zotto, Infinitely many $N = 2$ SCFT with ADE flavor symmetry, J. High Energy Phys. 2013 (2013) 191.
[38] S. Cecotti, M. Del Zotto, 4D $N = 2$ gauge theories and quivers: the non-simply laced case, J. High Energy Phys. 10 (2012) 190, arXiv:1207.7205 [hep-th].
[39] S.H. Katz, A. Klemm, C. Vafa, Geometric engineering of quantum field theories, Nucl. Phys. B 497 (1997) 173–195, arXiv:hep-th/9609239.
[40] Sheldon Katz, Cumrun Vafa, Geometric engineering of $N = 1$ quantum field theories, Nucl. Phys. B 497 (1997) 196–204, arXiv:hep-th/9611090.
[41] S. Katz, P. Mayr, C. Vafa, Mirror symmetry and exact solution of 4-D $N = 2$ gauge theories, Adv. Theor. Math. Phys. 1 (1998) 53–114, arXiv:hep-th/9706110.
[42] M. Ait Ben Haddou, A. Belhaj, E.H. Saidi, Nucl. Phys. B 674 (2003) 593–614, arXiv:hep-th/0307244.
[43] M. Ait Ben Haddou, A. Belhaj, E.H. Saidi, J. Phys. A 38 (2005) 1793–1806, arXiv:hep-th/0308005.
[44] A. Belhaj, E.H. Saidi, J. Phys. A 38 (2005) 721–748, arXiv:hep-th/0210167.
[45] J.E. Humphreys, Introduction to Lie Algebras and Representation Theory, Springer, 1972.
[46] N. Seiberg, Electric–magnetic duality in supersymmetric non Abelian gauge theories, Nucl. Phys. B 435 (1995) 129–146, arXiv:hep-th/9411149.
[47] P. Di Francesco, R. Kedem, Q-systems, cluster algebras, paths and total positivity, arXiv:0906.3421 [math.CO].
[48] P. Di Francesco, R. Kedem, Q-systems as cluster algebras II: Cartan matrix of finite type and the polynomial property, arXiv:0803.0362 [math.RT].
[49] L. Bonora, R. Savelli, Non-simply laced Lie algebras via F theory strings, J. High Energy Phys. 1011 (2010) 025, arXiv:1007.4668.
[50] A. Belhaj, E.H. Saidi, Toric geometry, enhanced non-simply laced gauge symmetries in superstrings and F-theory compactifications, arXiv:hep-th/0012131.
[51] P.C. Argyres, M.R. Douglas, New phenomena in SU (3) supersymmetric gauge theory, Nucl. Phys. B 448 (1995) 93, arXiv:hep-th/9505062.
[52] Dan Xie, General Argyres–Douglas theory, J. High Energy Phys. 01 (2013) 100, arXiv:1204.2270.
[53] M. Kontsevich, Y. Soibelman, Stability structures, motivic Donaldson–Thomas invariants and cluster transformations, arXiv:0811.2435 [math.AG].